



An integrated approach for water quality assessment and pollution source identification using optimized machine learning and water quality index model in a Tidal River of Bangladesh

Title	An integrated approach for water quality assessment and pollution source identification using optimized machine learning and water quality index model in a Tidal River of Bangladesh
Author(s)	Faruq, Omur;Hossain, Nahrin Jannat;Sajib, Abdul Majed;Diganta, Mir Talas Mahammad;Moniruzzaman, Md.;Olbert, Agnieszka I.;Uddin, Md Galal
Publication Date	2026-02-06
Publisher	Elsevier
Repository DOI	https://doi.org/10.1016/j.ejrh.2026.103215

1 **An Integrated Approach for Water Quality Assessment and Pollution Source**
2 **Identification Using Optimized Machine Learning and Water Quality Index**
3 **Model in a Tidal River of Bangladesh**

4 **Omur Faruq¹, Nahrin Jannat Hossain¹, Abdul Majed Sajib^{2,3,4}, Mir Talas Mahammad**
5 **Diganta^{2,3,4}, Md. Moniruzzaman¹, Agnieszka I. Olbert^{2,3,4}, Md Galal Uddin^{2,3,4,5}**

6 ¹ Department of Geography and Environment, Jagannath University, Dhaka, Bangladesh

7 ² School of Engineering, College of Science and Engineering, University of Galway, Ireland

8 ³ Ryan Institute, University of Galway, Ireland

9 ⁴ Eco-HydroInformatics Research Group (EHIRG), Civil Engineering, University of Galway,

10 Ireland

11 ⁵ Department of Civil, Structural and Environmental Engineering, and Sustainable Infrastructure

12 Research & Innovation Group, Munster Technological University, Cork, Ireland

13 Corresponding author: **Md Galal Uddin** (mdgalal.uddin@universityofgalway.ie,

14 jalaluddinbd1987@gmail.com)

15 **Abstract**

16 *Study region:* The Bhairab River is located in the south of Bangladesh. It is an active tidal river
17 that supports a wide range of aquatic environments.

18 *Study focus:* The present research utilized a holistic approach by incorporating the optimized root
19 mean squared water quality index (RMS-WQI) model and machine learning/artificial intelligence
20 (ML/AI) techniques to assess the water quality (WQ) of the Bhairab River. The study utilized four
21 years (2021-2024) of WQ data, including temperature, pH, electrical conductivity, chloride, total
22 solids, dissolved oxygen, and biochemical oxygen demand, from 8 monitoring sites of the Bhairab
23 River.

24 *New hydrological insights of the region:* The results of the RMS-WQI model showed a decreasing
25 trend of water quality index (WQI) scores between 2021-2024, with most of the monitoring sites
26 rated as ‘fair’ to ‘poor’ WQ categories, indicating that the majority of WQ indicators failed to meet
27 World Health Organization (WHO, 2022) and Environmental Conservation Rules (ECR, 2023)
28 standards. The declining trend of WQI scores was statistically validated by the Friedman test
29 statistic of 21.75 (p-value < 0.05) and the Mann-Kendall Tau value of -1.0 (p-value < 0.05).
30 Moreover, the study utilized eight ML/AI algorithms with the Optuna optimizer, where the
31 Artificial Neural Network (ANN) model demonstrated excellent performance with high accuracy
32 and reliability in predicting WQI scores. In terms of reliability assessment, the ANN-Optuna model
33 showed high effectiveness (Average model efficiency factor: MEF = 0.47; average percentage of
34 relative error index: PREI = 0.39), excellent sensitivity (Average coefficient of determination: R^2
35 = 0.95), and low uncertainty throughout the study period. In addition to assessing WQ trends, the
36 study identified major pollution hotspots along the Bhairab River, where various types of industrial
37 activities, brick kilns, and urban dumping stations were identified as the major sources of pollution
38 around the monitoring sites. In summary, the declining trend of WQ indicated that the Bhairab
39 River was under notable pressure from various point and non-point pollution sources during the
40 study period, which requires site-specific WQ management strategies to protect the Bhairab River
41 ecosystem and living organisms.

42 **Keywords:** Tidal River Water Quality; Pollution Hotspot; Water Quality Index; Machine
43 Learning; Model Reliability.

44 **1. Introduction**

45 Surface water, especially river water, accounts for 0.49% of the world’s freshwater (USGS, 2019)
46 and serves as an important source for drinking, irrigation, and healthy ecosystems. However,

47 maintaining good water quality (WQ) has become a notable global issue due to rapid
48 industrialization and urbanization (Bilal et al., 2023; Hossain et al., 2024; Sajib et al., 2024; Uddin
49 et al., 2024a). Specifically, industrial and municipal runoff is becoming a notable concern around
50 the world because it directly impacts river ecosystems and living organisms (Ameta et al., 2023;
51 Hassan et al., 2023; Mallin, 2024). As a result, maintaining acceptable WQ in rivers has become
52 significantly more challenging than in the past.

53 Typically, surface water pollution is driven by multiple anthropogenic and natural factors, which
54 include industrial discharges, agricultural runoff, municipal sewage, oil and gas contaminants,
55 mining effluents, etc. (Fakron, 2023; Hasan et al., 2019; Walker et al., 2019). These factors
56 introduce polymers, plastics, toxic chemicals, and other contaminants like pharmaceuticals,
57 nanomaterials, and microplastics into the environment (Morin-Crini et al., 2022). However,
58 through strict regulations and wastewater treatment processes, developed countries are attempting
59 to manage and monitor industrial and municipal discharges (Kato & Kansha, 2024), but continue
60 to face challenges in effectively establishing these systems (Chavoshani et al., 2020; Liu et al.,
61 2025; Varatharajan et al., 2025). In contrast, with limited resources, developing and least developed
62 countries face enormous challenges in managing untreated industrial effluents, urban wastewater,
63 and agrochemicals (Islam et al., 2018; Kumar et al., 2023; Sha et al., 2024). In order to address
64 these challenges, developed countries adopted strong policy frameworks, such as the European
65 Union Water Framework Directive (Sajib et al., 2025a; Söderberg, 2016; Uddin et al., 2022b) and
66 the USA Clean Water Act (Keiser & Shapiro, 2018). Nevertheless, weak institutional capacity and
67 implementation gaps often undermine their effectiveness (Gedamu et al., 2025; Handoyo, 2024;
68 Kirschke et al., 2020). Thus far, researchers have utilized several tools and techniques to identify
69 pollution sources in the surface water, including laboratory-based physicochemical assessment

70 (Musa et al., 2025; Sarkar et al., 2016), remote sensing and GIS-based spatial monitoring (Faruq
71 et al., 2025; Gani et al., 2023; Sajib et al., 2025b; Zhu et al., 2024), nutrient load modeling (Dada
72 et al., 2025; Pinichka et al., 2025), and the Water Quality Index (WQI) approach (Gupta & Gupta,
73 2021; Sutadian et al., 2017). Among them, the WQI model has gained notable attention in the last
74 few decades due to its simplistic approach (Uddin et al., 2021).

75 Around the world, WQ monitoring and management is quite challenging, as it involves the
76 collection and analysis of large datasets (Essamlali et al., 2024). On the other hand, established
77 monitoring systems struggle to capture real-world scenarios of waterbodies due to poor
78 management frameworks and a lack of universal tools (Kumar et al., 2023). Furthermore, most of
79 the countries around the world have developed their own guideline values for various WQ
80 indicators; however, they didn't suggest any specific tools/techniques to comprehensively assess
81 the overall status of waterbodies (Uddin et al., 2021). As a result, the WQI model is often utilized
82 by different researchers/organizations/WQ managers to evaluate the status of a waterbody.
83 Generally, the WQI model aggregates WQ data into a single numerical value (e.g., 0 to 100), which
84 effectively makes it easier to interpret and report (Essamlali et al., 2024). The WQI model consists
85 of five key steps: (i) selecting relevant WQ indicators, (ii) determining weighting factors for each
86 WQ indicator, (iii) converting WQ indicator concentrations into dimensionless sub-indices, (iv)
87 calculating the final WQI score using an aggregation function, and (v) rating the WQ based on
88 WQI scores. To date, several studies have utilized the WQI approach to evaluate the WQ status of
89 different waterbodies (Faruq et al., 2025; Gani et al., 2023; Sajib et al., 2025a; Sutadian et al.,
90 2017; Uddin et al., 2021).

91 Since 1960, numerous WQI models, such as the Horton index, the Scottish research development
92 department index, the Ross index, the environmental quality index, the Smith index, the Dojildo

93 index, the British Columbia index, the Liou index, the Said index, the Malaysian index, and the
94 Almedia index, the Canadian Council of Ministers of the Environment Water Quality Index Model,
95 the National Sanitation Foundation Water Quality Index, the Weighted Arithmetic Mean Water
96 Quality Index Model, the Entropy-based Water Quality Index Model, the Irish Water Quality Index
97 (IEWQI) Model, etc. (Chidiac et al., 2023; Gupta & Gupta, 2021; Sutadian et al., 2017; Uddin et
98 al., 2023a; Uddin et al., 2021) developed by different researchers and organizations. Despite this
99 progress in the WQI model field, a number of studies have highlighted notable uncertainty in
100 existing WQI models, which vary between 15% to 37% (Uddin et al., 2021; Uddin et al., 2022b;
101 Uddin et al., 2023a). To address this challenge, a group of water researchers proposed an improved
102 Root Mean Squared (RMS) WQI model for surface waters (Uddin et al., 2022b), which has shown
103 high performance in rating WQ with an uncertainty of less than 1% (Ding et al., 2023; Uddin et
104 al., 2023a). In particular, the RMS-WQI model demonstrated high reliable performance in
105 reducing common WQI problems, such as ambiguity, eclipsing, metaphoring issues, and data
106 outliers (Faruq et al., 2025; Sajib et al., 2024; Uddin et al., 2024b). As a result, several researchers
107 from countries such as Bangladesh, India, China, Romania, Ireland, and the UK adopted this
108 method for assessing surface WQ (Ding et al., 2023; Faruq et al., 2025; Gani et al., 2023; Sajib et
109 al., 2024; Uddin et al., 2023a).

110 In recent years, application of data-driven ML/AI (Machine learning/ Artificial Intelligence)
111 models has gained notable popularity for water resource management and monitoring,
112 supplementing traditional WQI methods (Ahmed et al., 2024). Additionally, several studies
113 highlighted that ML/AI methods can reduce costs and time for WQ assessment by using fewer
114 physical measurements, offering an efficient alternative by predicting WQ trends (Essamlali et al.,
115 2024; Rahman et al., 2025a; Zhang et al., 2024). Moreover, the ML/AI approach optimizes

116 resource allocation in low resource settings and offers accurate predictions that help
117 researchers/organizations/WQ managers make effective decisions for pollution control, regulatory
118 enforcement, and public health interventions (Ahmed et al., 2024; Azha et al., 2023; Ngwenya et
119 al., 2025). To date, several studies have incorporated various ML/AI models to enhance the
120 performance and precision of WQI models, often using techniques such as Random Forest
121 (Rahman et al., 2025a), Decision Trees (Lu & Ma, 2020), k-Nearest Neighbors (Zamri et al., 2022),
122 Support Vector Machines/Regression (Kamyab-Talesh et al., 2019), Extreme Gradient Boosting
123 (Zhang et al., 2024), and Gaussian Processes Regression (Wan et al., 2022), etc., for the WQI score
124 prediction (Sajib et al., 2024; Shahid et al., 2024; Uddin et al., 2022a, 2022c, 2022d). However,
125 contextual differences between locations pose a critical challenge for high-performance models in
126 the ML/AI field, as models trained in one environment may fail to generalize due to changing
127 factors, including data distribution, outliers, etc. (Sajib et al., 2025a; Uddin et al., 2021). As a
128 result, location-based upgradation in prediction models has become essential to cope with spatial
129 variations in data and to ensure accuracy and reliability across different geographic locations.

130 Globally, rivers and estuaries form a vital ecosystem that supports a variety of plant and animal
131 life (Fortune et al., 2023). Specifically, these ecosystems are under threat due to compound
132 anthropogenic impacts and climate change in South Asian countries (Fiaz et al., 2025). Among the
133 South Asian countries, Bangladesh is well known for its dynamic rivers and estuaries, which
134 support a wide range of flora and fauna (Chowdhury et al., 2020). However, environmental
135 degradation and sedimentation pose major challenges for these ecosystems (Uddin & Jeong, 2021).
136 To date, numerous studies have concluded that Bangladesh's river WQ are in danger due to three
137 important factors, which are increasing population, urbanization, and industrialization (Hasan et
138 al., 2021; Kabir et al., 2021a; 2021b; Uddin & Jeong, 2021). Furthermore, several studies have

139 reported deteriorating conditions across various tidal rivers, including the Bhairab River in Khulna,
140 Bangladesh (Ali et al., 2022; Alom et al., 2022; Anzum et al., 2023; Bari et al., 2025; Bari &
141 Sayeed, 2022; Hasan et al., 2019; Khan et al., 2019; Musa et al., 2025; Ridika et al., 2023). The
142 Bhairab River is located in the southern part of Bangladesh and plays an important role in the
143 economy by supporting several industrial facilities along its banks (Hashan et al., 2023; Islam et
144 al., 2018). Furthermore, this river network serves as a primary inland water transportation route
145 for various goods, including oil (Rafizul et al., 2017). All these facilities have not only accelerated
146 rapid urbanization and internal migration in their vicinity but also increased municipal waste
147 discharge and industrial runoff into the Bhairab River (Hashan et al., 2023; Islam et al., 2018;
148 Rafizul et al., 2017; Uddin, 2015). These combined pressures emphasize the urgent need for
149 sustainable WQ management of the Bhairab River to preserve its ecological and economic
150 functions. Thus far, numerous researchers have assessed the WQ of the Bhairab River for various
151 purposes, including drinking WQ (Uddin, 2015), irrigation WQ (Islam et al., 2016), and pollution
152 level assessment (Alom et al., 2022; Bari et al., 2025; Khan et al., 2019; Rafizul et al., 2017).
153 However, none of these studies incorporated the WQI model and ML/AI algorithm to assess and
154 predict the temporal WQ of this river. Additionally, to the best of the author's knowledge, this
155 research is one of the first initiatives to assess a tidal river WQ utilizing the RMS-WQI model
156 incorporating the ML/AI framework in this region. Therefore, the current research utilized the
157 RMS-WQI model for effectively assessing the WQ of the Bhairab River. The objectives of the
158 present research are as follows:

- 159 • To assess the temporal variation of WQ in the Bhairab River.
- 160 • To compute the WQI score and rate the WQ of the Bhairab River by using optimized RMS-
161 WQI framework.

- 162 • To evaluate the model's spatio-temporal performance by utilizing ML/AI framework in
163 terms of model reliability.
- 164 • To identify the major pollution sources in the Bhairab river.

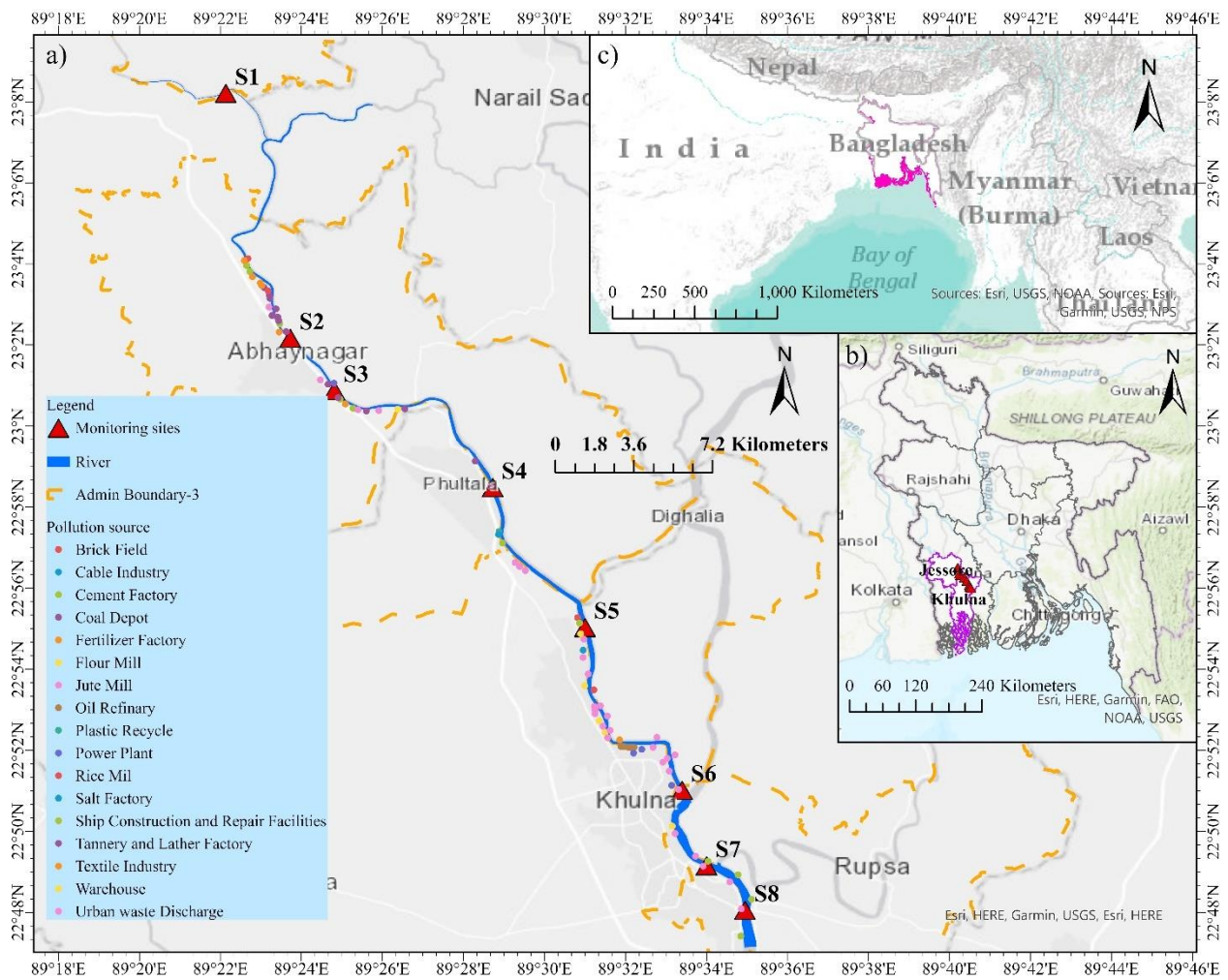
165 The outcome of the study will provide a time-series scenario of WQ in the Bhairab River and
166 provide an optimized framework for assessing tidal river WQ utilizing the RMS-WQI model and
167 ML/AI approach. This adaptive framework could guide WQ managers, institutions, and
168 organizations with a practical tool to monitor and manage the WQ of the region in a sustainable
169 manner.

170 **2. Materials and Method**

171 **2.1 Study Area**

172 The Bhairab River (latitude N 23° 34' 27.804" and longitude E 88° 44' 36.744") system flows to
173 the south of Bangladesh (Fig. 1). It originates from the Tengamari border of the Meherpur district
174 and passes through Narail, Jashore town, and Khulna area. After finishing long journey, the
175 Bhairab River falls on the Rupsha River at Jailkhana Ghat, Khulna City. The Bhairab River divided
176 Khulna city into two parts (Fig. 1). The river is approximately 100 miles long and 300 feet wide,
177 including an average depth of 4 to 5 feet with minimal water flow (Azad et al., 2020). This river
178 is a tributary of the Ganges River and experiences semi-diurnal flood tides from the Bay of
179 Bengal (Wang et al., 2023). It is an active tidal river with a strong current that carries coarser
180 sediments from upstream and finer sediments, mainly clay from downstream by flood tide (Roy et
181 al., 2005). Typically, the semi-diurnal tides with a tidal period of about 12 hours 25 minutes are
182 predominant in the Bay of Bengal (Wang et al., 2023). The tidal range at the coast is strong, ranging
183 from 0.27 m at neap tide to 3.38 m at spring tide (BIWTA, 2006). The area is blessed with a warm
184 tropical climate and sufficient rainfall, which supports a wide biological diversity (Islam et al.,

185 2024). The major water source of the Bhairab River network is the Ganges River water flow, which
 186 significantly dries up during the dry season (Uddin, 2015), but its lower part remains navigable
 187 throughout the year due to influences of tide water. The average annual rainfall and temperatures
 188 in the region vary between 1500-2500 mm and 12-35 °C, respectively (Anzum et al., 2023; BMD,
 189 2020).



190

191 Fig. 1. Map of the monitoring site in the Bhairab River. The map (a) shows eight water quality monitoring sites along
 192 with different pollution sources in the Bhairab River. The inset maps (b) and (c) show the location of the Bhairab River
 193 in Bangladesh and the location of Bangladesh in the South Asia, respectively.

194 **2.2 Data collection**

195 The current research obtained four years (2021–2024) of monthly WQ data from the Department
196 of Environment (DoE), Bangladesh (<https://doe.gov.bd/>), which encompassed eight monitoring
197 stations along the Bhairab River (Fig. 1). A detailed description of monitoring sites (e.g., longitude,
198 latitude, and site description) can be found in supplementary Table S1. In Bangladesh, the DoE is
199 responsible for routine monitoring of WQ data across 405 rivers, including the Bhairab River
200 (DoE, 2021). They established a nationwide monitoring network under which monthly surface
201 water samples from preselected locations are collected for laboratory analysis (DoE, 2021; 2022;
202 2023).

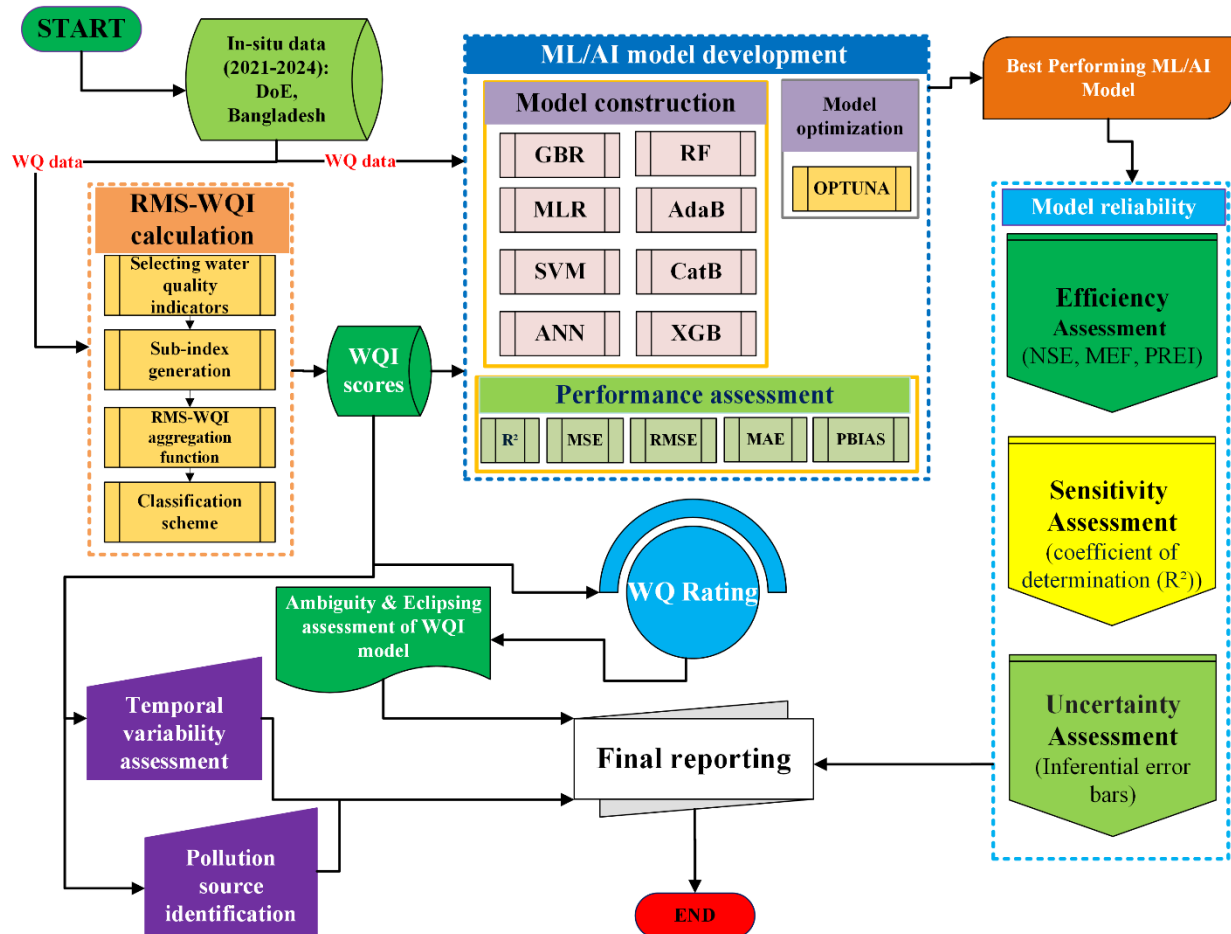
203 For the purposes of WQ assessment in the Bhairab River, seven WQ indicators, including
204 temperature (TEMP), pH, electrical conductivity (EC), chloride (Cl⁻), total solid (TS), dissolved
205 oxygen (DO), and biochemical oxygen demand (BOD₅) were utilized in this study. A detailed
206 description of WQ indicators, units, analytical methods and guideline values is presented in Table
207 1. The DoE follows strict guidelines to collect and analyze the WQ data. A detailed methodological
208 procedure, including sample collection and laboratory analysis can be found in the annual surface
209 and ground WQ reports of DoE, Bangladesh (DoE, 2021; 2022; 2023). On the other hand, the
210 selection of monitoring sites within the river was based on data availability. Regarding data
211 processing, the raw datasets for individual years (2021-2024) were cleaned, and yearly average
212 values were computed for each monitoring site. A detailed representation of the entire research
213 process is illustrated in (Fig. 2).

214 Table 1. WQ indicators and measurement units used in this study

Indicators	Unit	Analytical methodology	ECR, (2023)
Temperature	°C	Method 2550 B (APHA et al., 2005)	25
pH	-	Method 4500-H+ B (APHA et al., 2005)	6.5-9
EC	µS/cm	Method 2510 B (APHA et al., 2005)	2250

Cl ⁻	mg/L	Method 4110 B (APHA et al., 2005)	1000
TS	mg/L	Method 2540 (APHA et al., 2005)	1010
DO	mg/L	Method 4500-O C (APHA et al., 2005)	5-8*
BOD ₅	mg/L	Method 5210B (APHA et al., 2005)	≤ 6

215 *WHO (2022)



216
217 Fig 2. Methodological flowchart of the present study.
218

219 2.3 WQI score calculation

220 In this study, the WQI score was calculated using the RMS-WQI model based on the methodology
221 proposed by Uddin et al. (2022b). Previously, several studies utilized WQI models such as the
222 NSF-WQI and WAM-WQI to assess WQ status in the study region (Hashan, 2023; Rafizul et al.,
223 2017; Uddin, 2015). However, recent studies have highlighted notable limitations of these models
224 in accurately representing the WQ status of any waterbody (Sajib et al., 2023; Uddin et al., 2022c).
225 Specifically, issues such as aggregation functions, classification schemes, model eclipsing, and

226 ambiguity have led to considerable uncertainty in these WQI models (Uddin et al., 2021; Uddin et
227 al., 2023a). Furthermore, recent research suggests that unweighted WQI models such as the RMS-
228 WQI model offered improved performance compared to weighted approaches, particularly in
229 terms of reducing uncertainty and enhancing the accuracy of WQ assessments (Sajib et al., 2024;
230 Uddin et al., 2022d). To date, several studies have concluded that the RMS-WQI model is an
231 effective unweighted tool for assessing WQ with less than 1% uncertainty in various aquatic
232 environments, including rivers, lakes, coastal waters, and groundwater systems (Faruq et al., 2025;
233 Gani et al., 2023; Sajib et al., 2024; Uddin et al., 2021; Uddin et al., 2022b; Uddin et al., 2023a;
234 Uddin et al., 2024a). Based on these insights, the RMS-WQI model was selected for the WQ
235 assessment of the Bhairab River. The conceptual framework and mathematical structure of the
236 RMS-WQI model are illustrated in Fig. 2. The RMS-WQI model consists of four steps, which are
237 described as follows:

238 **2.3.1 Selecting WQ indicators**

239 Typically, several approaches, including expert judgement, data availability, ML/AI methods,
240 environmental significance, statistical techniques (e.g., principal component analysis, correlation),
241 etc., are widely utilized to select WQ indicators for WQI score calculation (Abed et al., 2022;
242 Uddin et al., 2022b; Uddin et al., 2023a). The current research adopted the approach of availability
243 of data to finalize pivotal WQ indicators as input in the RMS-WQI model. This approach ensures
244 comparability across monitoring sites and reduces uncertainty in RMS-WQI calculation.
245 Additionally, the selection of WQ indicators is in line with the Environmental Conservation Rules
246 (ECR, 2023) of Bangladesh and requirements of the RMS-WQI model input attributes. The ECR
247 (2023) is a legal framework (developed by the Government of Bangladesh) to protect the aquatic
248 environment and promote sustainable development that is implemented by the DoE, Bangladesh

249 (ECR, 2023). Several studies used similar approaches for WQ indicator selection (Faruq et al.,
250 2025; Gani et al., 2023; Parween et al., 2022; Sajib et al., 2024; Uddin et al., 2021; Uddin et al.,
251 2022b; Uddin et al., 2023a; Uddin et al., 2024a). The WQ indicators utilized for WQI score
252 calculation are Temp, pH, DO, EC, Cl⁻, TS, and BOD₅.

253 **2.3.2 Sub-index (SI) generation**

254 The SI approach standardizes diverse WQ indicators by converting them into a uniform numerical
255 scale ranging from 0 to 100 (Sajib et al., 2024). On this scale, a value of 0 denotes poor WQ, while
256 a value of 100 represents good WQ (Gupta & Gupta, 2021). In this study, sub-index values for
257 each WQ indicator were determined in accordance with the guidelines set by the ECR (2023) and
258 WHO (2022). Specifically, SI functions proposed by Uddin et al. (2022b) were utilized to convert
259 raw WQ measurements into this standardized scale. The SI equation utilized in this study can be
260 found in Table S2 (Supplementary materials).

261 **2.3.3 Aggregation formula**

262 The aggregation function is responsible for combining the SI values into a single numerical
263 expression that represents the WQI score. The mathematical expression for the RMS-WQI model
264 aggregation function is presented below (Eq. 1).

$$265 \text{ RMS - WQI} = \sqrt{\frac{1}{n} \sum_{i=1}^n (S_i)^2} \quad (1)$$

266 where n indicates the total number of indicators, and S_i is the sub-index value of the ith WQ
267 indicators.

268 **2.3.4 Classification of the WQ status**

269 The primary objective of the WQI model is to interpret and report the computed WQI score to
270 categorize WQ status. Based on the classification scheme of the specific WQI model utilized, WQ
271 status is usually declared as excellent, good, or poor (Uddin et al., 2021). However, recent studies

272 have highlighted a complex issue known as the metaphoring problem, where identical WQ
 273 indicators may lead to varying classifications under different WQI models (Gupta and Gupta,
 274 2021; Sutadian et al., 2017; Uddin et al., 2021). A detailed description of this problem can be found
 275 in Uddin et al. (2021). To address this challenge, the current study utilized a classification scheme
 276 developed by Uddin et al. (2022b). Further details of this classification scheme can be found in
 277 Uddin et al. (2022b), and the specific categories utilized in the RMS-WQI model are presented in
 278 Table 2.

279 Table 2: Classification categories of WQ utilized in this study (Uddin et al., 2022b)

WQ category	RMS score range
Good	80-100
Fair	50-79
Marginal	30-49
Poor	0-29

280 **2.4 Error assessment in WQI score calculation**

281 A number of studies highlighted that eclipsing and ambiguity are two notable limitations in any
 282 WQI models (Chidiac et al., 2023; Gupta & Gupta, 2021; Sutadian et al., 2017; Uddin et al., 2021).
 283 These problems can arise during the sub-index calculation, WQI score calculation using the
 284 aggregation function, and rating of WQ based on the WQI score, leading to either overestimation
 285 or underestimation of WQ status (Uddin et al., 2021). The eclipsing occurs from inaccurate rating
 286 of WQ (Table S3-supplementary materials), while ambiguity results from overestimation or
 287 underestimation between the average sub-index value and the WQI score. A detailed explanation
 288 of these phenomena and their measurement techniques can be found in Uddin et al. (2021). The
 289 current study utilized the methodological framework proposed by Uddin et al. (2022b) to measure
 290 eclipsing and ambiguity issues of the RMS-WQI model. The selection of this approach is based
 291 on the previous research conducted to measure the eclipsing and ambiguity issues of the RMS-

292 WQI model (Ding et al., 2023; Khan et al., 2025; Parween et al., 2022; Sajib et al., 2023, 2024,
293 2025a).

294 **2.5 ML/AI framework for WQI score prediction**

295 Over the past few years, several studies have applied sophisticated ML/AI techniques to predict
296 WQ across various aquatic environments (Ahmed et al., 2019; Bilali et al., 2020; Fan et al., 2018;
297 Sajib et al., 2023; Uddin et al., 2022a). The methodological framework applied in this study is
298 presented in Fig. 2. Moreover, the different steps employed to predict the RMS-WQI score using
299 the ML/AI framework can be found as follows:

300 **2.5.1 Training and testing dataset**

301 Typically, in the ML/AI field, 50-50, 80-20, 70-30, etc. data splitting ratios are frequently utilized
302 by different researchers (Joseph, 2022; Sarker et al., 2021). The current study utilized 80% (six
303 monitoring sites) and 20% (two monitoring sites) ratios for splitting the training and testing
304 datasets. A similar number or fewer sample locations were utilized in various previous studies
305 (Abba et al., 2020; Deng et al., 2022; Khoi et al., 2022; Nafsin & Li et al., 2022; Tiwari et al.,
306 2018; Wang & Wang et al., 2020; Rodríguez-López et al., 2023). Subsequently, both the training
307 and testing datasets were standardized utilizing the Z-score formula. The Z-score process helps to
308 minimize model errors by ensuring that all input variables are scaled consistently (Rahman, 2019).
309 After partitioning and standardizing the data, eight ML/AI models were trained and tested on the
310 training and testing datasets. The Z-score transformation equation used in this process is defined
311 as follows:

$$312 \quad Z = \frac{x_i - \bar{X}}{\sigma} \quad (2)$$

313 where, Z represents the standardized score, X_i denotes the i^{th} variable of WQ indicator dataset, \bar{X}
314 refers to the mean value of WQ indicator data, and σ is the standard deviation of WQ indicator
315 data.

316 **2.5.2 ML/AI algorithms**

317 The study utilized eight of the most popular ML/AI algorithms, namely Gradient Boosting
318 Regressor (GBR), Multiple Linear Regression (MLR), Support Vector Machine (SVM), Artificial
319 Neural Network (ANN), Random Forest (RF), AdaBoost (AdaB), CatBoost (CatB), and Extreme
320 Gradient Boosting (XGB), to identify the best model for predicting RMS-WQI scores. These
321 models were selected based on the prior studies conducted by authors and the performance of these
322 models in WQ modelling in various studies (Goodarzi et al., 2023; Kouadri et al., 2021; Shams et
323 al., 2023; Uddin et al., 2022a; Yudina et al., 2021; Yusri et al., 2022). A detailed description of
324 these models can be found in the supplementary materials as a continuation of subsection 2.5.2.
325 The implementation of these models was carried out using a combination of various Python
326 libraries such as Scikit-learn, Keras, NumPy, Pandas, Matplotlib, etc. in the Anaconda platform.

327 **2.5.3 Model hyper-parameterization**

328 To optimize and improve the accuracy of the ML/AI models, the current research incorporated a
329 cutting-edge hyperparameter optimization technique using the Optuna optimizer. Optuna is an
330 efficient and automated framework for hyperparameter tuning that can identify the best set of
331 parameters for each ML/AI model (Lai et al., 2024; Srinivas & Katarya, 2021). Typically, its
332 mathematical architecture is based on the Tree-structured Parzen Estimators (TPE), which enables
333 it to dynamically sample and evaluate parameter combinations that improve model performance
334 (Dada et al., 2025). Optuna framework enhances model performance by systematically exploring
335 the hyperparameter space to find the best configurations, resulting in improved accuracy and

336 generalization compared to exhaustive grid or random search optimizers (Pinichka et al., 2025;
337 Yuan et al., 2024). However, Optuna is computationally expensive, especially for models that
338 require many hyperparameter settings. Despite this disadvantage, several recent studies utilized
339 Optuna to optimize hyperparameters in various environmental and hydrological modeling, where
340 it has effectively demonstrated its ability to fine-tune models (Abbaszadeh et al., 2022; Islam et
341 al., 2024; Khan et al., 2025; Olbert et al., 2025; Uddin et al., 2022a, 2024a). In this study, Optuna
342 was used to optimize several key parameters such as learning rate, maximum depth, number of
343 estimators, regularization factors, and neural architecture configurations, depending on the specific
344 model.

345 **2.5.4 Model performance evaluation**

346 A 10-fold cross-validation was employed in this study to assess model reliability and reduce the
347 risk of overfitting, following the methodology of Uddin et al. (2022a). Cross-validation remains
348 one of the most widely utilized techniques in model evaluation because it provides a robust and
349 reliable assessment of a model's performance on unseen data (Tsamardinos et al., 2018; Wainer
350 and Cawley, 2021; Wong, 2015). It is especially valuable in environmental datasets, which are
351 often small, sparse, or imbalanced (Charilaou and Battat, 2022; López et al., 2022).

352 Furthermore, the prediction performance of utilized ML/AI models in this study was assessed
353 using a set of established performance statistics, including Mean Absolute Error (MAE), Mean
354 Squared Error (MSE), Root Mean Square Error (RMSE), and the Percent of Absolute Bias Error
355 (PABE). These metrics are adopted in this study based on the prior research conducted by the
356 authors (Khan et al., 2025; Sajib et al., 2023; Uddin et al., 2022a, 2022b, 2023) and findings from
357 various research (Ahmed et al., 2019; Chen et al., 2020; Islam et al., 2024). One of the key
358 advantages of these statistics is that they collectively provide a quantitative understanding of

359 prediction deviation (Chicco et al., 2021; Karunasingha, 2022; Nicolson & Paliwal, 2019). The
360 mathematical functions of these statistics are presented as follows:

$$361 \quad MAE = \frac{1}{m} \sum_{i=1}^m |Y_i - \hat{Y}_i| \quad (3)$$

$$362 \quad MSE = \frac{1}{m} \sum_{i=1}^m (Y_i - \hat{Y}_i)^2 \quad (4)$$

$$363 \quad RMSE = \sqrt{\frac{1}{m} \sum_{i=1}^m (Y_i - \hat{Y}_i)^2} \quad (5)$$

$$364 \quad PABE = \frac{1}{m} \sum_{i=1}^m \left| \frac{Y_i - \hat{Y}_i}{Y_i} \right| \times 100 \quad (6)$$

365 In the above equations, m is the number of observations, \hat{Y}_i is the predicted value and Y_i is the
366 actual value.

367 **2.5.5 Ranking of the ML/AI Models**

368 The current research utilized a rank-based method proposed by Uddin et al. (2022a) to collectively
369 assess the ML/AI models' performance based on the training and testing outcomes. In this study,
370 ML/AI models were ranked between 1 to 8 based on the performance metrics, where 1 indicates
371 the higher accuracy and 8 indicates the lower accuracy of the models. The cumulative score
372 obtained from all performance metrics (training and testing) determines the final ranking of each
373 model. The primary strength of this approach is that it allows for objective comparisons by
374 incorporating multiple evaluation dimensions. A number of studies utilized a similar approach to
375 identify the best-fitting model (Sajib et al., 2024; Uddin et al., 2023a).

376 **2.6 Model reliability assessment**

377 **2.6.1 Model efficiency assessment**

378 In order to assess the effectiveness of the model at each monitoring site, the current study utilized
379 Percentage of Relative Error Index (PREI), Nash-Sutcliffe Efficiency (NSE), and Model
380 Efficiency Factor (MEF) statistical metrics. Numerous studies utilized similar methods to assess

381 the effectiveness of the model (Sajib et al., 2025a; Sajib et al. 2024; Uddin et al., 2023a). Typically,
 382 the PREI score is utilized to evaluate the model overestimation (+' value) and underestimation (-'
 383 value) problems, which are presented in percentage. Usually, the NSE value can range between ∞
 384 to 1, where a value close to 1 represents the optimal value. Similarly, the MEF value close to 0
 385 represents the optimal value. A detailed description of these metrics can be found in Sajib et al.
 386 (2025a). The equations of PREI (Eq. 7), NSE (Eq. 8), and MEF (Eq. 9) are as follows:

$$387 \quad PREI = \left(\frac{Y_i - \hat{Y}_i}{Y_i} \right) \times 100 \quad (7)$$

388 where Y_i actual WQI score for i^{th} sample and \hat{Y}_i is the mean predicted WQI score.

$$389 \quad NSE = 1 - \frac{\sum_{i=1}^m (Y_i - \hat{Y}_i)^2}{\sum_{i=1}^m (Y_i - \bar{Y}_i)^2} \quad (8)$$

390 where, m is the number of samples, Y_i is the actual value, and the \hat{Y}_i is the predicted value and \bar{Y}_i
 391 mean of the actual value.

$$392 \quad MEF = \sqrt{1 - NSE} \quad (9)$$

393 where, NSE is the Nash–Sutcliffe efficiency index score.

394 **2.6.2 Model sensitivity evaluation**

395 To evaluate the model sensitivity and explanatory power, the coefficient of determination (R^2) was
 396 used. This metric measures the proportion of variance in the observed data that is explained by the
 397 model predictions and is commonly used in WQ modeling studies (Fan et al., 2018; Sajib et al.,
 398 2023; Uddin et al., 2022a). The R^2 value is closer to 1, indicating stronger model performance.
 399 Numerous studies utilized similar approaches to measure model sensitivity (Bilali et al., 2020;
 400 Ding et al., 2023; Goodarzi et al., 2023; Sajib et al., 2023, 2024). The R^2 formula is given as:

$$401 \quad R^2 = 1 - \frac{\sum_{i=1}^m (Y_i - \hat{Y}_i)^2}{\sum_{i=1}^m (Y_i - \bar{Y}_i)^2} \quad (10)$$

402 Here, m is the number of samples, Y_i is the actual value, \hat{Y}_i is the predicted value and \bar{Y}_i mean of
403 the actual value.

404 **2.6.3 Model uncertainty assessment**

405 The current study utilized inferential error bars with a 95% confidence interval (CI) to measure the
406 uncertainty of the model. This approach helps to visualize the uncertainty associated between two
407 groups (Cumming et al., 2007). Moreover, an overlapping error bar (especially CIs) indicates that
408 the difference between the groups might not be statistically significant, whereas a non-overlapping
409 error bar might indicate a significant difference. One of the key advantages of inferential error bars
410 is that their length indicates how much uncertainty there is in the data (Uddin et al., 2024b). For
411 example, wide bars indicate higher error, and shorter bars indicate higher accuracy. A detailed
412 description of this approach can be found in Cumming et al. (2007). Several environmental studies
413 have utilized similar methods to assess and visualize model uncertainty (Fang et al., 2025; Uddin
414 et al., 2024b).

415 **2.7 Trend analysis of water quality**

416 Analysis of temporal variability was conducted to examine the variation in WQ of the study area
417 during 2021 to 2024. Typically, variability analysis helps to understand how much fluctuation
418 occurs in WQ over time. The current study utilized the Friedman test and Mann-Kendall test to
419 assess the temporal variability analysis. A detailed description of these techniques can be found as
420 follows:

421 **2.7.1 Friedman test**

422 The Friedman test was originally developed by Milton Friedman in 1937. This statistical tool is
423 particularly utilized to assess repeated measures or matched pairs (Pereira et al., 2015). It ranks
424 the data for each subject and compares the sums of ranks across different groups. The Friedman

425 test can be defined as a generalization of the sign test (Hoffman, 2015). However, it has been
426 argued that the statistical power of the Friedman test slightly exceeds the sign test when there are
427 more than two treatment groups (Cleophas & Zwinderman, 2016). Since the present research
428 accounted for four different years data evaluation, the Friedman test is an optimum choice. A
429 detailed description of this technique can be found in Pereira et al. (2015). The tests were initiated
430 with the following hypothesis.

- 431 • Null Hypothesis (H_0): There is no significant difference in overall WQ from 2021 to 2024.
- 432 • Alternative Hypothesis (H_1): There is a significant difference in the overall WQ between
433 2021 to 2024.

434 The Friedman test statistics are calculated using the following formulas:

$$435 \chi_F^2 = \frac{12}{nk(k+1)} \sum_{nk(k+1)}^k R_j^2 - 3n(k+1) \quad (11)$$

436 Here, χ_F^2 is the Friedman test statistics (T_1), n is the number of blocks, k is the number of groups
437 (e.g., years) and R_j^2 is the sum of ranks for group j .

438 **2.7.2 Mann-Kendall trend analysis test**

439 The study utilized the Mann-Kendall test for the purpose of trend analysis in WQ. This is a non-
440 parametric method that identifies monotonic trends in time series data (Coccia & Roshani, 2024).
441 Typically, the Mann-Kendall test provides three types of information, including the Kendall Tau
442 (measures the monotony of slope and Tau value - value varies between -1 to 1), the Sen slope
443 (measures the overall slope of time series data), and the significance value (indicates trend or no
444 trend in the time series data based on statistical significance with a p -value < 0.05). This method
445 is widely adopted by different researchers for assessing trends in time series data (Coccia &
446 Roshani, 2024; Uddin et al., 2023b).

447 **2.8 Field observation for pollution source identification**

448 To identify the major hotspots of pollution around the monitoring site in the Bhairab River, the
449 study documented environmental conditions by field observations and photography. This method
450 increases the accuracy of the calculated RMS-WQI score by validating the measured WQ
451 indicators and comparing them with the actual conditions at the monitoring sites. A key advantage
452 of this combined approach is that it provides a more holistic and reliable assessment of WQ than
453 relying solely on numerical data. Therefore, a field visit was conducted on the 18th of July 2025
454 during daylight hours, which included photography, pollution source identification, and informal
455 interviews with local residents. A standardized field notebook with a pre-designed checklist was
456 utilized to note down field observations. Each site was photographed to capture these conditions
457 utilizing the RMX2193 device. Additionally, GPS location was collected for the same location
458 using the GPS Test Android application which supports GPS, GLONASS, GALILEO, SBAS,
459 BEIDOU, and QZSS satellites. The sampling site was selected based on a random approach, which
460 has consistently shown a poor WQ rating during the study period.

461 **2.9 Statistical processing and geo-spatial mapping**

462 To assess significant similarities/differences between the actual and predicted RMS-WQI scores,
463 this research utilized the Bland-Altman plot analysis. The Bland-Altman plot analysis is a widely
464 utilized statistical method for evaluating statistical agreement/disagreement between two
465 quantitative measurement techniques at a 95% confidence level (Doğan, 2018). Recently, this
466 statistical approach has been widely used in the domain of hydrological modelling for assessing
467 significant differences/similarities between model outcomes (Diganta et al., 2025; Sy et al., 2020;
468 Zubaidi et al., 2022). A detailed description of the Bland-Altman plot analysis can be found in

469 Bland and Altman (1986). For implementing this analysis, the research followed the approach of
470 Bland and Altman (1986).

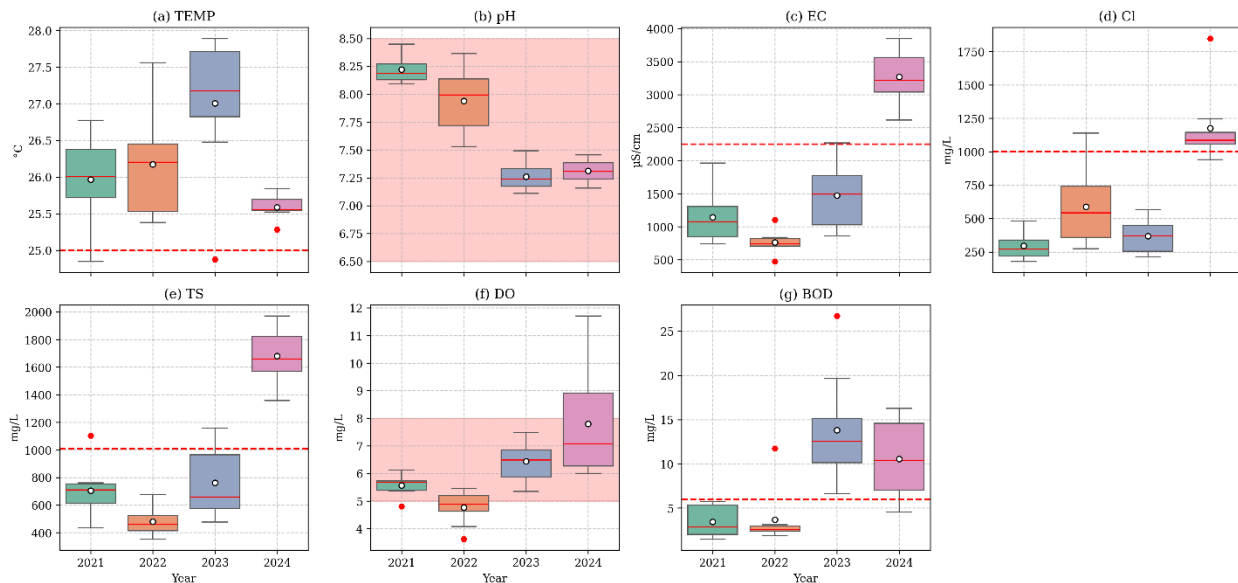
471 The current research utilized a proportional distribution approach on the ArcGIS Pro 3.5.2 platform
472 for geospatial mapping and visualization of WQI scores in the study area. Typically, this method
473 utilizes symbols shaped consistent with the data values to visually represent quantitative
474 information on the map. The size of the symbol (e.g., circle) directly corresponds to the dimensions
475 of the mapped features, making it easier to understand spatial patterns and distribution (Faruq et
476 al., 2025; Sajib et al., 2024). Apart from this, all statistical analyses and visualizations for this
477 research were performed using Microsoft Excel and the Python programming environment.

478 **3. Result and Discussion**

479 **3.1 Statistical distribution of WQ indicators**

480 The study assessed the WQ of the Bhairab River between 2021-2024 utilizing seven WQ
481 indicators. The WQ data was collected from DoE, Bangladesh, and evaluated against the ECR
482 (2023) and WHO (2022) standards to identify breached WQ indicators. Fig. 3 shows a statistical
483 summary of the WQ indicators utilized in this study. Notably, most of the WQ indicators in the
484 study area, such as TEMP, TS, Cl⁻, DO, and BOD₅, have breached the guideline values for years.
485 In particular, the TEMP (°C) at all monitoring sites consistently exceeded the standard level (25
486 °C) for surface water during 2021-2024 (Fig. 3). Similarly, studies by Ali et al. (2022) and Anzum
487 et al. (2023) reported high TEMP (> 25 °C) as a result of various anthropogenic activities in the
488 vicinity of the river. In contrast, water pH remained within the acceptable range (6.5 – 8.5) at all
489 monitoring sites throughout the study period. The average pH value in the study area during 2021-
490 2022 was between 7.9 - 8.2, while in 2023-2024 it decreased slightly to between 7.3 – 7.2.

491 Furthermore, EC concentrations, which indicate dissolved substances in the surface water,
 492 exceeded the ECR (2023) standards with high variability at all monitoring sites in 2024. The
 493 average EC concentration during the study period was 3269.44 $\mu\text{S}/\text{cm}$ (SD \pm 394.04 $\mu\text{S}/\text{cm}$).
 494 Generally, higher EC concentrations in river water indicate an increase in dissolved ion
 495 concentrations, which may be due to mineral runoff or anthropogenic activities like industrial
 496 pollution and sewage discharge (Rahman et al., 2025b; Zhu et al., 2022). Similarly, Cl⁻ ($1175.81 \pm$
 497 266.16 mg/L) and TS (1680.49 ± 191.04 mg/L) concentrations at most monitoring sites in 2024
 498 exceeded the ECR (2023) standard. The higher Cl⁻ concentrations in 2024 may reflect the influence
 499 of high tides compared to previous years (Cereja et al., 2021; Feng et al., 2025; Skibbe et al., 2024).
 500 Additionally, DO (mg/L) and BOD₅ (mg/L) concentrations at the monitoring sites showed
 501 considerable variability. Specifically, DO value exceeded WHO (2022) standards at most sites in
 502 2022, while BOD₅ exceeded the ECR (2023) thresholds in 2023 and 2024. Prior studies have
 503 documented similar higher BOD₅ values because of the discharge of sewage and industrial
 504 effluents into the river (Ali et al., 2022; Anzum et al., 2023).



505
 506 Fig. 3. The statistical summary of physicochemical indicators in the Bhairab River. Here red line indicates the
 507 guideline value suggested by ECR (2023) and WHO (2022).

508 The study also utilized the Spearman's correlation (based on the Shapiro-Wilk test – see Table S4)
509 approach to evaluate the relationship between the WQ indicators and WQI scores (Fig. 4). Over
510 the years, the data has indicated varying correlations between WQ indicators and WQI scores. For
511 example, Cl^- concentrations consistently exhibited a negative correlation with WQI scores during
512 the study period. Moreover, strong negative correlations were observed between BOD_5 and Cl^-
513 concentrations with WQI scores ($\text{BOD}_5 = -0.52$; $\text{Cl}^- = -0.93$) in 2021, while weak positive
514 correlations were observed between DO concentrations and WQI scores ($r = 0.31$). These strong
515 negative relationships indicate that increases in these indicators may lead to decreases in WQI
516 scores (Rahman et al., 2021). Furthermore, in the 2022 dataset, a high positive correlation was
517 found between the DO and WQI scores ($r = 0.81$). However, in the 2024 dataset, DO concentrations
518 showed a strong negative correlation with WQI scores ($r = -0.95$). In contrast, DO concentrations
519 exhibited a weak negative correlation with WQI scores ($r = -0.21$) in 2023. Moreover, TS showed
520 strong negative correlation ($r = -0.57$) with WQI scores for the year 2022 and 2023, respectively.
521 Nevertheless, none of the WQ indicators showed a strong positive relationship with WQI scores
522 in 2023 (Fig. 4).

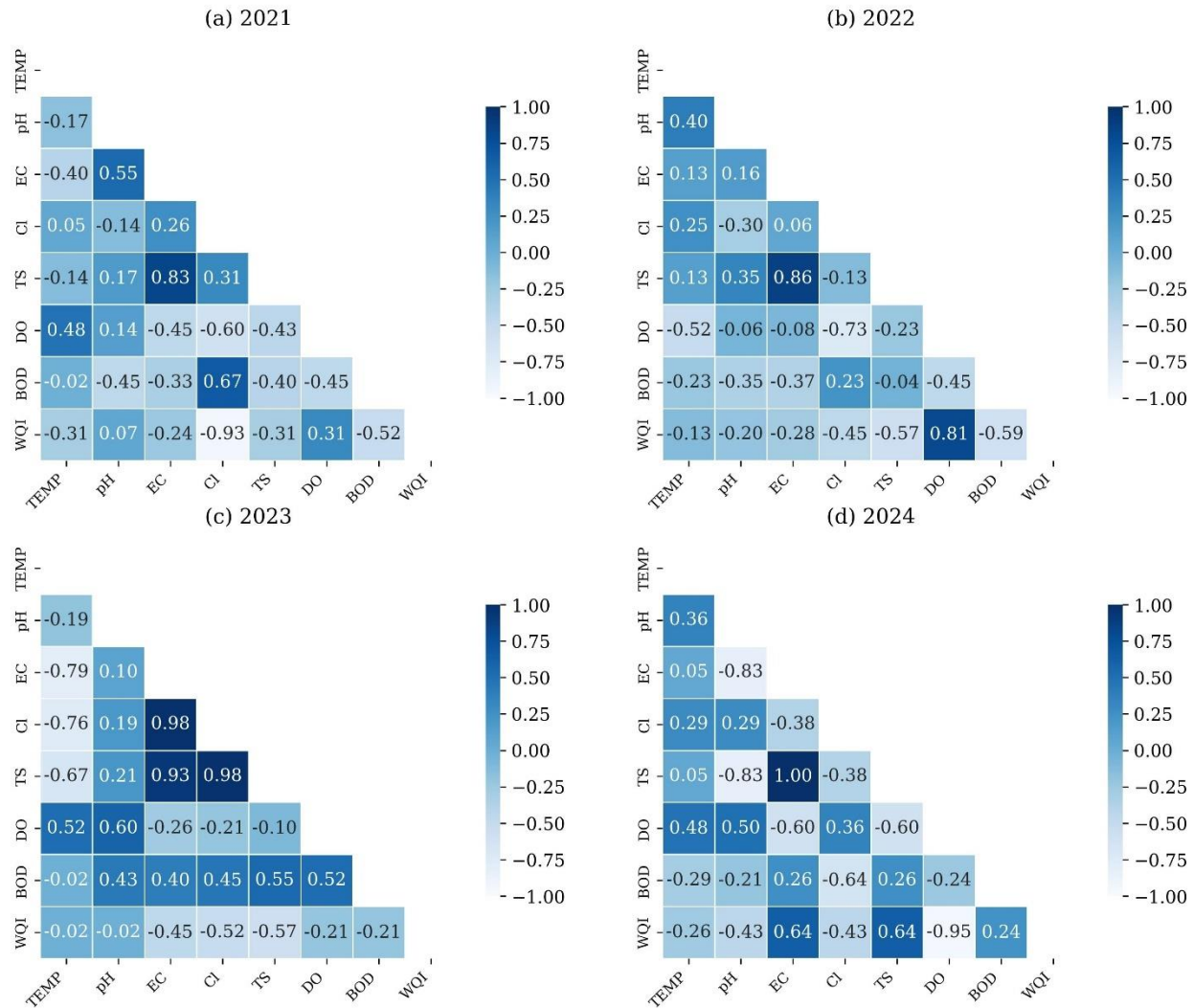
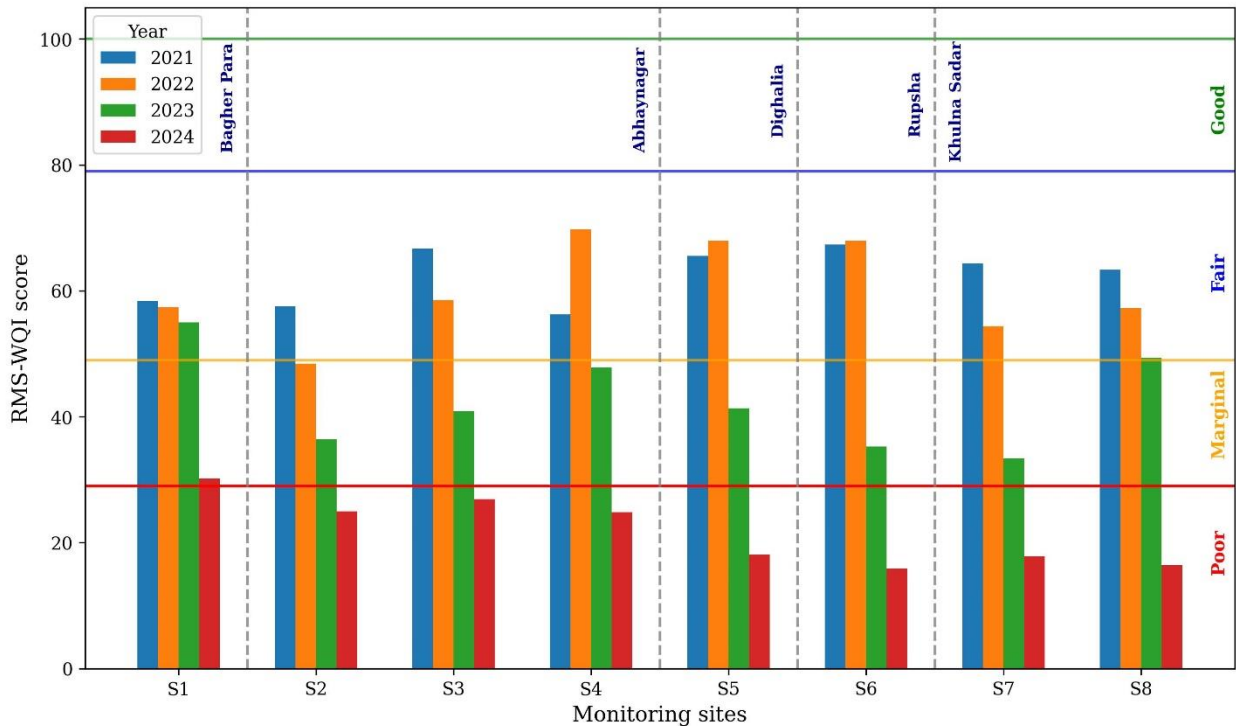


Fig. 4. Spearman's correlation between the WQ indicators and RMS-WQI scores.

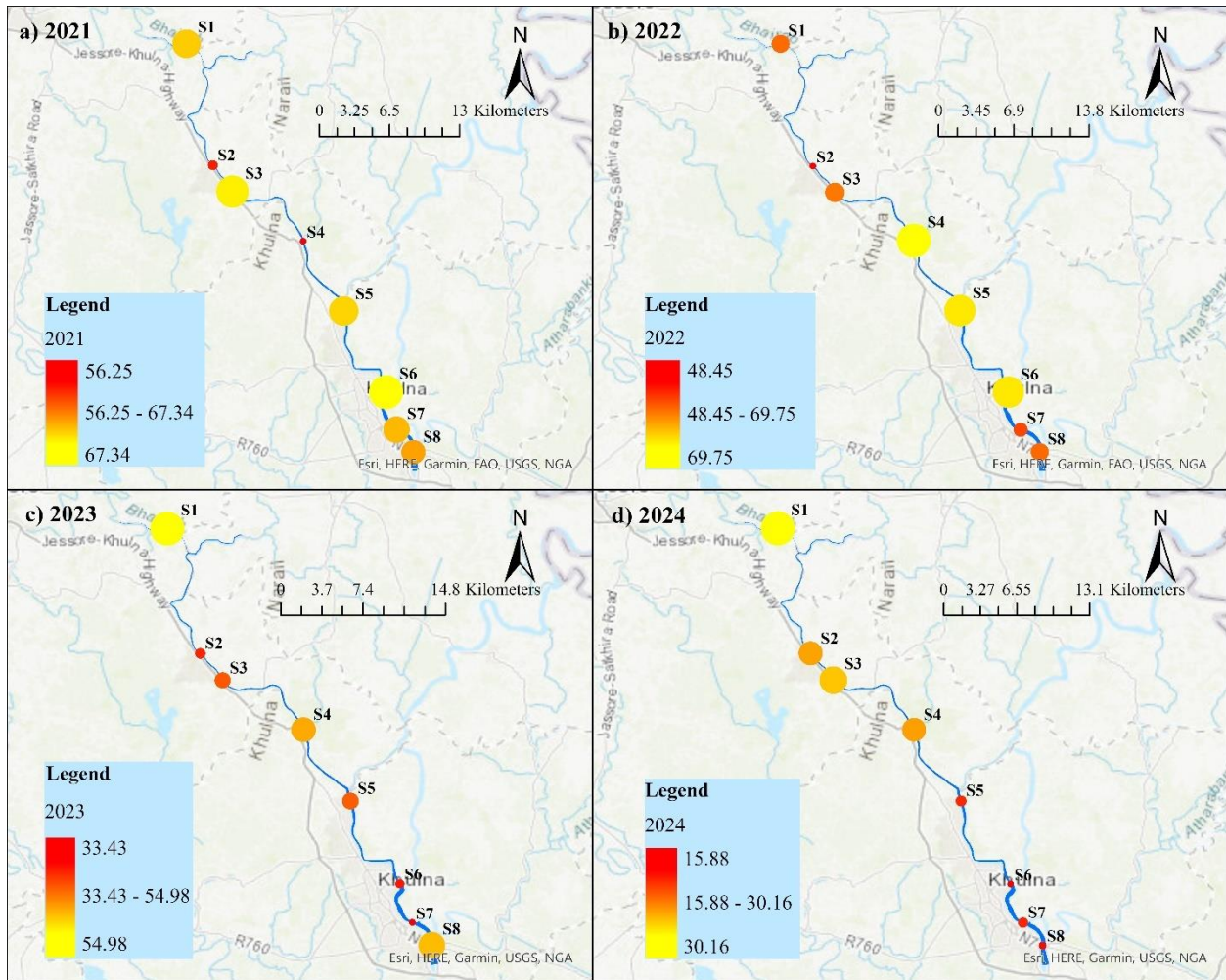
3.2 Results of the RMS-WQI model

The present study utilized the RMS-WQI model to assess the WQ status of the Bhairab River. Prior to this, numerous studies utilized a similar approach for calculating WQI scores (Faruq et al., 2025; Gani et al., 2023; Sajib et al., 2024; Uddin et al., 2024a; Uddin et al., 2023a; Uddin et al., 2022b). Fig. 5 shows the summary of the RMS-WQI scores at various monitoring sites throughout the study period, whereas Fig. 6 presents the spatio-temporal distribution of RMS-WQI scores in the Bhairab River. Additionally, a detailed calculation of the SI value of each WQ indicator during 2021-2024 can be found in Table S5 (Supplementary materials). During the study period (2021-

533 2024), WQI scores at eight monitoring sites (S1 to S8) of the Bhairab River showed a consistent
 534 decreasing trend. Specifically, WQI scores are relatively higher in 2021 compared to other years
 535 The WQI scores in 2021 ranged from 56.25 (S4) to 67.34 (S6) (Fig. 5). Furthermore, the proportion
 536 distribution map of WQI scores validates these findings, as site S6 represented the largest circle,
 537 indicating the highest WQI score, whereas S4 is exhibited with the smallest, reflecting the lowest
 538 WQI score (Fig. 6a). In 2022, WQI scores range from 48.45 (S2) to 69.75 (S4). The sites S4, S5,
 539 and S6 exhibited higher WQI scores than other sites on the distribution map in 2022 (Fig. 6b).
 540 However, there was a notable downward trend of WQI scores observed between 2023-2024. The
 541 WQI scores ranged from 33.43 (S7) to 54.98 (S1) in 2023, while in 2024, WQI scores reached
 542 their lowest levels, ranging from 15.88 (S6) to 30.16 (S1). In summary, a consistently decreasing
 543 trend in WQI scores was observed over the study period across all monitoring sites.



544 Fig. 5. Computed RMS-WQI scores at each monitoring site in the Bhairab River during the study period.
 545
 546
 547



548

549 Fig. 6. Geo-spatial distribution of WQI scores in the Bhairab River during the study period. Here, (a), (b), (c), and (d)
 550 show the distribution of WQI scores at each monitoring site for 2021, 2022, 2023, and 2024, respectively.

551 3.3 ML/AI models result for WQI prediction

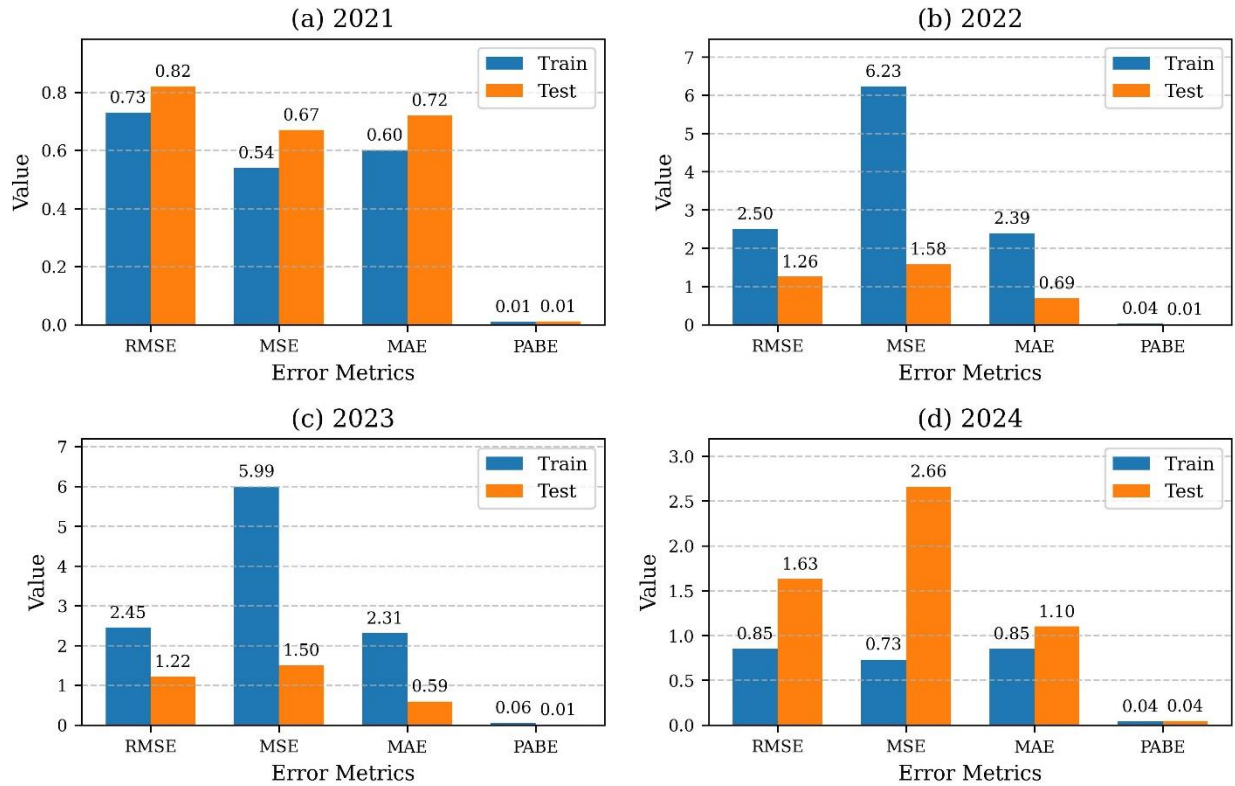
552 The study utilized eight ML/AI algorithms (GBR, CatB, XGB, AdaB, ANN, RF, SVM, and MLR)
 553 to predict WQI scores in the study area. The performance of these models was evaluated utilizing
 554 RMSE, MSE, MAE, PABE, and R^2 . Additionally, a ranking method was utilized to identify the
 555 best-fit model.

556 3.3.1 Performance of ML models

557 Table S6 (Supplementary materials) shows the performance metrics of different ML/AI models
 558 based on RMSE, MSE, MAE, PABE, and R^2 scores. Among the eight ML/AI models utilized in
 559 the study to predict WQI scores, the ANN model showed outstanding performance, ranking first

560 based on prediction accuracy and overall ranking score during the study period (2021-2024).
561 Moreover, SVM and CatB models showed notable performance on various datasets, but the
562 consistency of predicted performance over the years was not stable. In contrast, the GBR exhibited
563 the weakest performance overall among the utilized models (Table S6).

564 Specifically, the ANN model performed best compared to other models with remarkably lower
565 RMSE (0.82), MSE (0.67), MAE (0.72), and PABE (0.01) for the 2021 dataset (Fig. 7). Although
566 the test performance metrics are slightly higher than the training metrics in 2021, but the difference
567 was not notable. The ANN maintained consistent accuracy for the 2022 and 2023 datasets.
568 However, its performance is slightly declined for the 2024 dataset, with higher RMSE (1.63), MSE
569 (2.66), MAE (1.1), and PABE (0.04). On the other hand, SVM showed good performance during
570 the training phase but suffered severe overfitting, ranking poorly in testing across all the years
571 (Table S6). Furthermore, boosting algorithms such as AdaB, CatB, and XGB models have shown
572 good accuracy with balanced performance and low overfitting compared to other models.
573 Conversely, GBR, MLR, and RF models showed poor performance over the years, indicating poor
574 generalization capabilities with these WQ datasets (Table S6). In this study, the consistent
575 performance of the ANN model validated that the neural networks are well-suited for capturing
576 long-term trends and complex dependencies within yearly aggregated data (Ubah et al., 2021). The
577 research results are consistent with prior studies conducted on WQI score prediction in various
578 waterbodies (Chen et al., 2020; Chen & Hao, 2025; Frincu, 2024; Sajib et al., 2023; Satish et al.,
579 2024).



580
581 Fig. 7. Performance metrics of the ANN model during the training and testing phase.

582 **3.3.2 Role of Optuna optimizer on prediction capabilities**

583 The current study utilized the Optuna optimizer to enhance the prediction accuracy of applied
584 ML/AI models. Due to its flexibility and effective performance in hyperparameter tuning, this
585 method has been utilized to optimize the models in numerous water research studies (Islam et al.,
586 2024; Olbert et al., 2025; Uddin et al., 2024b). Table 3 shows the optimal hyperparameter values
587 utilized for model testing. In the hyperparameter setting, the logistic and tanh activation functions
588 were identified as the best functions for utilized datasets. Typically, these functions were utilized
589 as the base for developing ANN models to solve non-linear problems (Althubiti et al., 2023).

590 Furthermore, the optimizer results revealed that the alpha value (L2 regularization parameter) was
591 notably higher in 2021, indicating strong regularization to reduce overfitting. However, from 2022
592 to 2024, the alpha value decreased notably, indicating minimal regularization (Table 3). For

593 instance, the lowest alpha value was observed for the 2024 dataset, which may be an optimal value
 594 for a well-structured dataset to prevent overfitting (Fiorentini et al., 2022; Frazier, 2018; Huang &
 595 Le, 2021). Typically, the number of neurons in the hidden layer of an ANN model defines the
 596 overall structure of the model (Huang & Le, 2021). In the 2021 dataset, the developed ANN-
 597 Optuna model utilized a single hidden layer with 100 neurons, indicating a simpler architecture.
 598 In contrast, from 2022 to 2024, the model was transformed into a deeper architecture with two
 599 hidden layers (150 and 200 neurons).

600 Furthermore, the Optuna optimizer also determined that the ‘adaptive’ learning strategy was
 601 effective for the developed ANN model. The primary strength of this setting is that it stabilizes the
 602 model and avoids slow learning problems (Qian et al., 2021). Additionally, in terms of max
 603 iterations, Optuna has consistently identified 1000 training epochs as optimal across the years. The
 604 consistency of the 1000 iterations over the years indicates that this value is sufficient for the ANN
 605 model to achieve convergence without early stopping (Miseta et al., 2023). Moreover, the
 606 ‘Stochastic Gradient Descent’ (sgd) solver was suggested by Optuna throughout the years to
 607 minimize the loss function of the ANN model.

608 Table 3. Best hyperparameter value utilized in the ANN-OPUTNA model

Hyperparameters	2021	2022	2023	2024
Activation function	logistic	tanh	tanh	tanh
Alpha	0.99	1.00165E-08	1.2118E-08	1.001E-08
Hidden layer sizes	100	150, 100	150, 100	150, 100
Learning rate	adaptive	adaptive	adaptive	adaptive
Max iterations	1000	1000	1000	1000
Solver	sgd	sgd	sgd	sgd

609

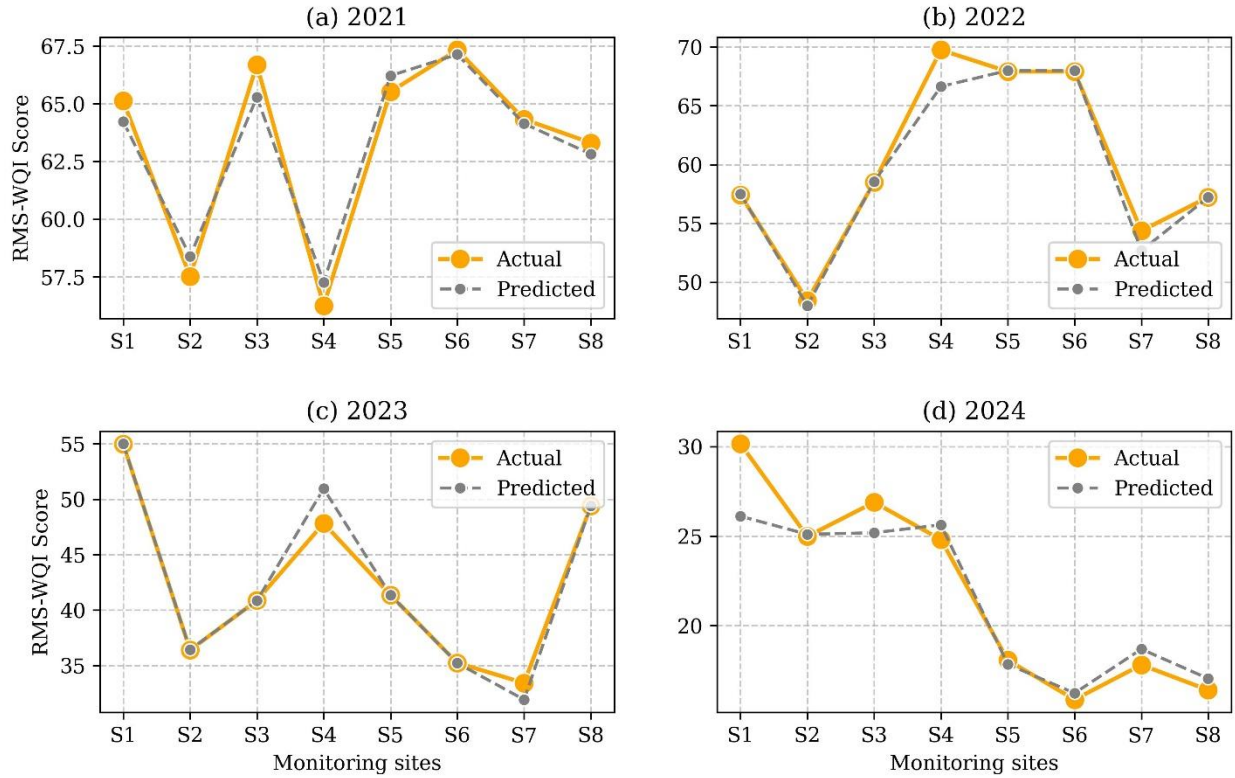
610 3.3.3 Comparison between actual and predicted WQI scores

611 The study evaluated the differences between actual and predicted WQI scores to assess the
 612 accuracy of the ANN-Optuna model at each monitoring site. The line plot (Fig. 8) shows the actual

613 and predicted WQI scores for all the years. It can be seen from the plot (Fig. 8) that across the
614 years an underfitting and overfitting problem has emerged at different monitoring sites.

615 Specifically, high overfitting and underfitting were found at sites S3 and S4 in 2021, respectively.
616 Moreover, an underfitting was observed at sites S2 and S5 in 2021. Conversely, a notable
617 overfitting was observed for site S7 during 2022-2023. However, the same monitoring site (S7)
618 experienced an underfitting problem in 2024. Typically, these problems (e.g., underfitting and
619 overfitting) indicate that the ANN model either failed to capture the complexity of the independent
620 variables (e.g., WQ indicators) or was affected by a small training size/noisy data (Kariri et al.,
621 2023; Maier et al., 2023; Sakizadeh et al., 2015).

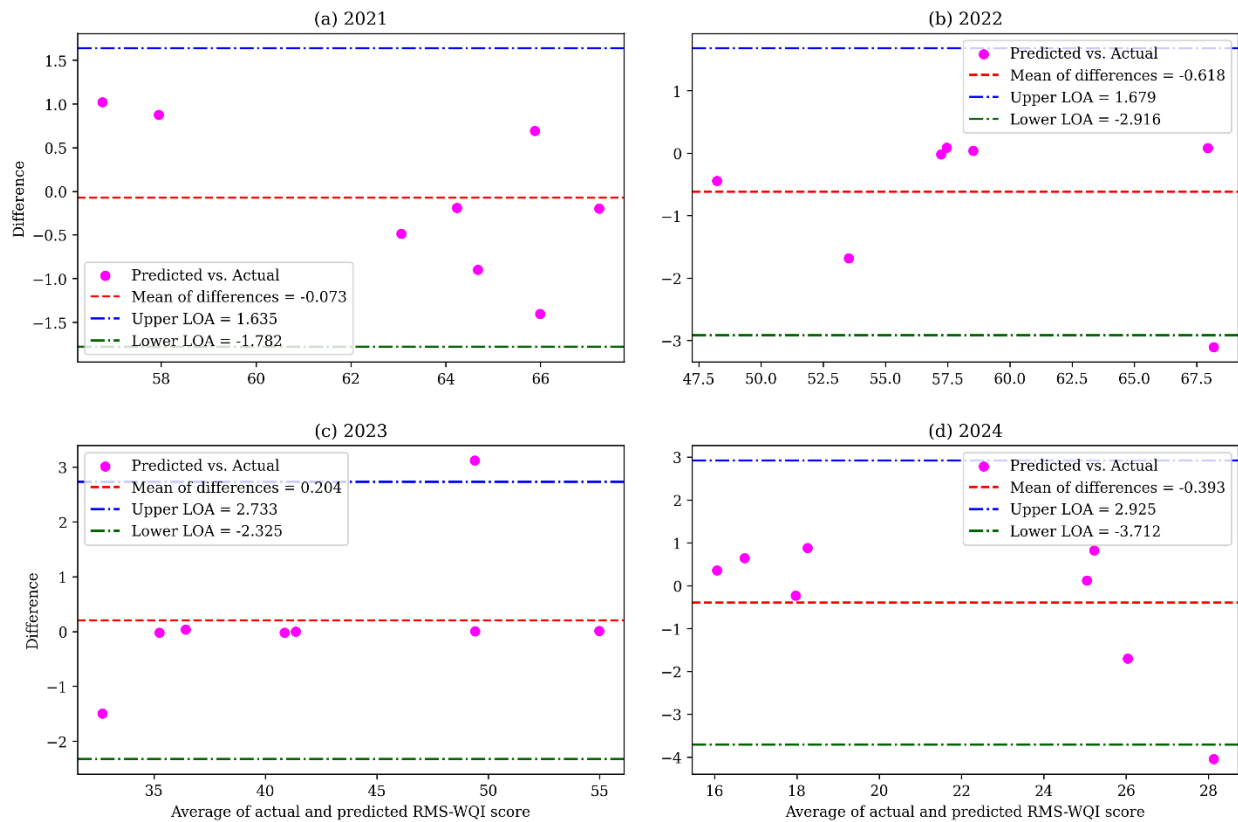
622 It is worth noting that the highest levels of overfitting and underfitting were observed at site S4 in
623 2022 and 2023 (Fig. 8). Moreover, the highest differences between the actual and predicted WQI
624 scores were observed in 2024. The result suggests that the model failed to capture the complexity
625 of the input data at all monitoring sites in 2024 (Chen et al., 2020). In contrast, the lowest variance
626 was found in the 2023 dataset, indicating that the model successfully captures the complexity of
627 data input for that year. Overall, the research findings demonstrated the accuracy of the ANN-
628 Optuna model in predicting WQI scores at each monitoring site across all the years. Nevertheless,
629 temporal variations were observed at different sites (e.g., S5, S4, S7, S8) in predicting WQI score,
630 which required further attention (Fig. 8).



631
 632 Fig 8. Difference between actual and predicted RMS-WQI scores at each monitoring site across all the years along
 633 the Bhairab River.

634 The study further utilized Bland-Altman analysis to assess the agreement/disagreement between
 635 actual and predicted WQI scores in the study area (Fig. 9). In particular, this method evaluated the
 636 performance of the ANN-Optuna model by comparing the differences between actual and
 637 predicted WQI scores against their mean values, with a 95% confidence interval in this study. In
 638 2021, the LOA (limit of agreement) ranged from -1.782 to 1.635, with a slight underprediction
 639 (bias of -0.073) found between actual and predicted WQI scores. This range suggests moderate
 640 variability with reasonable agreement. However, as the LOA range increased in 2022 (-2.916 to
 641 1.679), with the negative bias value (-0.618), indicating a lower level of agreement compared to
 642 2021. In contrast, the bias is minimal (0.204) in the 2023 dataset, indicating better agreement
 643 between actual and predicted WQI scores (Fig. 9). However, the LOA range (-2.325 to 2.733) is
 644 quite wide in 2023 dataset, indicating greater variability. This variability may be due to the weak

645 prediction performance at sites S4 and S7 by the ANN-Optuna model (Fig. 9). Furthermore, in
 646 2024, the model showed an underestimation bias (-0.393), with the widest LOA range (-3.712 to
 647 2.925), verifying the model's weak performance in S1, S3, S4, S7, and S8 monitoring sites (Fig.
 648 9). Although the ANN-Optuna model showed few over- and underestimation at certain monitoring
 649 sites, the overall performance of this model is high compared to other models.



650
 651 Fig. 9. Bland-Altman plot analysis at 95% confidence level showing the differences against the average values of
 652 actual and predicted RMS-WQI scores (the blue and green lines indicate the upper and lower limits of agreement
 653 (LOA), respectively).

654 3.4 Model reliability assessment

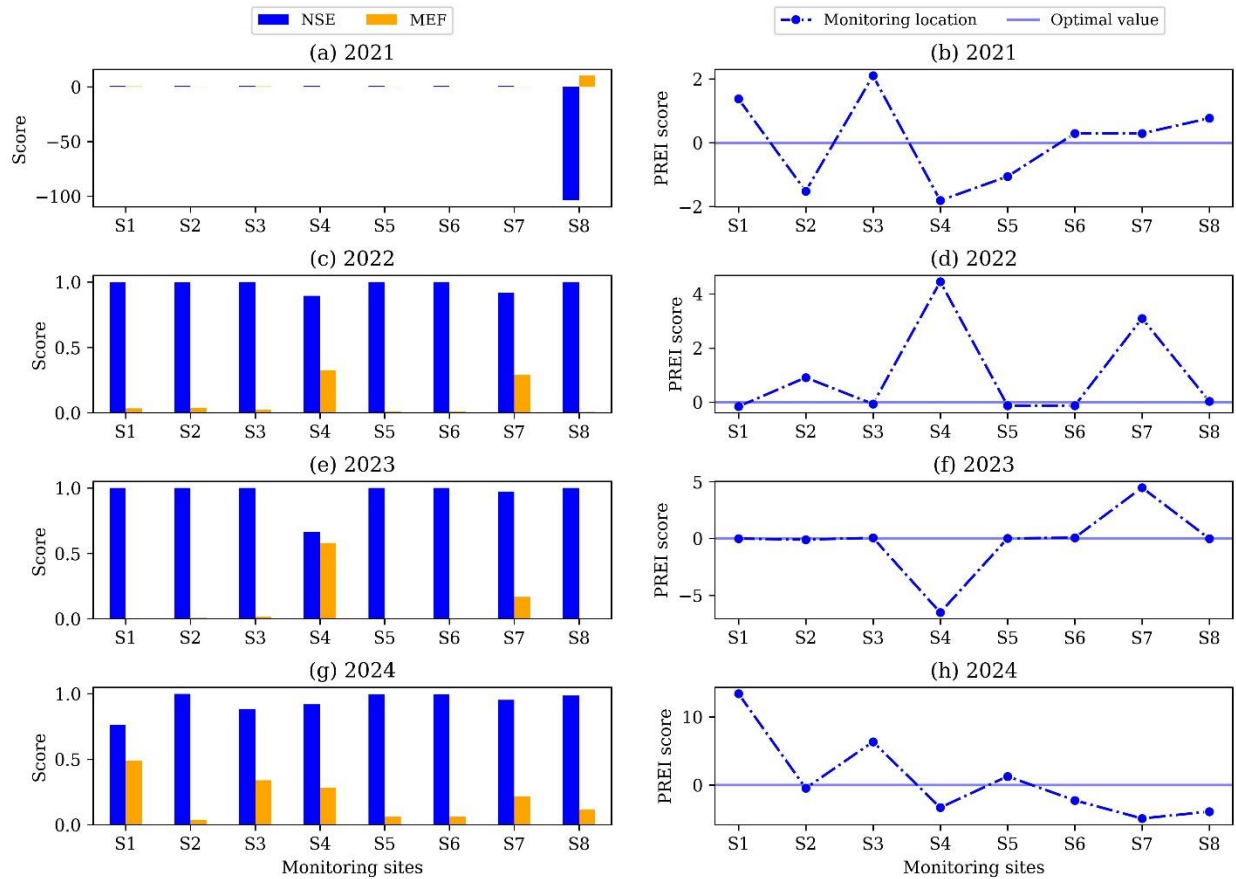
655 3.4.1 Result of model efficiency

656 In order to assess the performance of the ANN-Optuna model in predicting WQI scores at each
 657 monitoring site during the study period, the study utilized NSE, MEF, and PREI statistics. These
 658 metrics were commonly utilized by researchers to assess model efficiency and reliability (Khan et

659 al., 2025; Sajib et al., 2024; Uddin et al., 2023a). Fig. 10 presents the NSE, MEF, and PREI results
660 for eight monitoring sites along the Bhairab River.

661 It is apparent from Fig. 10 that among the eight monitoring sites, site S8 exhibited a high negative
662 NSE value (-104) and a high MEF value (10.2) in 2021 WQI scores, which may indicate poor
663 model performance. Although the difference between actual and predicted scores is 0.5, it is worth
664 noting that the NSE value appears larger due to the site's greater deviation from the average WQI
665 score of the 2021 dataset. On the other hand, a stable performance was observed across all
666 monitoring sites during the 2022-2024 period, with an average NSE value of 0.98 in 2022, 0.95 in
667 2023, and 0.94 in 2024, and consistent MEF values across monitoring sites (average MEF 2022 =
668 0.1; 2023 = 0.1; 2024 = 0.2). The result indicates effective performance of the ANN-Optuna model
669 in the study area. Furthermore, the current research utilized PREI statistics to evaluate the accuracy
670 of the ANN-Optuna model in predicting WQI score at each monitoring site. Typically, PREI
671 statistics highlight the problems of overestimation (+ value) and underestimation (- value) in model
672 predictions. It can be seen from Fig. 10(b,d,f,h) that a number of overestimations and
673 underestimations were observed at the monitoring sites during the study period. Specifically, S1,
674 S4, and S7 showed consistent overestimation and underestimation problems during the study
675 period (2021-2024), which required further investigation. The highest overestimation problem was
676 observed at site S1 (PREI = 13.4) in 2024, while the highest underestimation problem was
677 observed at site S4 (PREI = -6.53) in 2023. Nevertheless, the average PREI score for each year
678 indicates that the ANN-Optuna model is suitable for predicting WQI scores in the Bhairab River.
679 These results are consistent with previous research (Abbaszadeh et al., 2022; Dada et al., 2025;
680 Pinichka et al., 2025; Uddin et al., 2022a; Yuan et al., 2024), further strengthening the reliability

681 of the model. Overall, these results indicate that the ANN-Optuna model is highly efficient in
 682 predicting WQI scores in the study area.

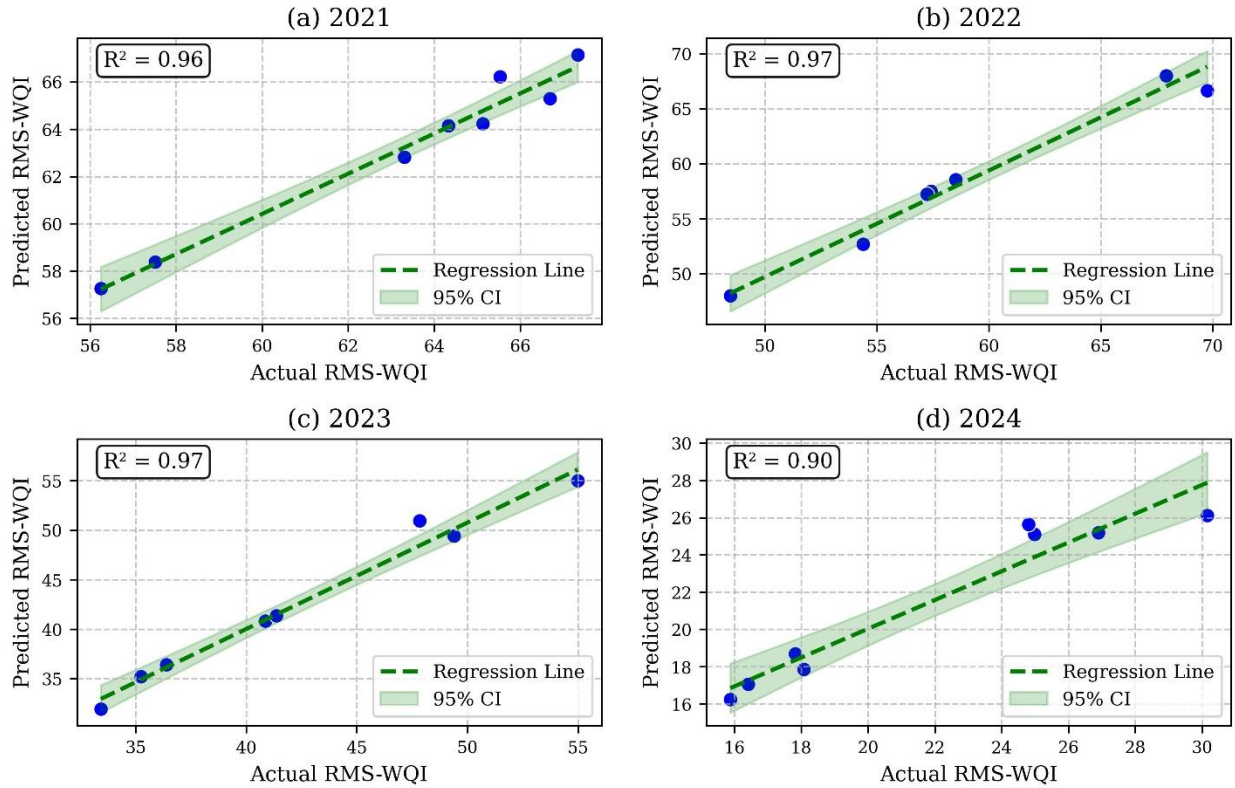


683
 684 Fig. 10. The ANN-Optuna model efficiency assessment at each monitoring site using NSE, MEF, and PREI metrics.

685 3.4.2 Sensitivity of model

686 The current study utilized R^2 to assess the sensitivity of the model. Fig. 11 shows the scatter plot
 687 with regression lines and 95% confidence interval, comparing the actual and predicted WQI scores
 688 during the study period in the Bhairab River. In terms of sensitivity, the ANN-Optuna model
 689 showed high sensitivity with $R^2 > 0.90$ during the study period, indicating excellent sensitivity.
 690 Specifically, the model demonstrated that the predicted values could explain approximately 96%
 691 of the variability in the actual WQI score from 2021 to 2023. Additionally, a narrow 95%
 692 confidence interval further validates reliable prediction by the ANN-Optuna model in the Bhairab

693 River (Fig. 11). However, a wider 95% confidence interval was found in 2023 compared to 2021-
694 2022, indicating slight variability in WQI score predictions. In contrast, the sensitivity score drops
695 to $R^2 = 0.90$ with a wider 95% confidence interval in 2024, showing a limited variability in
696 predicted WQI scores (Fig. 11). Consequently, the lower R^2 and wider confidence interval in 2024
697 suggest that the ANN-Optuna model might be less responsive to the lower range of WQI scores.
698 These notable decreases in sensitivity score require further investigation. Nevertheless, it is worth
699 noting that overall, the ANN-Optuna model showed high sensitivity across the Bhairab River for
700 all years, indicating a high level of agreement between dependent and independent variables in the
701 developed model. The result is consistent with previous research (Chen et al., 2020; Chen & Hao,
702 2025; Frincu, 2024; Rustam et al., 2022; Sajib et al., 2023; Satish et al., 2024), which has
703 consistently demonstrated that the neural network models are highly effective in capturing long-
704 term trends and complex dependencies. In summary, the result collectively indicates that the
705 developed model may be utilized in other tidal rivers with similar characteristics to assess surface
706 water in terms of sensitivity.

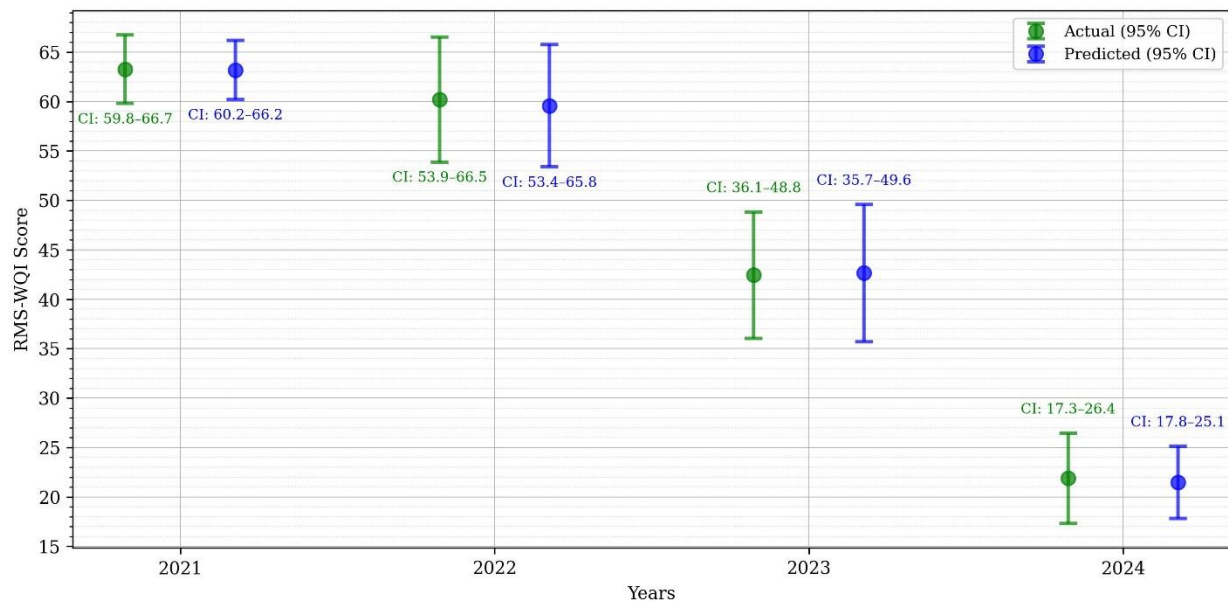


707
708 Fig. 11. The scatter plot between actual and predicted WQI scores with regression lines and a 95% confidence interval.

709 **3.4.3 Uncertainty of model**

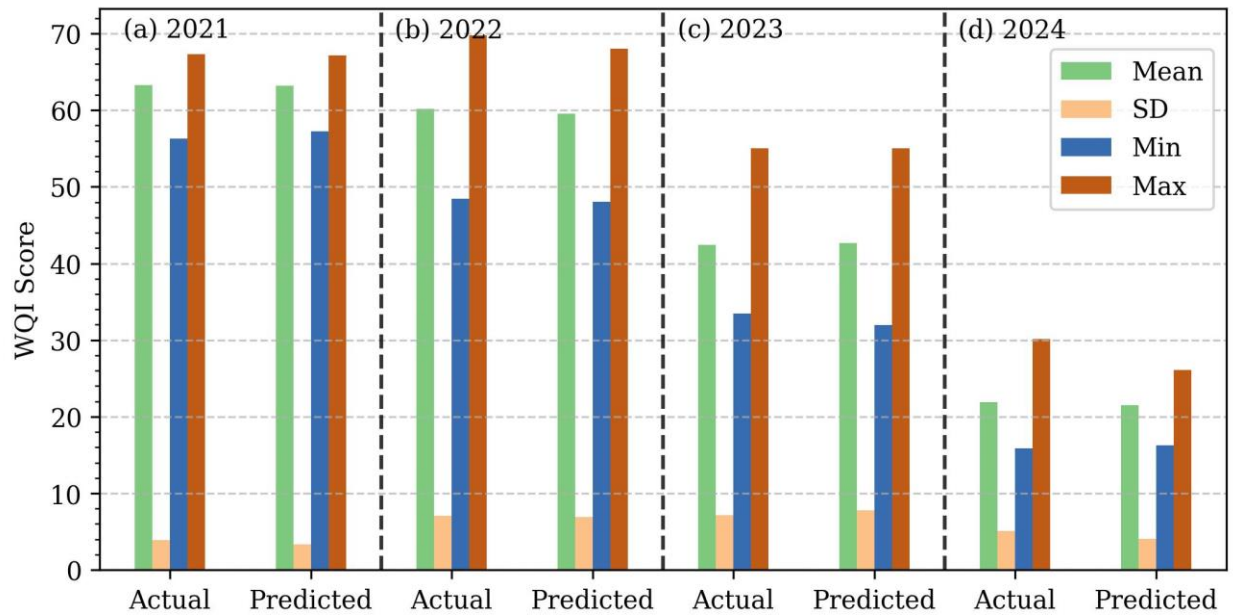
710 The study utilized inferential error bars with 95% confidence interval to assess model uncertainty.
711 Additionally, a statistical summary of actual and predicted scores is presented to support this
712 uncertainty measure. Fig. 12 presents the error bars of actual and predicted WQI scores, while Fig.
713 13 shows a statistical summary of actual and predicted WQI scores across the years for the Bhairab
714 River. It can be seen from Fig. 12 that the mean predicted WQI scores are slightly lower than the
715 actual mean WQI scores in 2021, yet the overlapping 95% confidence interval indicates low
716 uncertainty. A similar consistent result was observed in 2022 WQI scores, where predicted WQI
717 scores are very close to the calculated WQI scores mean (Fig. 12). However, there is a slight wider
718 95% confidence interval range observed in 2023 WQI scores, indicating greater uncertainty
719 compared to previous years. On the other hand, mean predicted WQI scores are quite lower than
720 the actual mean WQI scores in 2024, indicating higher uncertainty than the 2021-2023 WQI scores.

721 Overall, it is noteworthy that the observed uncertainty between actual and predicted WQI scores
 722 in this study was not high, indicating a good level of accuracy and reliability in the predictions of
 723 the ANN-Optuna model. Furthermore, the results of the inferential error bars are further validated
 724 by the statistical summary of the actual and predicted WQI scores (Fig. 13). Fig. 13 shows that
 725 there is apparently slight difference between actual and predicted mean and standard deviation
 726 (SD), indicating the excellent performance of the model. The ANN model's result is consistent
 727 with earlier research (Ding et al., 2023; Nishat et al., 2025; Rustam et al., 2022; Sajib et al., 2023;
 728 Satish et al., 2024; Uddin et al., 2022c). In summary, these results indicate that the developed
 729 model can be utilized for future WQ prediction for the Bhairab River.



730
 731 Fig. 12. Error bars of actual and predicted WQI scores with 95% confidence interval. Here a dot (circle) represents
 732 the mean value, with caps around the dot indicating the 95% confidence interval for the mean value.

733



734 Fig. 13. Statistical summary of actual and predicted WQI scores in the Bhairab River during 2021-2024. (Here SD =
 735 standard deviation)
 736

737 3.5 Result of the WQI score calculation error assessment

738 The degree of ambiguity and eclipsing of the RMS-WQI model was assessed in this study to
 739 determine the reliability and interpretability of the model. Table 4 presents a summary of ambiguity
 740 and eclipsing problems observed during calculation of the RMS-WQI scores. It is apparent from
 741 Table 4 that the highest levels of ambiguity and eclipsing problems were found in the calculation
 742 of 2023 WQI scores, while the 2024 dataset recorded the lowest (Table 4). In 2021, two monitoring
 743 sites (S2 and S4) showed ambiguity problems due to their average SI values, which should be in
 744 the range of 50-79 (refer to 'fair' WQ rating). However, both sites scored below 50, resulting in a
 745 'marginal' rating. In terms of eclipsing issues, no eclipsing issues were observed in the 2021
 746 dataset, as the data followed the eclipsing criteria addressed in Table S3 (Supplementary
 747 materials). In contrast, during 2022-2023, an average of more than three sites showed eclipsing
 748 and ambiguity problems, which required further investigation. Moreover, at S1 monitoring site,
 749 both eclipsing and ambiguity problems were observed due to a slight increase in WQI score (WQI

750 ≈ 30), indicating the inherent limitations of the WQI framework. The outcome aligns with previous
 751 research (Faruq et al., 2025; Gani et al., 2023; Sajib et al., 2023; Uddin et al., 2024a). In summary,
 752 the results of ambiguity and eclipsing indicate that the RMS-WQI framework suitable for
 753 assessment of tidal rivers by addressing eclipsing and ambiguity problems.

754 Table 4. Results of ambiguity and eclipsing assessment

Year	Eclipsing		Ambiguity	
	Number of sites ($N = 8$)	Percent (%)	Number of sites ($N = 8$)	Percent (%)
2021	0	0	2	25
2022	3	37.5	4	50
2023	6	75	5	62.5
2024	1	12.5	1	12.5

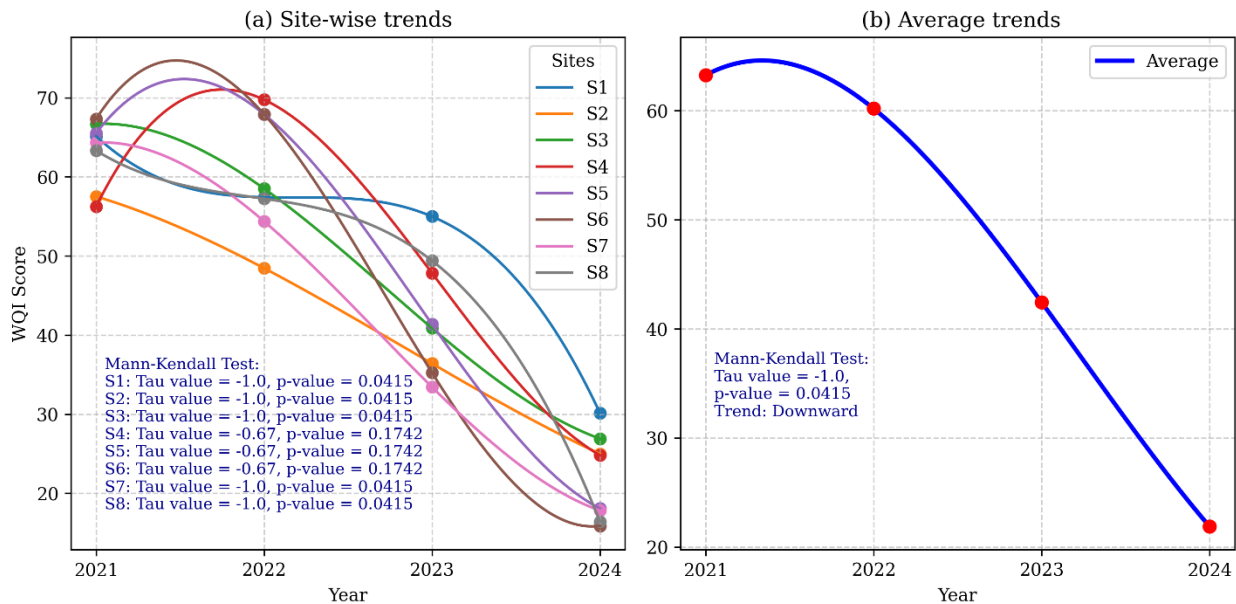
755

756 3.6 Assessment of water quality in the Bhairab River

757 3.6.1 Result of trend analysis

758 In order to assess the temporal variability and trend assessment of WQ in the Bhairab River during
 759 the study period, the current research utilized the Friedman test and the Mann-Kendall test. Fig.
 760 14 shows the decreasing trend of WQI scores across monitoring sites between 2021-2024.
 761 Temporal variability was observed in WQI scores during the study period (2021-2024) with the
 762 Friedman test statistic of 21.75 and a p-value of 7.35×10^{-5} ($p < 0.05$). The results of this test
 763 suggest that there is a significant difference in the overall WQ between 2021 to 2024. This data
 764 supports the alternative hypothesis and indicates that the river was unable to maintain a consistent
 765 WQ status during the study period. In addition, the results are validated by the downward trend of
 766 WQI scores, where the average WQI score decreased from 65 to 22 between 2021 to 2024,
 767 respectively (Fig. 5). The similar downward trend results of WQ across the study area have been
 768 reported in literature (Ali et al., 2022; Hasan et al., 2019; Islam et al., 2018; Khan et al., 2019).

769 Also, the Mann-Kendall trend result showed a statistically perfect monotonic decrease trend with
 770 a Tau value = -1.0 and a p-value < 0.05 for sites S1, S2, S3, S7, and S8 (Fig. 14a). On the contrary,
 771 the sites S4, S5, and S6 have a decreasing trend in terms of the Kendall Tau value (-0.67), but the
 772 trend is not statistically significant (p-value > 0.05). On the other hand, a strong, perfect, and
 773 significant decreasing trend (Tau value = -1.0, p < 0.05) was observed in yearly average WQI
 774 scores in the Bhairab River during 2021-2024 (Fig. 14b). However, the results of the trend analysis
 775 revealed that the Bhairab River WQ deteriorated gradually over the years due to the loading of
 776 higher anthropogenic stressors (see Fig. 16).



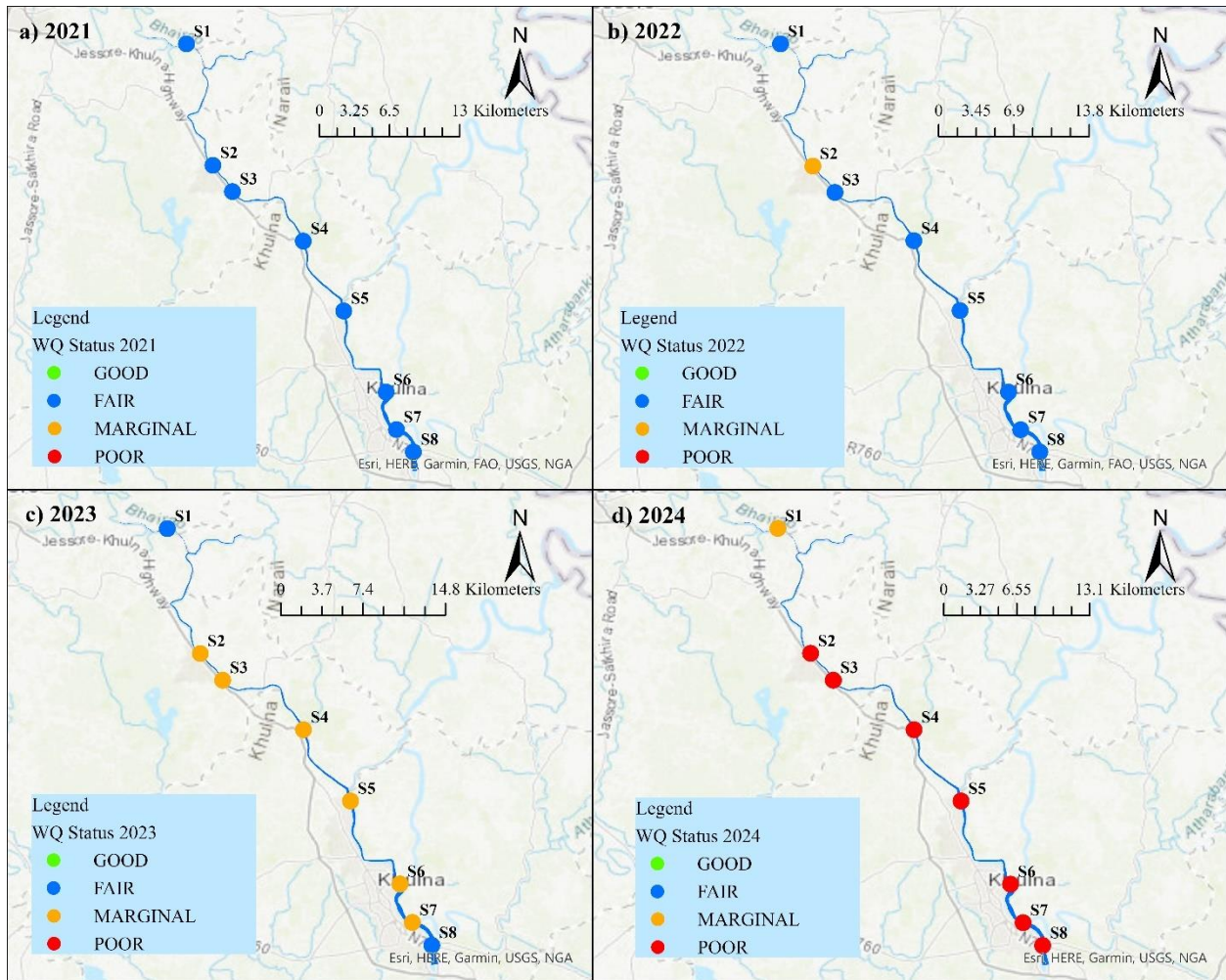
777
 778 Fig. 14. Trend of WQ (using WQI scores) in the Bhairab River from 2021 to 2024.

779 3.6.2 Water quality status in the Bhairab River over the years

780 The research utilized the RMS-WQI model to assess the WQ status of the Bhairab River across
 781 eight monitoring sites from 2021 to 2024. Fig. 15 shows the spatio-temporal distribution of WQ
 782 status at different monitoring sites in the Bhairab River. It can be seen from the figure that the WQ
 783 status at all monitoring sites remained relatively stable for 2021 and 2022 except for the S2 site,
 784 whereas most monitoring sites presented a ‘fair’ WQ rating (Fig. 15 a,b). However, a decreasing

785 trend was observed between 2023-2024, as most of the monitoring sites presented ‘marginal’ to
786 ‘poor’ WQ ratings, indicating notable deterioration of WQ in the Bhairab River (Fig. 15 c,d). The
787 worst scenario was observed in 2024, as most of the monitoring sites (> 87.5% of monitoring sites)
788 showed a ‘poor’ WQ rating in the study area. Furthermore, the rating for 2023-2024 collectively
789 indicates that most of the WQ indicators in these years breached the standards recommended by
790 ECR (2023) and WHO (2022). According to Table 2, ‘marginal’ and ‘poor’ rated WQ is unsuitable
791 for any type of use and poses a notable threat to aquatic life. These findings are consistent with
792 earlier studies on the Bhairab River, which also reported a steady decline in WQ due to increasing
793 domestic, industrial, and urban discharges (Bari et al., 2025; Hashan et al., 2023; Rafizul et al.,
794 2017; Uddin, 2015). The convergence of results reinforces the evidence that the Bhairab River is
795 under severe anthropogenic pressure.

796 The findings of the current research indicate that there may be weak implementation of laws and
797 regulations in the Bhairab River WQ management. To achieve Sustainable Development Goals
798 (SDG) 6, the Bhairab and other rivers in Bangladesh require an integrated river monitoring and
799 management system, along with strict implementation of the Bangladesh Environment
800 Conservation Act (1995) and the Environmental Conservation Rules (ECR, 2023). This combined
801 approach could safeguard the Bhairab River ecosystem and its living organisms. The research
802 supports some of the key targets of SDG-6, including target 6.3 (reducing pollution and untreated
803 wastewater for improving WQ), target 6.5 (holistic water resources management for all types of
804 waters), target 6.6 (protection of water-related ecosystems), and target 6.8 (capacity building in
805 water monitoring and management through local engagement) (SDG, 2015).



806

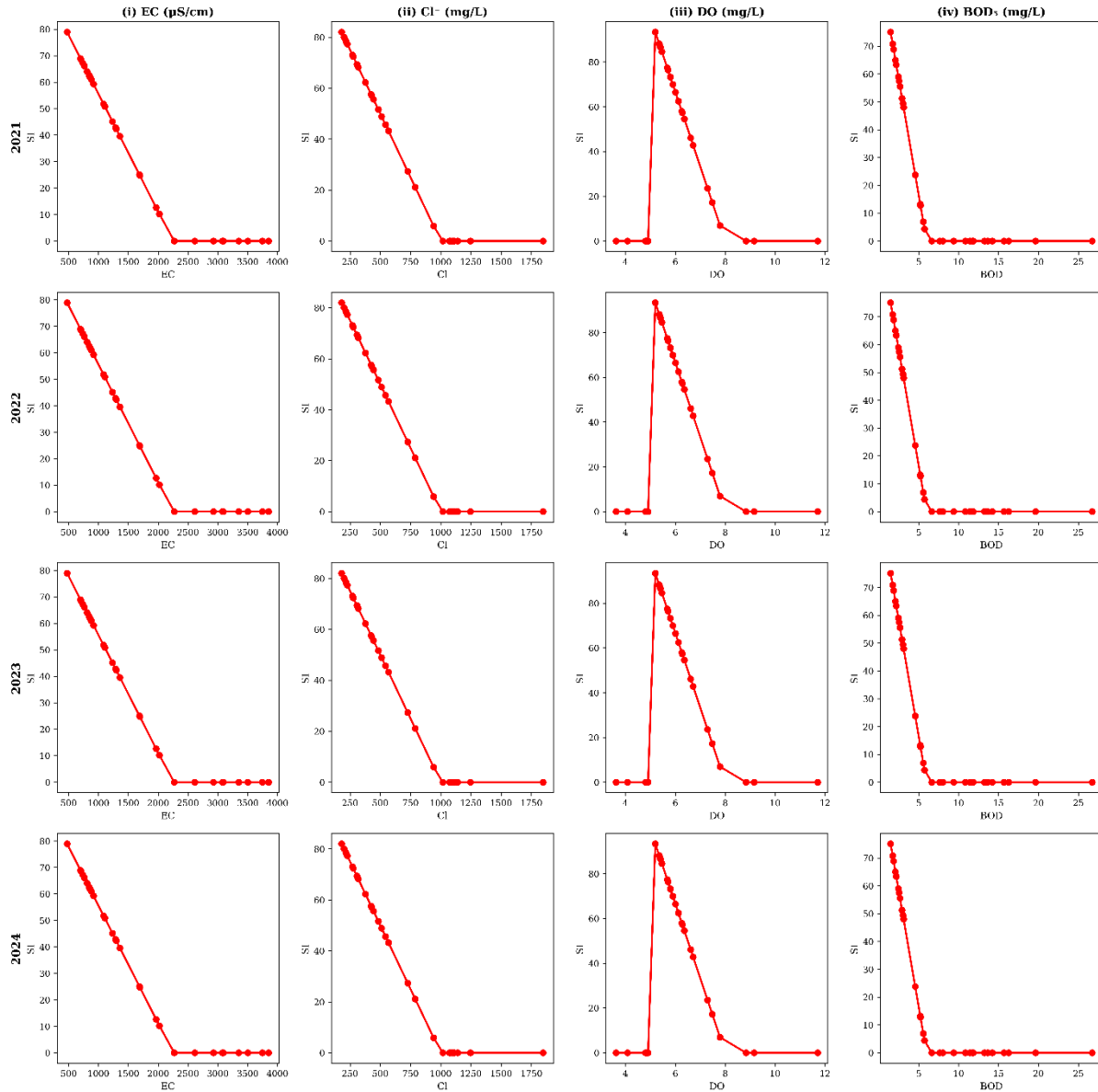
807 Fig. 15. Status of WQI in the Bhairab River. Here, (a), (b), (c), and (d) show the individual ratings (e.g., good to poor)
 808 of WQI scores at each monitoring site for 2021, 2022, 2023, and 2024, respectively.

809 **3.6.3 Response results to tidal events of the RMS-WQI framework**

810 Across all years (2021–2024), based on the tidal influences in tidal dominated domains, the
 811 research identified four WQ indicators which are highly affected by the tidal attributes in Bhairab
 812 river. Based on the tidal pressures, the analyzed indicators can be addressed into two associations
 813 (i) physical tidal forcing indicators EC and Cl⁻ these are crucial factors as the dominant physical
 814 drivers (Cereja et al., 2021; Feng et al., 2025; Skibbe et al., 2024), reflecting the magnitude of
 815 salinity intrusion associated with tidal exchange; and (ii) biogeochemical response DO and BOD₅
 816 these can be able to capture the ecological response linked to oxygen depletion and organic loading

817 (Kar et al., 2022; Zhang et al., 2025). As a response to the tidal events of these WQ indicators, Fig.
818 16 shows the SI response/sensitivity and Fig. 17 presents the association between measured
819 indicators concentration (raw) and SI with computed RMS-WQI scores, respectively.

820 It can be seen from Fig. 16 clearly how each WQ indicator propagates through the RMS-WQI
821 framework. Considering physical tidal forcing indicators EC and Cl^- , increasing salinity produces
822 a monotonic decline in SI, followed by consistent lower RMS-WQI scores. This result reveals that
823 the SI functions could be effective to address the impact of short-term salinity variation due to the
824 tidal effects instead of smoothing them out. Contrary, as biogeochemical response DO, a
825 considerable threshold response is observed (Fig. 16(iii)); whereas the SI remains high under well-
826 oxygenated conditions but drops sharply once hypoxic thresholds are crossed (Uddin et al., 2021;
827 Uddin et al., 2022b), and this consequence also reveals that the RMS-WQI framework could be
828 more effective to assess the tidal dominated waterbodies. Similarly, elevated BOD_5 shows a similar
829 attribute, with rapid SI deterioration propagating into reduced RMS-WQI values over the four
830 years indicating higher organic loading in the river (Anzum et al., 2023; Bari et al., 2025; Khan et
831 al., 2019).



832

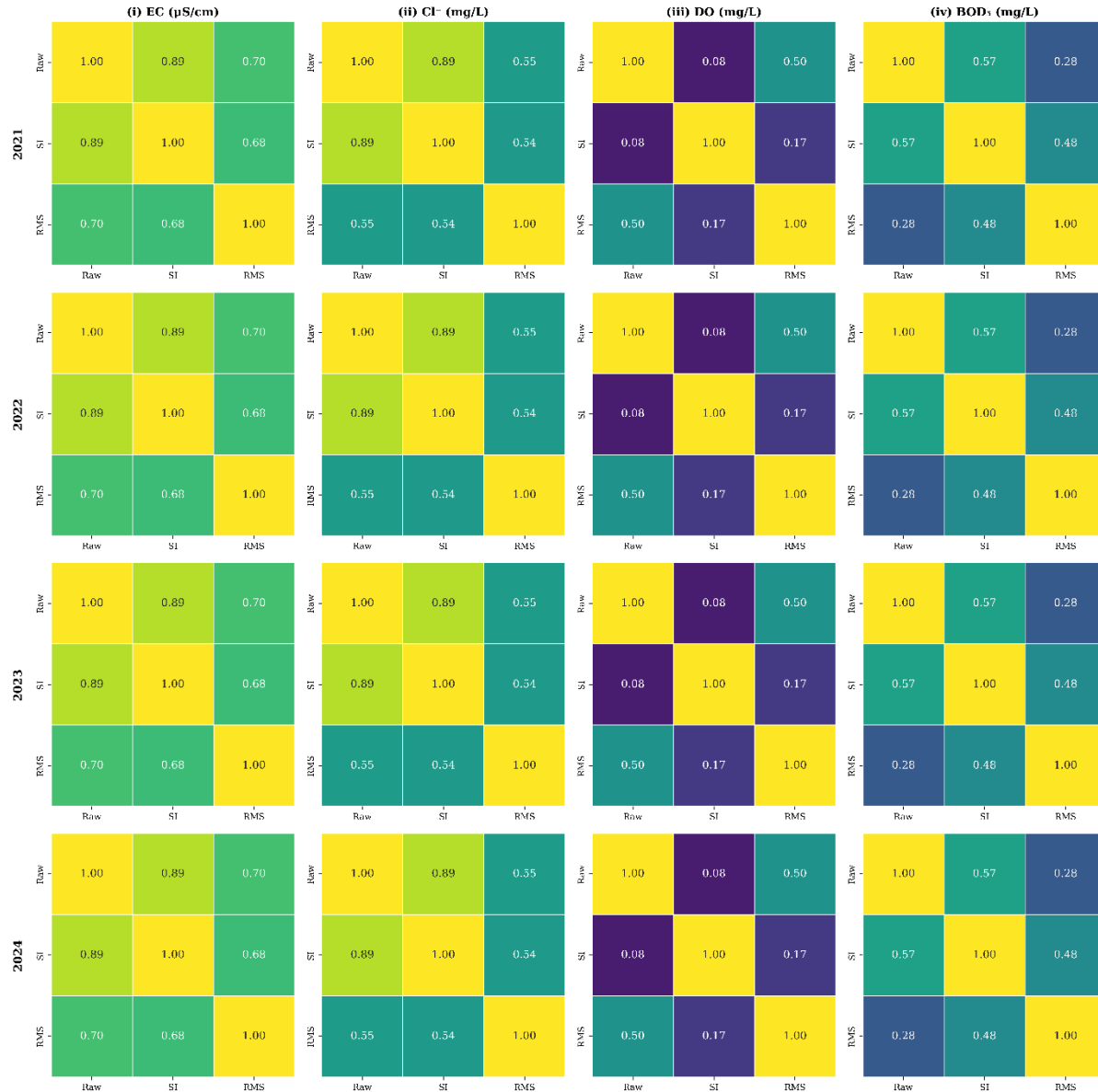
833 Fig. 16. Response the SI functions to the tidal dominated WQ indicators.

834 In addition, the Fig. 17 clearly demonstrate that the EC and Cl⁻ exhibit the strongest and most
 835 stable associations along the Raw (each indicators field measured values)–SI–RMS–WQI scores,
 836 confirming the salinity variability as the primary control on RMS–WQI framework behavior in this
 837 tidal ecosystem. Although, DO and BOD₅ show moderate but highly sensitive, indicating that
 838 biogeochemical stress could be influenced the RMS–WQI by the hydrodynamics factors like
 839 regular or irregular tidal events.

840 The results of the sensitivity (R^2 heatmap from Fig. 17) between tidal dominated WQ indicators
841 like EC, Cl^- , DO and BOD_5 highlight the RMS-WQI framework could be effective under the
842 highly non-stationary conditions. Relatively, the conventional WQI approaches based on linear
843 averaging, the advanced RMS-WQI using a quadratic aggregation that amplifies degraded sub-
844 indices, thereby avoiding the masking of episodic stress events. It can be seen from the Raw-SI-
845 RMS relationships in Fig. 17, the RMS-WQI framework could be enhanced detection of short-lived
846 extremes, reduced eclipsing of key stressors by stable indicators like temperature, pH, these
847 indicate the structural robustness of the model under strong temporal variability over the years.

848 However, the results of the tidal dominated indicators reveal that the RMS-WQI framework could
849 be effective to address various stressors due to the regular or irregular tidal attributes in any tidal
850 dominated domains at any geospatial resolution across the globe.

851



852

853 Fig. 17. Sensitivity of the various WQ indicators and their behavior within the RMS-WQI framework under the tidal
 854 events in the Bhairab river.

855 **3.7 Pollution hotspot analysis**

856 To identify the pollution hotspots in the Bhairab River, the study conducted a field visit around the

857 WQ monitoring sites. Fig. 18 presents the major pollution sources in the study area. It can be seen

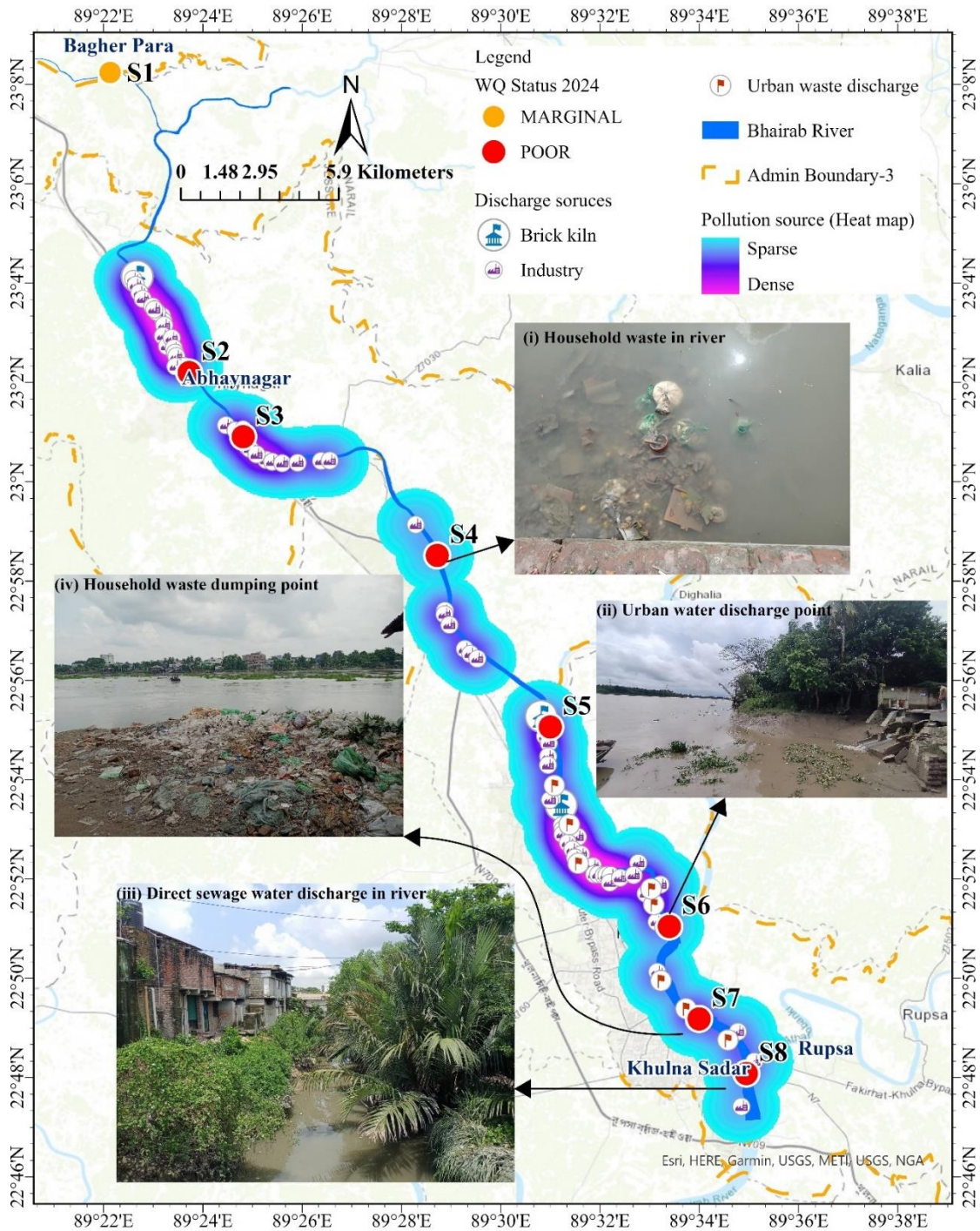
858 from Fig. 18 that the main sources of pollutants in the Bhairab River are various types of industries

859 (such as cable, fertilizer, flour, jute, oil, plastic, rice, salt, ship construction, tannery and leather,

860 and textiles), along with brick kilns and urban waste dumping stations. Additionally, the region

861 was historically dominated by the jute industry (Haque et al., 2021; Islam & Alauddin, 2012;
862 Rahman et al., 2025b), currently with 19 jute mills along the banks (Fig. 1). Based on the field
863 visit, it is also revealed that a range of various industries, such as cement, leather, textile, and power
864 plants, are being built along the river catchment area and could be expected to grow in the near
865 future. These pollution sources can release various types of pollutants, such as particulate matter,
866 sulfur dioxide, heavy metals, etc. (Ayilara & Babalola, 2023; Bărbulescu & Hosen, 2025; Raj &
867 Das, 2023; Sathya et al., 2022). On the other hand, the key driver behind this industrial growth is
868 the notable development of transportation networks, which is leading to an increase in new
869 industrial establishments (Islam et al., 2021). As a result, the river is at risk of receiving more
870 industrial waste from the factories. Subsequently, this industrial development accelerated internal
871 migration and urban development in this region (Alam et al., 2023). Additionally, the field survey
872 also revealed several domestic/market waste dumping sites and urban wastewater discharge into
873 the river at monitoring sites S4, S6, S7, and S8 (Fig. 18). These sources include plastics, domestic
874 organic/inorganic waste, and sewage, which might elevate the BOD₅ level and reduce the DO level
875 in the study area, as evident in the 2023 and 2024 datasets. Furthermore, urban wastewater could
876 introduce heavy metal pollution in water (Ali et al., 2022; Musa et al., 2025; Sarkar et al., 2016).
877 Apart from these pollution sources, frequent movement of oil- and coal-carrying ships, coal
878 dumping, ship manufacturing activities, etc., have been identified as the major sources of pollution
879 in this area. In summary, the water of the Bhairab river is under stress due to various points (e.g.,
880 industrial and urban waste discharge) and non-point (e.g., rainfall runoff from urban and
881 agricultural surface) pollution sources. These sources are not only deteriorating WQ (Bari et al.,
882 2025; Chowdhury et al., 2024; Hashan et al., 2023; Rafizul et al., 2017; Uddin, 2015) but also
883 exposing the water to more complex scenarios such as microplastic (Shakik et al., 2025) and heavy

884 metal pollution (Sarkar et al., 2016). Consequently, water becomes unsuitable for most domestic
 885 and human uses (Ali et al., 2022; Hasan et al., 2019; Musa et al., 2025). Overall, field observation
 886 visually validates the numerical results of the present study.



887
 888 Fig. 18. Sources of pollution in the Bhairab River

889 4. Summary and Conclusion

890 The research was carried out to investigate the spatio-temporal variation in WQ in the Bhairab
891 River from 2021 to 2024. The main objective of this research was to assess the WQ status by
892 leveraging the advanced RMS-WQI model incorporating the ML/AI algorithms, whereas the
893 research also addressed the major pollution sources across different monitoring sites in the Bhairab
894 River. The findings of the study are summarized as follows:

- 895 • Among the WQ indicators, TEMP, DO, and BOD₅ breached the standard guidelines at most
896 monitoring sites over the study period. It should be noted that TS and Cl⁻ concentrations
897 were found at risk levels (with a mean TS value of 1680.49 ± 191.04 mg/L and Cl⁻ value
898 of 1175.81 ± 266.16 mg/L in 2024, respectively). Although the DO and BOD₅
899 concentrations showed considerable variability, whereas DO exceed WHO standards at
900 63% of sites in 2022, and BOD₅ consistently breached the ECR (2023) guideline at 100%
901 and 75% of sites in 2024 and 2023, respectively.
- 902 • The RMS-WQI scores showed a significant (Friedman test statistics = 21.75, $p < 0.05$;
903 Kendall Tau value = -1.0, $p < 0.05$) and consistent decline in WQI scores at all monitoring
904 sites during the study period, with WQ status falling from the 'fair' category in 2021 to
905 'poor' status by 2024.
- 906 • The ANN-Optuna model showed excellent performance with minimal errors in predicting
907 WQI scores compared to the other seven ML/AI models utilized in this study. However,
908 some overfitting and underfitting issues were observed in 2024. Despite these issues, the
909 ANN-Optuna model demonstrated strong accuracy and reliability in predicting WQI
910 scores.

- 911 • The model efficiency (NSE, MEF, and PREI) results indicate that the model is reliable for
912 predicting WQI scores. However, certain monitoring sites such as S1, S3, and S7 showed
913 discrepancies that require further investigation.
- 914 • The outcome of the model’s sensitivity and uncertainty indicated that the ANN-Optuna
915 model was highly sensitive in capturing WQI variability ($R^2 \geq 0.9$) with low uncertainty
916 across all the years.
- 917 • Different types of industries, brick kilns, and urban waste disposal sites have been
918 identified as the major pollution sources in the study area.

919 The study has identified that the WQ of the Bhairab River has consistently declined in the last few
920 years, posing a notable threat to the Bhairab River ecosystem. One of the key findings that emerged
921 from this research is that poor management of industrial discharge and urban waste are the primary
922 sources of increased pollution levels in the study area. As a result, the local government needs to
923 impose strict pollution control measures, including sustainable WQ management strategies, to
924 reduce the impact of pollution around the river. Although this study provides valuable insights into
925 the WQ status of the study area, it has some limitations. For instance, the study did not consider
926 other aspects, such as seasonal variation and tidal effects on WQ in the study area. Additionally,
927 while investigating pollution sources, riverside land use plays a pivotal role in altering WQ (Anh
928 et al., 2023; Faruq et al., 2025; Gani et al., 2023; Zhu et al., 2024). Therefore, future research
929 should incorporate seasonal variation in WQ, including full spatial coverage of the monitoring
930 sites, and it could receive potential attention to explore pollution pressures resulting from land
931 cover changes over the years. Additionally, future research should expand this adaptive framework
932 by incorporating remote sensing, climate change scenarios, and cross-basin applications to
933 enhance the resilience of tidal river ecosystems in South Asia. The findings of this study can be

934 useful for different stakeholders (e.g., local communities, government organizations,
935 policymakers, environmental agencies, non-governmental organizations, and researchers) for
936 developing integrated sustainable development plans, which include pollution control, aquatic
937 ecosystem restoration, and ensuring sustainable water resource management. In summary, the
938 research emphasizes the urgent need to develop comprehensive management practices and
939 pollution control strategies for the Bhairab River. The findings of this study also provide a robust
940 framework for evaluating the WQ status of tidal rivers using the RMS-WQI model and ML/AI
941 techniques.

942 **Acknowledgement**

943 We sincerely acknowledge Department of Environment of Bangladesh for the data. The authors
944 gratefully acknowledge the editor's and anonymous reviewers' contributions to the improvement
945 of this paper. Additionally, the authors extend their gratitude to the Eco-HydroInformatics
946 Research Group (EHIRG) at the School of Engineering, College of Science and Engineering,
947 University of Galway, Ireland, for providing computational laboratory facilities essential for
948 completing this research. The authors also acknowledge the University of Galway for providing
949 open-access funding

950 **References**

- 951 Abba, S.I., Pham, Q.B., Saini, G., Linh, N.T.T., Ahmed, A.N., Mohajane, M., Khaledian, M., Abdulkadir, R.A.,
952 Bach, Q.-V., 2020. Implementation of data intelligence models coupled with ensemble machine learning for
953 prediction of water quality index. *Environ. Sci. Pollut. Res.* 27, 41524–41539.
954 <https://doi.org/10.1007/s11356-020-09689-x>
- 955 Abbaszadeh, M., Soltani-Mohammadi, S., Ahmed, A.N., 2022. Optimization of support vector machine parameters
956 in modeling of Iju deposit mineralization and alteration zones using particle swarm optimization algorithm
957 and grid search method. *Comput. Geosci.* 165, 105140. <https://doi.org/10.1016/j.cageo.2022.105140>
- 958 Abed, I.F., Nashaat, M.R., Mirza, N.N., 2022. Evaluation of the effects of Tigris River water quality on the rotifers
959 community in northern Baghdad by using the Canadian Water Quality Index (CCME-WQI). *Iraqi J. Sci.* 63,
960 480–490. <https://doi.org/10.24996/ijs.2022.63.2.6>
- 961 Ahmed, A.A., Sayed, S., Abdoulhalik, A., Moutari, S., Oyedele, L., 2024. Applications of machine learning to water
962 resources management: a review of present status and future opportunities. *J. Clean. Prod.* 441, 140715.
963 <https://doi.org/10.1016/j.jclepro.2024.140715>

- 964 Ahmed, A.N., Othman, F.B., Afan, H.A., Ibrahim, R.K., Fai, C.M., Hossain, M.S., Elshafie, A., 2019. Machine
 965 learning methods for better water quality prediction. *J. Hydrol.* 578, 124084.
 966 <https://doi.org/10.1016/j.jhydrol.2019.124084>
- 967 Alam, I., Nahar, K., Morshed, M.M., 2023. Measuring urban expansion pattern using spatial matrices in Khulna
 968 City, Bangladesh. *Heliyon* 9, e13193. <https://doi.org/10.1016/j.heliyon.2023.e13193>
- 969 Ali, M.M., Rahman, S., Islam, M.S., Rakib, M.R.J., Hossen, S., Rahman, M.Z., Kormoker, T., Idris, A.M.,
 970 Phoungthong, K., 2022. Distribution of heavy metals in water and sediment of an urban river in a developing
 971 country: a probabilistic risk assessment. *Int. J. Sediment Res.* 37, 173–187.
 972 <https://doi.org/10.1016/j.ijsrc.2021.09.002>
- 973 Ali, M.S., Begum, S., Rabbi, F.M., Sumaia, Hasan, Md.K., Rahman, Md.A., Rahman, M.M., Rahaman, Md.H.,
 974 2024. Multivariate analysis of water quality in the Dhaleshwari River, Bangladesh: identifying pollution
 975 sources and environmental implications. *Water Pract. Technol.* 19, 4128–4147.
 976 <https://doi.org/10.2166/wpt.2024.251>
- 977 Alom, M.S., Yelmai, S.W., Noyon, M.A.R., Ahmed, M.T., 2022. Effects of industrial effluents on the water quality
 978 of Bhairab River. In: *Proceedings of the International Conference on Mechanical, Industrial and Energy
 979 Engineering 2022*, Khulna University of Engineering & Technology, Khulna, Bangladesh
- 980 Althubiti, S., Kumar, M., Goswami, P., Kumar, K., 2023. Artificial neural network for solving the nonlinear singular
 981 fractional differential equations. *Appl. Math. Sci. Eng.* 31. <https://doi.org/10.1080/27690911.2023.2187389>
- 982 Ameta, S.K., Kamaal, M., Ahamad, F., 2023. Impact of domestic and industrial effluent disposal on physicochemical
 983 characteristics of River Malin at Najibabad City, India. *AgroEnviron. Sustain.* 1, 246–256.
 984 <https://doi.org/10.59983/s2023010306>
- 985 Anh, N.T., Can, L.D., Nhan, N.T., Schmalz, B., Luu, T.L., 2023. Influences of key factors on river water quality in
 986 urban and rural areas: a review. *Case Stud. Chem. Environ. Eng.* 8, 100424.
 987 <https://doi.org/10.1016/j.cscee.2023.100424>
- 988 Anzum, H.M.N., Shaibur, M.R., Nahar, N., Akber, A., Hossain, M.S., Mamun, S.A., 2023. Changing dynamics of
 989 river ecosystem from aquatic to terrestrial: a case of Bhairab River, Jashore, Bangladesh. *Watershed Ecol.
 990 Environ.* 5, 134–142. <https://doi.org/10.1016/j.wsee.2023.05.001>
- 991 APHA (American Public Health Association), 2005. In: Rice, E.W., Baird, R.B., Eaton, A. D., Clesceri, L.S. (Eds.),
 992 *Standard Methods for the Examination of Water and Wastewater*, 20th edn. American Public Health
 993 Association, American Water Works Association, Water Pollution Control Federation, Washington, DC.
- 994 Ayilara, M.S., Babalola, O.O., 2023. Bioremediation of environmental wastes: the role of microorganisms. *Front.
 995 Agron.* 5, 1183691. <https://doi.org/10.3389/fagro.2023.1183691>
- 996 Azad, K.N., Hasan, N., Azad, K.N., 2020. Causes for drying up of Bhairab River in Bangladesh. *J. Fish. Livest. Vet.
 997 Sci.* 1, 18–27. <https://doi.org/10.18801/jflvs.010120.03>
- 998 Azha, S.F., Sidek, L.M., Ahmad, Z., Zhang, J., Basri, H., Zawawi, M.H., Noh, N.M., Ahmed, A.N., 2023. Enhancing
 999 river health monitoring: developing a reliable predictive model and mitigation plan. *Ecol. Indic.* 156, 111190.
 1000 <https://doi.org/10.1016/j.ecolind.2023.111190>
- 1001 Bărbulescu, A., Hosen, K., 2025. Cement industry pollution and its impact on the environment and population
 1002 health: a review. *Toxics* 13, 587. <https://doi.org/10.3390/toxics13070587>

- 1003 Bari, Q.H., Shafiquzzaman, M., Haider, H., 2025. Analyzing water quality dynamics using multivariate analysis for
1004 a tidal river in Bangladesh. *Adv. Civ. Eng.* 2025, 8733617. <https://doi.org/10.1155/adce/8733617>
- 1005 Bari, Q.H., Sayeed, Q.S., 2022. Monthly fluctuation of water quality parameters in an estuarine river: a study on
1006 River Bhairab in Khulna. In: *Proceedings of the 3rd International Conference on Water and Environmental
1007 Engineering (iCWEE2022)*.
- 1008 Bilal, H., Li, X., Iqbal, M.S., Mu, Y., Tulcan, R.X.S., Ghufuran, M.A., 2023. Surface water quality, public health, and
1009 ecological risks in Bangladesh—a systematic review and meta-analysis over the last two decades. *Environ.
1010 Sci. Pollut. Res.* 30, 91710–91728. <https://doi.org/10.1007/s11356-023-28879-x>
- 1011 Bilali, A.E., Taleb, A., Brouziyne, Y., 2020. Groundwater quality forecasting using machine learning algorithms for
1012 irrigation purposes. *Agric. Water Manag.* 245, 106625. <https://doi.org/10.1016/j.agwat.2020.106625>
- 1013 BIWTA (Bangladesh Inland Water Transport Authority), 2006. Bangladesh tide tables, tidal research and computer.
1014 Department of Hydrology. Ministry of Shipping. Government of the People’s Republic of Bangladesh.
- 1015 Bland, J.M., Altman, D., 1986. Statistical methods for assessing agreement between two methods of clinical
1016 measurement. *Lancet* 327, 307–310. [https://doi.org/10.1016/S0140-6736\(86\)90837-8](https://doi.org/10.1016/S0140-6736(86)90837-8)
- 1017 BMD (Bangladesh Meteorological Department), 2020. Ministry of Defense. Government of the People’s Republic
1018 of Bangladesh.
- 1019 Bui, D.T., Khosravi, K., Tiefenbacher, J., Nguyen, H., Kazakis, N., 2020. Improving prediction of water quality
1020 indices using novel hybrid machine-learning algorithms. *Sci. Total Environ.* 721, 137612.
1021 <https://doi.org/10.1016/j.scitotenv.2020.137612>
- 1022 Cereja, R., Brotas, V., Cruz, J.P.C., Rodrigues, M., Brito, A.C., 2021. Tidal and Physicochemical Effects on
1023 Phytoplankton Community Variability at Tagus Estuary (Portugal). *Front Mar Sci* 8.
1024 <https://doi.org/10.3389/fmars.2021.675699>
- 1025 Charilaou, P., Battat, R., 2022. Machine learning models and over-fitting considerations. *World J. Gastroenterol.* 28,
1026 605–607. <https://doi.org/10.3748/wjg.v28.i5.605>
- 1027 Chavoshani, A., Hashemi, M., Amin, M.M., Ameta, S.C., 2020. Pharmaceuticals as emerging micropollutants in
1028 aquatic environments, in: Chavoshani, A., Hashemi, M., Amin, M.M., Ameta, S.C. (Eds.), *Micropollutants
1029 and Challenges*. Elsevier, pp. 35–90. <https://doi.org/10.1016/b978-0-12-818612-1.00002-7>
- 1030 Chen, C., Hao, J., 2025. A water quality prediction model based on neural network at data-scarce sites. *Water-
1031 Energy Nexus*. <https://doi.org/10.1016/j.wen.2025.05.001>
- 1032 Chen, Y., Song, L., Liu, Y., Yang, L., Li, D., 2020. A review of the artificial neural network models for water quality
1033 prediction. *Appl. Sci.* 10, 5776. <https://doi.org/10.3390/app10175776>
- 1034 Chicco, D., Warrens, M.J., Jurman, G., 2021. The coefficient of determination R-squared is more informative than
1035 SMAPE, MAE, MAPE, MSE and RMSE in regression analysis evaluation. *PeerJ Comput. Sci.* 7, e623.
1036 <https://doi.org/10.7717/peerj-cs.623>
- 1037 Chidiac, S., Najjar, P.E., Ouaini, N., Rayess, Y.E., Azzi, D.E., 2023. A comprehensive review of water quality
1038 indices (WQIs): history, models, attempts and perspectives. *Rev. Environ. Sci. Bio/Technol.* 22, 349–395.
1039 <https://doi.org/10.1007/s11157-023-09650-7>

- 1040 Chowdhury, G.W., Koldewey, H.J., Duncan, E., Napper, I.E., Niloy, M.N.H., Nelms, S.E., Sarker, S., Bhola, S.,
 1041 Nishat, B., 2020. Plastic pollution in aquatic systems in Bangladesh: a review of current knowledge. *Sci.*
 1042 *Total Environ.* 761, 143285. <https://doi.org/10.1016/j.scitotenv.2020.143285>
- 1043 Chowdhury, M.D.A., Billah, T., Rahman, M.R., Bakri, M.K.B., Barua, S., Morshed, A.J.M., Uddin, M.M., 2024.
 1044 Evaluation of water quality indexes and heavy metal pollution indexes of different industrial effluents and
 1045 Karnaphuli River Water in Chattogram, Bangladesh. *Environ. Qual. Manag.* 34, e22290.
 1046 <https://doi.org/10.1002/tqem.22290>
- 1047 Cleophas, T.J., Zwinderman, A.H., 2016. Non-parametric tests for three or more samples (Friedman and Kruskal-
 1048 Wallis), in: Cleophas, T.J., Zwinderman, A.H. (Eds.), *Clinical Data Analysis on a Pocket Calculator*. Springer,
 1049 pp. 193–197. https://doi.org/10.1007/978-3-319-27104-0_34
- 1050 Coccia, M., Roshani, S., 2024. Evolution of topics and trends in emerging research fields: multiple analyses with
 1051 entity linking, Mann–Kendall test and burst methods in cloud computing. *Scientometrics* 129, 5347–5371.
 1052 <https://doi.org/10.1007/s11192-024-05139-4>
- 1053 Cumming, G., Fidler, F., Vaux, D.L., 2007. Error bars in experimental biology. *J. Cell Biol.* 177, 7–11.
 1054 <https://doi.org/10.1083/jcb.200611141>
- 1055 Dada, B.A., Nwulu, N.I., Olukanmi, S.O., 2025. Bayesian optimization with Optuna for enhanced soil nutrient
 1056 prediction: a comparative study with genetic algorithm and particle swarm optimization. *Smart Agric.*
 1057 *Technol.* 101136. <https://doi.org/10.1016/j.atech.2025.101136>
- 1058 Deng, T., Duan, H.F., Keramat, A., 2022. Spatiotemporal characterization and forecasting of coastal water quality in
 1059 the semi-enclosed Tolo Harbour based on machine learning and EKC analysis. *Eng. Appl. Comput. Fluid*
 1060 *Mech.* 16, 694–712. <https://doi.org/10.1080/19942060.2022.2035257>
- 1061 Diganta, M.T.M., Sajib, A.M., Hasan, M.A., Saifullah, A.S.M., Ashekuzzaman, S.M., Moniruzzaman, M., Yunhui
 1062 Zhang, Y., Rahman, A., Olbert, A.I., Uddin, M.G., 2025. A methodological framework for assessing aquatic
 1063 contamination using data science approaches. (Submitted to publication).
- 1064 Ding, F., Zhang, W., Cao, S., Hao, S., Chen, L., Xie, X., Li, W., Jiang, M., 2023. Optimization of water quality index
 1065 models using machine learning approaches. *Water Res.* 243, 120337.
 1066 <https://doi.org/10.1016/j.watres.2023.120337>
- 1067 DoE (Department of Environment), 2021. Surface and ground water quality report 2021. Department of
 1068 Environment, Ministry of Environment, Forest & Climate Change, Government of the People’s Republic of
 1069 Bangladesh.
- 1070 DoE (Department of Environment), 2022. Surface and ground water quality report 2022. Department of
 1071 Environment, Ministry of Environment, Forest & Climate Change, Government of the People’s Republic of
 1072 Bangladesh.
- 1073 DoE (Department of Environment), 2023. Surface and ground water quality report 2023. Department of
 1074 Environment, Ministry of Environment, Forest & Climate Change, Government of the People’s Republic of
 1075 Bangladesh.
- 1076 Doğan, N.Ö., 2018. Bland-Altman analysis: a paradigm to understand correlation and agreement. *Turk. J. Emerg.*
 1077 *Med.* 18, 139–141. <https://doi.org/10.1016/j.tjem.2018.09.001>
- 1078 ECR (Environmental Conservation Rules), 2023. Department of Environment. Ministry of Environment and Forest.
 1079 Government of the People’s Republic of Bangladesh.

- 1080 Essamlali, I., Nhaila, H., Khaili, M.E., 2024. Advances in machine learning and IoT for water quality monitoring: a
1081 comprehensive review. *Heliyon* 10, e27920. <https://doi.org/10.1016/j.heliyon.2024.e27920>
- 1082 Fakron, M., 2023. Surface water pollution & restoration. *SSRN Electron. J.* <https://doi.org/10.2139/ssrn.4444153>
- 1083 Fan, J., Li, M., Guo, F., Yan, Z., Zheng, X., Zhang, Y., Xu, Z., Wu, F., 2018. Priorization of river restoration by
1084 coupling soil and water assessment tool (SWAT) and support vector machine (SVM) models in the Taizi
1085 River basin, northern China. *Int. J. Environ. Res. Public Health* 15, 2090.
1086 <https://doi.org/10.3390/ijerph15102090>
- 1087 Fang, P., Wang, Y., Zhao, Y., Kang, J., 2025. Analysis of prediction confidence in water quality forecasting
1088 employing LSTM. *Water* 17, 1050. <https://doi.org/10.3390/w17071050>
- 1089 Faruq, O., Malak, M.A., Hossain, N.J., Sami, M.S., Sajib, A.M., 2025. Investigating the relationship between land
1090 use and water quality in urban waterbodies. *Clean. Water* 100070.
1091 <https://doi.org/10.1016/j.clwat.2025.100070>
- 1092 Feng, G., Liu, J., Wang, N., Xia, L., Fan, J., Mu, Q., Sun, Y., He, P., Zhang, J., 2025. Synergistic effects of nutrient
1093 competition, biotic interactions, and hydrological regulation drive green tide outbreaks in the South Yellow
1094 Sea. *Harmful Algae* 149, 102943. <https://doi.org/10.1016/j.hal.2025.102943>
- 1095 Fiaz, A., Rahman, G., Kwon, H.H., 2025. Impacts of climate change on the south asian monsoon: a comprehensive
1096 review of its variability and future projections. *J. Hydro-environ. Res.* 59, 100654.
1097 <https://doi.org/10.1016/j.jher.2025.100654>
- 1098 Fiorentini, N., Pellegrini, D., Losa, M., 2022. Overfitting prevention in accident prediction models: Bayesian
1099 regularization of artificial neural networks. *Transp. Res. Rec.* 2677, 1455–1470.
1100 <https://doi.org/10.1177/03611981221111367>
- 1101 Fortune, J., Butler, E.C., Gibb, K., 2023. Estuarine benthic habitats provide an important ecosystem service
1102 regulating the nitrogen cycle. *Mar. Environ. Res.* 190, 106121.
1103 <https://doi.org/10.1016/j.marenvres.2023.106121>
- 1104 Frazier, P.I., 2018. A tutorial on Bayesian optimization. *arXiv (Cornell University)*.
1105 <https://doi.org/10.48550/arxiv.1807.02811>
- 1106 Friedman, M., 1937. The use of ranks to avoid the assumption of normality implicit in the analysis of variance. *J.*
1107 *Am. Stat. Assoc.* 32, 675–701. <https://doi.org/10.1080/01621459.1937.10503522>
- 1108 Frincu, R.M., 2024. Artificial intelligence in water quality monitoring: a review of water quality assessment
1109 applications. *Water Qual. Res. J.* <https://doi.org/10.2166/wqrj.2024.049>
- 1110 Gani, M.A., Sajib, A.M., Siddik, M.A., Moniruzzaman, N.M., 2023. Assessing the impact of land use and land cover
1111 on river water quality using water quality index and remote sensing techniques. *Environ. Monit. Assess.* 195.
1112 <https://doi.org/10.1007/s10661-023-10989-1>
- 1113 Gedamu, G., Mitiku, K.W., Belay, M.A., Simegn, M.B., Chanie, S.D., Tilahun, W.M., Menber, Y., Wasihun, Y.,
1114 Gebreegziabher, Z.A., Anduale, Z., Alemu, A.T., Geddif, A., 2025. Barriers to the sustainability of rural water
1115 schemes in Sub-Saharan African countries: a systematic review. *J. Water Sanit. Hyg. Dev.*
1116 <https://doi.org/10.2166/washdev.2025.101>
- 1117 Goodarzi, M.R., Niknam, A.R.R., Barzkar, A., Niazkar, M., Zare Mehrjerdi, Y., Abedi, M.J., Heydari Pour, M.,
1118 2023. Water quality index estimations using machine learning algorithms: a case study of Yazd-Ardakan
1119 plain, Iran. *Water (Switzerland)* 15. <https://doi.org/10.3390/w15101876>

- 1120 Gupta, S., Gupta, S.K., 2021. A critical review on water quality index tool: genesis, evolution and future directions.
1121 Ecol. Inform. 63, 101299. <https://doi.org/10.1016/j.ecoinf.2021.101299>
- 1122 Handoyo, S., 2024. Public governance and national environmental performance nexus: evidence from cross-country
1123 studies. Heliyon 10, e40637. <https://doi.org/10.1016/j.heliyon.2024.e40637>
- 1124 Haque, M.N., Sresto, M.A., Siddika, S., 2021. Suitable locations for industrial setup in urban context: way forward
1125 to meet the SDGs for Khulna City, Bangladesh. Int. J. Built Environ. Sustain. 8, 89–102.
1126 <https://doi.org/10.11113/ijbes.v8.n2.679>
- 1127 Hasan, M.F., Nur-E-Alam, M., Salam, M.A., Rahman, H., Paul, S.C., Rak, A.E., Ambade, B., Islam, A.R.M.T.,
1128 2021. Health risk and water quality assessment of surface water in an urban river of Bangladesh.
1129 Sustainability 13, 6832. <https://doi.org/10.3390/su13126832>
- 1130 Hasan, M.K., Shahriar, A., Jim, K.U., 2019. Water pollution in Bangladesh and its impact on public health. Heliyon
1131 5, e02145. <https://doi.org/10.1016/j.heliyon.2019.e02145>
- 1132 Hashan, M.M., 2023. A comprehensive assessment of water quality and mass balance of the Bhairab River, Khulna.
1133 Int. J. Res. Appl. Sci. Eng. Technol. 11, 2254–2269. <https://doi.org/10.22214/ijraset.2023.57816>
- 1134 Hassan, H.B., Moniruzzaman, M., Majumder, R.K., Ahmed, F., Bhuiyan, M.A.Q., Ahsan, M.A., Al-Asad, H., 2023.
1135 Impacts of seasonal variations and wastewater discharge on river quality and associated human health risks: a
1136 case of northwest Dhaka, Bangladesh. Heliyon 9. <https://doi.org/10.1016/j.heliyon.2023.e18171>
- 1137 Hoffman, J.I., 2015. Analysis of variance II. More complex forms, in: Hoffman, J.I. (Ed.), Biostatistics for Medical
1138 and Biomedical Practitioners. Elsevier, pp. 421–447. <https://doi.org/10.1016/b978-0-12-802387-7.00026-3>
- 1139 Hossain, M.N., Howladar, M.F., Siddique, M.A.B., 2024. A comprehensive evaluation of the contamination scenario
1140 and water quality in the gas fields of north-east region, Bangladesh. Heliyon 10.
1141 <https://doi.org/10.1016/j.heliyon.2024.e34323>
- 1142 Huang, S., Le, T., 2021. Neural networks, in: Huang, S., Le, T. (Eds.), Principles of Data Science for Engineers.
1143 Elsevier, pp. 27–55. <https://doi.org/10.1016/b978-0-323-90198-7.00006-9>
- 1144 Islam, A.R.M.T., Mamun, M.A., Hasan, M., Aktar, M.N., Uddin, M.N., Siddique, M.A.B., Chowdhury, M.H., Islam,
1145 M.S., Bari, A.B.M.M., Idris, A.M., Senapathi, V., 2024. Optimizing coastal groundwater quality predictions:
1146 a novel data mining framework with cross-validation, bootstrapping, and entropy analysis. J. Contam.
1147 Hydrol. 269, 104480. <https://doi.org/10.1016/j.jconhyd.2024.104480>
- 1148 Islam, M.D., Islam, K.S., Ahasan, R., Mia, M.R., Haque, M.E., 2021. A data-driven machine learning-based
1149 approach for urban land cover change modeling: a case of Khulna City Corporation area. Remote Sens. Appl.
1150 Soc. Environ. 24, 100634. <https://doi.org/10.1016/j.rsase.2021.100634>
- 1151 Islam, M.M., Abid, A.-A., Jyoti, L.T.Z., Siddikui, A., Sultana, N., 2024. Assessing the dynamics of climate change in
1152 Khulna city: a comprehensive analysis of temperature, rainfall, and humidity trends. Int. J. Sci. Eng. 1, 15–
1153 32. <https://doi.org/10.62304/ijse.v1i1.118>
- 1154 Islam, M.M., Azad, A.K., Ara, M.H., Rahman, M., Hassan, N., Swarnokar, S.C., Rabeya, I., 2016. Environmental
1155 study on a coastal river of Bangladesh with reference to irrigation water quality assessment: a case study on
1156 Shailmari River, Khulna. J. Geosci. Environ. Prot. 4, 41–64. <https://doi.org/10.4236/gep.2016.410003>
- 1157 Islam, M.S., Alauddin, M., 2012. World production of jute: a comparative analysis of Bangladesh. Int. J. Manag.
1158 Bus. Stud. 2, 014–022.

- 1159 Islam, M.S., Mohanta, S.C., Siddique, M.A.B., Abdullah-Al-Mamun, M., Hossain, N., Bithi, U.H., 2018. Physico-
 1160 chemical assessment of water quality parameters in Rupsha River of Khulna region, Bangladesh. *Int. J. Eng.*
 1161 *Sci.* 7, 57–62. <https://doi.org/10.9790/1813>
- 1162 Joseph, V.R., 2022. Optimal ratio for data splitting. *Stat. Anal. Data Min.* 15, 531–538.
 1163 <https://doi.org/10.1002/sam.11583>
- 1164 Kabir, A., Sraboni, H.J., Hasan, M.M., Sorker, R., 2021a. Eco-environmental assessment of the Turag River in the
 1165 megacity of Bangladesh. *Environ. Chall.* 6, 100423. <https://doi.org/10.1016/j.envc.2021.100423>
- 1166 Kabir, M.H., Tusher, T.R., Hossain, Md.S., Islam, Md.S., Shammi, R.S., Kormoker, T., Proshad, R., Islam, M.,
 1167 2021b. Evaluation of spatio-temporal variations in water quality and suitability of an ecologically critical
 1168 urban river employing water quality index and multivariate statistical approaches: a study on Shitalakhya
 1169 river, Bangladesh. *Hum. Ecol. Risk Assess. Int. J.* 27, 1388–1415.
 1170 <https://doi.org/10.1080/10807039.2020.1848415>
- 1171 Kamyab-Talesh, N.F., Mousavi, S., Khaledian, M., Yousefi-Falakdehi, O., Norouzi-Masir, M., 2019. Prediction of
 1172 water quality index by support vector machine: a case study in the Sefidrud Basin, Northern Iran. *Water*
 1173 *Resour.* 46, 112–116. <https://doi.org/10.1134/s0097807819010056>
- 1174 Kar, S., Ghosh, I., Chowdhury, P., Ghosh, A., Aitch, P., Bhandari, G., RoyChowdhury, A., 2022. A model-based
 1175 prediction and analysis of seasonal and tidal influence on pollutants distribution from city outfalls of river
 1176 Ganges in West Bengal, India and its mapping using GIS tool, *PLOS Water*.
 1177 <https://doi.org/10.1371/journal.pwat.0000008>
- 1178 Kariri, E., Louati, H., Louati, A., Masmoudi, F., 2023. Exploring the advancements and future research directions of
 1179 artificial neural networks: a text mining approach. *Appl. Sci.* 13, 3186. <https://doi.org/10.3390/app13053186>
- 1180 Karunasingha, D.S.K., 2022. Root mean square error or mean absolute error? Use their ratio as well. *Inf. Sci.* 585,
 1181 609–629. <https://doi.org/10.1016/j.ins.2021.11.036>
- 1182 Kato, S., Kansha, Y., 2024. Comprehensive review of industrial wastewater treatment techniques. *Environ. Sci.*
 1183 *Pollut. Res.* 31, 51064–51097. <https://doi.org/10.1007/s11356-024-34584-0>
- 1184 Keiser, D.A., Shapiro, J.S., 2018. Consequences of the Clean Water Act and the demand for water quality. *Q. J.*
 1185 *Econ.* 134, 349–396. <https://doi.org/10.1093/qje/qjy019>
- 1186 Khan, A.S., Hakim, A., Waliullah, N., Rahman, M., Mandal, B.H., Abdullah-Al-Mamun, N., Ahammed, F., 2019.
 1187 Seasonal water quality monitoring of the Bhairab River at Noapara industrial area in Bangladesh. *SN Appl.*
 1188 *Sci.* 1. <https://doi.org/10.1007/s42452-019-0583-4>
- 1189 Khan, I., Nizam, S., Bamal, A., Sajib, A.M., Diganta, M.T.M., Shaida, M.A., Ashekuzzaman, S., Nash, S., Olbert,
 1190 A.I., Uddin, M.G., 2025. Optimized intelligent learning for groundwater quality prediction in diverse aquifers
 1191 of arid and semi-arid regions of India. *Clean. Eng. Technol.* 26, 100984.
 1192 <https://doi.org/10.1016/j.clet.2025.100984>
- 1193 Khoi, D.N., Quan, N.T., Linh, D.Q., Nhi, P.T., Thuy, N.T., 2022. Using machine learning models for predicting the
 1194 water quality index in the La Buong River, Vietnam. *Water* 14. <https://doi.org/10.3390/w14101552>
- 1195 Kirschke, S., Avellán, T., Bärlund, I., Bogardi, J.J., Carvalho, L., Chapman, D., Dickens, C.W.S., Irvine, K., Lee, S.,
 1196 Mehner, T., Warner, S., 2020. Capacity challenges in water quality monitoring: understanding the role of
 1197 human development. *Environ. Monit. Assess.* 192. <https://doi.org/10.1007/s10661-020-8224-3>

- 1198 Kouadri, S., Elbeltagi, A., Islam, A.R.M.T., Kateb, S., 2021. Performance of machine learning methods in predicting
1199 water quality index based on irregular data set: application on Illizi region (Algerian southeast). *Appl. Water*
1200 *Sci.* 11. <https://doi.org/10.1007/s13201-021-01528-9>
- 1201 Kumar, D., Kumar, R., Sharma, M., Awasthi, A., Kumar, M., 2023. Global water quality indices: development,
1202 implications, and limitations. *Total Environ. Adv.* 9, 200095. <https://doi.org/10.1016/j.teadv.2023.200095>
- 1203 Lai, L., Lin, Y., Liu, Y., Lai, J., Yang, W., Hou, H., Pai, P., 2024. The use of machine learning models with Optuna in
1204 disease prediction. *Electronics* 13, 4775. <https://doi.org/10.3390/electronics13234775>
- 1205 Li, X., Song, Y., Gao, J., Zhang, B., Gui, L., Yuan, W., Li, Z., Han, S., 2023. Multi-objective optimization method
1206 for reactor shielding design based on SMS-EMOA. *Ann. Nucl. Energy* 194, 110097.
1207 <https://doi.org/10.1016/j.anucene.2023.110097>
- 1208 Liu, M., Saracevic, E., Oudega, T.J., Obeid, A.A.A., Nagy-Kovács, Z., László, B., Kittlaus, S., Zoboli, O., Krampe,
1209 J., Derx, J., Zessner, M., 2025. Investigating the extent of PFAS contamination in the Upper Danube Basin
1210 across environmental compartments. *Environ. Sci. Eur.* 37. <https://doi.org/10.1186/s12302-025-01141-6>
- 1211 López, O.A.M., López, A.M., Crossa, J., 2022. Multivariate statistical machine learning methods for genomic
1212 prediction. Springer. <https://doi.org/10.1007/978-3-030-89010-0>
- 1213 Lu, H., Ma, X., 2020. Hybrid decision tree-based machine learning models for short-term water quality prediction.
1214 *Chemosphere* 249, 126169. <https://doi.org/10.1016/j.chemosphere.2020.126169>
- 1215 Maier, H.R., Galelli, S., Razavi, S., Castelletti, A., Rizzoli, A., Athanasiadis, I.N., Sánchez-Marrè, M., Acutis, M.,
1216 Wu, W., Humphrey, G.B., 2023. Exploding the myths: an introduction to artificial neural networks for
1217 prediction and forecasting. *Environ. Model. Softw.* 167, 105776.
1218 <https://doi.org/10.1016/j.envsoft.2023.105776>
- 1219 Mallin, M.A., 2024. *River Ecology: Science and Management for a Changing World*. Oxford University Press.
- 1220 Miseta, T., Fodor, A., Vathy-Fogarassy, Á., 2023. Surpassing early stopping: a novel correlation-based stopping
1221 criterion for neural networks. *Neurocomputing* 567, 127028. <https://doi.org/10.1016/j.neucom.2023.127028>
- 1222 Morin-Crini, N., Lichtfouse, E., Liu, G., Balam, V., Ribeiro, A.R.L., Lu, Z., Stock, F., Carmona, E., Teixeira,
1223 M.R., Picos-Corrales, L.A., Moreno-Piraján, J.C., Giraldo, L., Li, C., Pandey, A., Hocquet, D., Torri, G.,
1224 Crini, G., 2022. Worldwide cases of water pollution by emerging contaminants: a review. *Environ. Chem.*
1225 *Lett.* 20, 2311–2338. <https://doi.org/10.1007/s10311-022-01447-4>
- 1226 Musa, M.A., Abdullah-Al-Mamun, N., Nasrin, S., Jakia, T., Sikdar, K., Siddik, M.N.A., Hasi, S.A., Hossain, M.I.S.,
1227 Halder, M., 2025. Heavy metals in water, sediment and fish species of the Bhairab River in southwest
1228 Bangladesh and their health implications. *Waste Manag. Bull.* 100237.
1229 <https://doi.org/10.1016/j.wmb.2025.100237>
- 1230 Nafsin, N., Li, J., 2022. Prediction of 5-day biochemical oxygen demand in the Buriganga River of Bangladesh
1231 using novel hybrid machine learning algorithms. *Water Environ. Res.* 94, 1–17.
1232 <https://doi.org/10.1002/wer.10718>
- 1233 Nasir, N., Kansal, A., Alshaltone, O., Barneih, F., Sameer, M., Shanableh, A., Al-Shamma'a, A., 2022. Water quality
1234 classification using machine learning algorithms. *J. Water Process Eng.* 48, 102920.
1235 <https://doi.org/10.1016/j.jwpe.2022.102920>

- 1236 Ngwenya, B., Paepae, T., Bokoro, P.N., 2025. Monitoring ambient water quality using machine learning and IoT: a
 1237 review and recommendations for advancing SDG indicator 6.3.2. *J. Water Process Eng.* 73, 107664.
 1238 <https://doi.org/10.1016/j.jwpe.2025.107664>
- 1239 Nicolson, A., Paliwal, K.K., 2019. Deep learning for minimum mean-square error approaches to speech
 1240 enhancement. *Speech Commun.* 111, 44–55. <https://doi.org/10.1016/j.specom.2019.06.002>
- 1241 Nishat, M.H., Khan, M.H.R.B., Ahmed, T., Hossain, S.N., Ahsan, A., El-Sergany, M.M., Shafiquzzaman, M.,
 1242 Imteaz, M.A., Alresheedi, M.T., 2025. Comparative analysis of machine learning models for predicting water
 1243 quality index in Dhaka's rivers of Bangladesh. *Environ. Sci. Eur.* 37. <https://doi.org/10.1186/s12302-025-01078-w>
 1244
- 1245 Olbert, A.I., Diganta, M.T.M., Bama, A., Burke, W., Sajib, A.M., Abioui, M., Ashekuzzaman, S., Rahman, A.,
 1246 Uddin, M.G., 2025. Developing river water quality prediction model incorporating reliable indexing
 1247 approach. *J. Environ. Sci.* <https://doi.org/10.1016/j.jes.2025.07.038>
- 1248 Parween, S., Siddique, N.A., Diganta, M.T.M., Olbert, A.I., Uddin, M.G., 2022. Assessment of urban river water
 1249 quality using modified NSF water quality index model at Siliguri city, West Bengal, India. *Environ. Sustain.*
 1250 *Indic.* 16, 100202. <https://doi.org/10.1016/j.indic.2022.100202>
- 1251 Pereira, D.G., Afonso, A., Medeiros, F.M., 2015. Overview of Friedman's test and post-hoc analysis. *Commun. Stat.*
 1252 *Simul. Comput.* 44, 2636–2653. <https://doi.org/10.1080/03610918.2014.931971>
- 1253 Pinichka, C., Chotpantararat, S., Cho, K.H., Siriwong, W., 2025. Comparative analysis of SWAT and SWAT coupled
 1254 with XGBoost model using Optuna hyperparameter optimization for nutrient simulation: a case study in the
 1255 Upper Nan River basin, Thailand. *J. Environ. Manag.* 388, 126053.
 1256 <https://doi.org/10.1016/j.jenvman.2025.126053>
- 1257 Qian, C., Tan, R.K., Ye, W., 2021. An adaptive artificial neural network-based generative design method for layout
 1258 designs. *Int. J. Heat Mass Transf.* 184, 122313. <https://doi.org/10.1016/j.ijheatmasstransfer.2021.122313>
- 1259 Rafizul, I.M., Sakib, S., Alamgir, M., 2017. Appropriate aggregation function for estimating of pollution index of a
 1260 selected river in Bangladesh. *J. Eng.* 8, 1–10.
- 1261 Rahman, A., 2019. Statistics-based data preprocessing methods and machine learning algorithms for big data
 1262 analysis. *Int. J. Artif. Intell.* 17, 44–65.
- 1263 Rahman, A., Jahanara, I., Jolly, Y.N., 2021. Assessment of physicochemical properties of water and their seasonal
 1264 variation in an urban river in Bangladesh. *Water Sci. Eng.* 14, 139–148.
 1265 <https://doi.org/10.1016/j.wse.2021.06.006>
- 1266 Rahman, A., Syeed, M.M.M., Karim, M.R., Fatema, K., Khan, R.H., Uddin, M.F., 2025a. An optimized ensemble
 1267 ML-WQI model for reliable water quality prediction by minimizing the eclipsing and ambiguity issues. *Appl.*
 1268 *Water Sci.* 15. <https://doi.org/10.1007/s13201-025-02450-0>
- 1269 Rahman, M., Sima, S.A., Hossain, M.T., 2025b. Sustainable organizational performance and Khulna's jute industry:
 1270 issues, challenges, and opportunities. *J. Bus. Manag. Stud.* 7, 351–363.
 1271 <https://doi.org/10.32996/jbms.2025.7.4.20.24>
- 1272 Raj, K., Das, A.P., 2023. Lead pollution: impact on environment and human health and approach for a sustainable
 1273 solution. *Environ. Chem. Ecotoxicol.* 5, 79–85. <https://doi.org/10.1016/j.enceco.2023.02.001>
- 1274 Ridika, J.A., Mia, M.R., Ahmed, M.T., Hashib, A.H., 2023. Water quality assessment in different areas of Khulna
 1275 City in Bangladesh. *Chem. Eng. Res. Bull.* 124-129. <https://doi.org/10.3329/cebr.v23i10.78508>

- 1276 Rodríguez-López, L., Bustos Usta, D., Bravo Alvarez, L., Duran-Llacer, I., Lami, A., Martínez-Retureta, R., Urrutia,
1277 R., 2023. Machine learning algorithms for the estimation of water quality parameters in Lake Llanquihue in
1278 Southern Chile. *Water* 15. <https://doi.org/10.3390/w15111994>
- 1279 Roy, M.K., Datta, D.K., Adhikari, D.K., Chowdhury, B.K., Roy, P.J., 2005. Geology of the Khulna City Corporation.
1280 *J. Life Earth Sci.* 1, 57–63.
- 1281 Rustam, F., Ishaq, A., Kokab, S.T., De La Torre Diez, I., Mazón, J.L.V., Rodríguez, C.L., Ashraf, I., 2022. An
1282 artificial neural network model for water quality and water consumption prediction. *Water* 14, 3359.
1283 <https://doi.org/10.3390/w14213359>
- 1284 Sajib, A.M., Bamal, A., Diganta, M.T.M., Ashekuzzaman, S., Rahman, A., Olbert, A.I., Uddin, M.G., 2025a. Novel
1285 groundwater quality index (GWQI) model: a reliable approach for the assessment of groundwater. *Results*
1286 *Eng.* 104265. <https://doi.org/10.1016/j.rineng.2025.104265>
- 1287 Sajib, A.M., Uddin, M.G., Rahman, A., Ahmadian, R., Olbert, A.I., 2025b. Remote sensing applications for
1288 monitoring optically inactive water quality indicators: a comprehensive review. *Earth-Sci. Rev.* 105259.
1289 <https://doi.org/10.1016/j.earscirev.2025.105259>
- 1290 Sajib, A.M., Diganta, M.T.M., Moniruzzaman, M., Rahman, A., Dabrowski, T., Uddin, M.G., Olbert, A.I., 2024.
1291 Assessing water quality of an ecologically critical urban canal incorporating machine learning approaches.
1292 *Ecol. Inform.* 80, 102514. <https://doi.org/10.1016/j.ecoinf.2024.102514>
- 1293 Sajib, A.M., Diganta, M.T.M., Rahman, A., Dabrowski, T., Olbert, A.I., Uddin, M.G., 2023. Developing a novel tool
1294 for assessing the groundwater incorporating water quality index and machine learning approach. *Groundw.*
1295 *Sustain. Dev.* 23, 101049. <https://doi.org/10.1016/j.gsd.2023.101049>
- 1296 Sakizadeh, M., Malian, A., Ahmadpour, E., 2015. Groundwater quality modeling with a small data set. *Ground*
1297 *Water* 54, 115–120. <https://doi.org/10.1111/gwat.12317>
- 1298 Sarker, I.H., 2021. Data science and analytics: an overview from data-driven smart computing, decision-making and
1299 applications perspective. *SN Comput. Sci.* 2, 377. <https://doi.org/10.1007/s42979-021-00765-8>
- 1300 Sarkar, T., Alam, M.M., Parvin, N., Fardous, Z., Chowdhury, A.Z., Hossain, S., Haque, M., Biswas, N., 2016.
1301 Assessment of heavy metals contamination and human health risk in shrimp collected from different farms
1302 and rivers at Khulna-Satkhira region, Bangladesh. *Toxicol. Rep.* 3, 346–350.
1303 <https://doi.org/10.1016/j.toxrep.2016.03.003>
- 1304 Sathya, K., Nagarajan, K., Carlin Geor Malar, G., Rajalakshmi, S., Raja Lakshmi, P., 2022. A comprehensive review
1305 on comparison among effluent treatment methods and modern methods of treatment of industrial wastewater
1306 effluent from different sources. *Appl. Water Sci.* 12, 70. <https://doi.org/10.1007/s13201-022-01594-7>
- 1307 Satish, N., Anmala, J., Varma, M.R.R., Rajitha, K., 2024. Performance of machine learning, artificial neural network
1308 (ANN), and stacked ensemble models in predicting water quality index (WQI) from surface water quality
1309 parameters, climatic and land use data. *Process Saf. Environ. Prot.* <https://doi.org/10.1016/j.psep.2024.10.054>
- 1310 SDG (Sustainable Development Goals), 2015. The 17 goals. Department of Economic and Social Affairs. United
1311 Nations. <https://sdgs.un.org/goals>
- 1312 Sha, C., Shen, S., Zhang, J., Zhou, C., Lu, X., Zhang, H., 2024. A review of strategies and technologies for
1313 sustainable decentralized wastewater treatment. *Water* 16, 3003. <https://doi.org/10.3390/w16203003>

- 1314 Shahid, T.A., Pinjaman, S.B., Amir, H., Bilal, K., Rehman, A.U., 2024. Assessing the nexus between health
 1315 expenditure, food production and water quality: policymaking for achieving sustainable development goals.
 1316 Crit. Rev. Soc. Sci. Stud. 2, 1168–1197.
- 1317 Shakik, A., Brohomo, P., Kabir, S., Islam, S., Mizan, M.H., 2025. Microplastic contamination in Rupsha River of
 1318 Bangladesh and its impacts on fish species. Reg. Stud. Mar. Sci. 104130.
 1319 <https://doi.org/10.1016/j.rsma.2025.104130>
- 1320 Shams, M.Y., Elshewey, A.M., El-Kenawy, E.M., Ibrahim, A., Talaat, F.M., Tarek, Z., 2023. Water quality prediction
 1321 using machine learning models based on grid search method. Multimed. Tools Appl. 83, 35307–35334.
 1322 <https://doi.org/10.1007/s11042-023-16737-4>
- 1323 Skibbe, N., Günther, T., Schwalfenberg, K., Meyer, R., Reckhardt, A., Greskowiak, J., Massmann, G., Müller-Petke,
 1324 M., 2024. Comparison of methods measuring electrical conductivity in coastal aquifers. J Hydrol (Amst) 643,
 1325 131905. <https://doi.org/10.1016/j.jhydrol.2024.131905>
- 1326 Söderberg, C., 2016. Complex governance structures and incoherent policies: implementing the EU water
 1327 framework directive in Sweden. J. Environ. Manag. 183, 90–97.
 1328 <https://doi.org/10.1016/j.jenvman.2016.08.040>
- 1329 Srinivas, P., Katarya, R., 2021. hyOPTXg: OPTUNA hyper-parameter optimization framework for predicting
 1330 cardiovascular disease using XGBoost. Biomed. Signal Process. Control 73, 103456.
 1331 <https://doi.org/10.1016/j.bspc.2021.103456>
- 1332 Sutadian, A.D., Muttil, N., Yilmaz, A.G., Perera, B., 2017. Development of a water quality index for rivers in West
 1333 Java Province, Indonesia. Ecol. Indic. 85, 966–982. <https://doi.org/10.1016/j.ecolind.2017.11.049>
- 1334 Sy, B., Frischknecht, C., Dao, H., Consuegra, D., Giuliani, G., 2020. Reconstituting past flood events: the
 1335 contribution of citizen science. Hydrol. Earth Syst. Sci. 24, 61–74. <https://doi.org/10.5194/hess-24-61-2020>
- 1336 The Bangladesh Environment Conservation Act, 1995. Ministry of Law. Government of the People’s Republic of
 1337 Bangladesh. <http://bdlaws.minlaw.gov.bd/act-791.html>
- 1338 Tiwari, S., Babbar, R., Kaur, G., 2018. Performance evaluation of two ANFIS models for predicting water quality
 1339 index of River Satluj (India). Adv. Civ. Eng. 2018, 8971079. <https://doi.org/10.1155/2018/8971079>
- 1340 Tsamardinos, I., Greasidou, E., Borboudakis, G., 2018. Bootstrapping the out-of-sample predictions for efficient and
 1341 accurate cross-validation. Mach. Learn. 107, 1895–1922. <https://doi.org/10.1007/s10994-018-5714-4>
- 1342 Ubah, J.I., Orakwe, L.C., Ogbu, K.N., Awu, J.I., Ahaneku, I.E., Chukwuma, E.C., 2021. Forecasting water quality
 1343 parameters using artificial neural network for irrigation purposes. Sci. Rep. 11.
 1344 <https://doi.org/10.1038/s41598-021-04062-5>
- 1345 Uddin, M.A., 2015. Study on water quality of Bhairab River in Khulna Region (Doctoral dissertation, Khulna
 1346 University of Engineering & Technology (KUET)).
- 1347 Uddin, M.G., Nash, S., Olbert, A.I., 2021. A review of water quality index models and their use for assessing surface
 1348 water quality. Ecol. Indic. 122, 107218. <https://doi.org/10.1016/j.ecolind.2020.107218>
- 1349 Uddin, M.G., Nash, S., Diganta, M.T.M., Rahman, A., Olbert, A.I., 2022a. Robust machine learning algorithms for
 1350 predicting coastal water quality index. J. Environ. Manag. 321, 115923.
 1351 <https://doi.org/10.1016/j.jenvman.2022.115923>

- 1352 Uddin, M.G., Nash, S., Rahman, A., Olbert, A.I., 2022b. A comprehensive method for improvement of water quality
1353 index (WQI) models for coastal water quality assessment. *Water Res.* 219, 118532.
1354 <https://doi.org/10.1016/j.watres.2022.118532>
- 1355 Uddin, M.G., Nash, S., Rahman, A., Olbert, A.I., 2022c. A novel approach for estimating and predicting uncertainty
1356 in water quality index model using machine learning approaches. *Water Res.* 229, 119422.
1357 <https://doi.org/10.1016/j.watres.2022.119422>
- 1358 Uddin, M.G., Nash, S., Rahman, A., Olbert, A.I., 2022d. Performance analysis of the water quality index model for
1359 predicting water state using machine learning techniques. *Process Saf. Environ. Prot.* 169, 808–828.
1360 <https://doi.org/10.1016/j.psep.2022.11.073>
- 1361 Uddin, M.G., Nash, S., Rahman, A., Olbert, A.I., 2023a. A sophisticated model for rating water quality. *Sci. Total*
1362 *Environ.* 868, 161614. <https://doi.org/10.1016/j.scitotenv.2023.161614>
- 1363 Uddin, M.G., Diganta, M.T.M., Sajib, A.M., Rahman, A., Nash, S., Dabrowski, T., Olbert, A.I., 2023b. Assessing the
1364 impact of COVID-19 lockdown on surface water quality in Ireland using advanced Irish water quality index
1365 (IEWQI) model. *Environ. Pollut.* 336, 122456. <https://doi.org/10.1016/j.envpol.2023.122456>
- 1366 Uddin, M.G., Rana, M.S.P., Diganta, M.T.M., Bamal, A., Sajib, A.M., Abioui, M., Shaibur, M.R., Ashekuzzaman, S.,
1367 Nikoo, M.R., Rahman, A., Moniruzzaman, M., Olbert, A.I., 2024a. Enhancing groundwater quality
1368 assessment in coastal area: a hybrid modeling approach. *Heliyon* 10, e33082.
1369 <https://doi.org/10.1016/j.heliyon.2024.e33082>
- 1370 Uddin, M.G., Dabrowski, T., Rahman, A., Taghikhah, F., Olbert, A.I., 2024b. Data-driven evolution of water quality
1371 models: an in-depth investigation of innovative outlier detection approaches—a case study of Irish Water
1372 Quality Index (IEWQI) model. *Water Res.* 121499. <https://doi.org/10.1016/j.watres.2024.121499>
- 1373 Uddin, M.J., Jeong, Y., 2021. Urban river pollution in Bangladesh during last 40 years: potential public health and
1374 ecological risk, present policy, and future prospects toward smart water management. *Heliyon* 7, e06107.
1375 <https://doi.org/10.1016/j.heliyon.2021.e06107>
- 1376 USGS, 2019. pH and water. U.S. Geological Survey. [https://www.usgs.gov/special-topics/water-science-
1377 school/science/ph-and-water#overview](https://www.usgs.gov/special-topics/water-science-school/science/ph-and-water#overview) (accessed 5.22.23).
- 1378 Varatharajan, G.R., Ndayishimiye, J.C., Nyirabuhoro, P., 2025. Emerging contaminants: a rising threat to urban
1379 water and a barrier to achieving SDG-aligned planetary protection. *Water* 17, 2367.
1380 <https://doi.org/10.3390/w17162367>
- 1381 Wainer, J., Cawley, G., 2021. Nested cross-validation when selecting classifiers is overzealous for most practical
1382 applications. *Expert Syst. Appl.* 182, 115222. <https://doi.org/10.1016/j.eswa.2021.115222>
- 1383 Walker, D., Baumgartner, D., Gerba, C., Fitzsimmons, K., 2019. Surface water pollution, in: Brusseau, M.L., Pepper,
1384 L.I., Gerba, C.P. (Eds.), *Environmental and Pollution Science*. Elsevier, pp. 261–292.
1385 <https://doi.org/10.1016/b978-0-12-814719-1.00016-1>
- 1386 Wan, X., Li, X., Wang, X., Yi, X., Zhao, Y., He, X., Wu, R., Huang, M., 2022. Water quality prediction model using
1387 Gaussian process regression based on deep learning for carbon neutrality in papermaking wastewater
1388 treatment system. *Environ. Res.* 211, 112942. <https://doi.org/10.1016/j.envres.2022.112942>
- 1389 Wang, Q., Wang, S., 2020. Machine learning-based water level prediction in Lake Erie. *Water* 12.
1390 <https://doi.org/10.3390/w12102654>

- 1391 Wang, Y., Deng, A., Feng, H., Wang, D., Guo, C., 2023. Tide-modulated river discharge division in the Ganges-
1392 Brahmaputra-Meghna delta channel network, Bangladesh. *J. Hydrol. Reg. Stud.* 49, 101493.
1393 <https://doi.org/10.1016/j.ejrh.2023.101493>
- 1394 WHO (World Health Organization), 2022. Guidelines for drinking-water quality: fourth edition incorporating the
1395 first and second addenda. World Health Organization.
1396 <https://www.who.int/publications/i/item/9789240045064>
- 1397 Wong, T., 2015. Performance evaluation of classification algorithms by k-fold and leave-one-out cross validation.
1398 *Pattern Recognit.* 48, 2839–2846. <https://doi.org/10.1016/j.patcog.2015.03.009>
- 1399 Yuan, Y., Lin, Z., Jiang, X., Fan, Z., 2024. Hyper-parameter optimization-based multi-source fusion for remote
1400 sensing inversion of non-photosensitive water quality parameters. *Int. J. Remote Sens.* 45, 6838–6859.
1401 <https://doi.org/10.1080/01431161.2024.2388878>
- 1402 Yudina, E., Petrovskaya, A., Shadrin, D., Tregubova, P., Chernova, E., Pukalchik, M., Oseledets, I., 2021.
1403 Optimization of water quality monitoring networks using metaheuristic approaches: Moscow Region use
1404 case. *Water* 13, 888. <https://doi.org/10.3390/w13070888>
- 1405 Yusri, H.I.H., Ab Rahim, A.A., Hassan, S.L.M., Halim, I.S.A., Abdullah, N.E., 2022. Water quality classification
1406 using SVM and XGBoost method, in: Proceedings of the 2022 IEEE 13th Control and System Graduate
1407 Research Colloquium (ICSGRC), pp. 231–236. <https://doi.org/10.1109/ICSGRC55096.2022.9845143>
- 1408 Zamri, N., Pairan, M.A., Azman, W.N.A.W., Abas, S.S., Abdullah, L., Naim, S., Tarmudi, Z., Gao, M., 2022. River
1409 quality classification using different distances in k-nearest neighbors algorithm. *Procedia Comput. Sci.* 204,
1410 180–186. <https://doi.org/10.1016/j.procs.2022.08.022>
- 1411 Zhang, K., Wang, X., Liu, T., Wei, W., Zhang, F., Huang, M., Liu, H., 2024. Enhancing water quality prediction with
1412 advanced machine learning techniques: an extreme gradient boosting model based on long short-term
1413 memory and autoencoder. *J. Hydrol.* 132115. <https://doi.org/10.1016/j.jhydrol.2024.132115>
- 1414 Zhang, H., Liu, J., Li, T., Zhang, S., Lin, Z., Jia, Z., Gong, W., Zhang, G., 2025. Evaluating impacts of hydrology
1415 and pollution loadings on low dissolved oxygen in an urbanized tidal river network using modeling and
1416 monitoring. *J. Hydrol. (Amst)* 661, 133630. <https://doi.org/10.1016/j.jhydrol.2025.133630>
- 1417 Zhu, J., Peng, S., Shen, X., Lin, Z., Gong, L., Zhang, R., Huang, B., 2024. Multiple scale impacts of land use
1418 intensity on water quality in the Chishui river source area. *Ecol. Indic.* 166, 112396.
1419 <https://doi.org/10.1016/j.ecolind.2024.112396>
- 1420 Zhu, X., Wang, L., Zhang, X., He, M., Wang, D., Ren, Y., Yao, H., Ngegla, J.N.V., Pan, H., 2022. Effects of different
1421 types of anthropogenic disturbances and natural wetlands on water quality and microbial communities in a
1422 typical black-odor river. *Ecol. Indic.* 136, 108613. <https://doi.org/10.1016/j.ecolind.2022.108613>
- 1423 Zubaidi, S.L., Hashim, K., Ethaib, S., Al-Bdairi, N.S.S., Al-Bugharbee, H., Gharghan, S.K., 2022. A novel
1424 methodology to predict monthly municipal water demand based on weather variables scenario. *J. King Saud
1425 Univ. Eng. Sci.* 34, 163–169. <https://doi.org/10.1016/j.jksues.2020.09.011>

Supplementary materials

An Integrated Approach for Water Quality Assessment and Pollution Sources Identification Using Optimized Machine Learning and Water Quality Index Model in a Tidal River of Bangladesh

Omur Faruq¹, Nahrin Jannat Hossain¹, Abdul Majed Sajib^{2,3,4}, Mir Talas Mahammad Diganta^{2,3,4}, Md. Moniruzzaman¹, Agnieszka I. Olbert^{2,3,4}, Md Galal Uddin^{2,3,4,5}

¹ Department of Geography and Environment, Jagannath University, Dhaka, Bangladesh

² School of Engineering, College of Science and Engineering, University of Galway, Ireland

³ Ryan Institute, University of Galway, Ireland

⁴ Eco-HydroInformatics Research Group (EHIRG), Civil Engineering, University of Galway, Ireland

⁵ Department of Civil, Structural and Environmental Engineering, and Sustainable Infrastructure Research & Innovation Group, Munster Technological University, Cork, Ireland

Corresponding author: **Md Galal Uddin** (mdgalal.uddin@universityofgalway.ie, jalaluddinbd1987@gmail.com)

Table S1. Description of monitoring sites in the Bhairab River

Sampling site	Sampling location		Site description	
	Longitude	Latitude	Type	Description
Within Jashore district				
S1	89.36887	23.13734	Rural	Agriculture-dominated areas are characterized by crop cultivation and livestock farming.
S2	89.39539	23.03663	Suburban	Presence of fertilizer, cement, textile factories, coal depots, and brick fields.
S3	89.41357	23.01507	Suburban	Industrial zone with jute mills, cement factories, tanneries, and power plants.
S4	89.47869	22.97521	Suburban	Mixed industrial and residential area with jute mills, cement factories, tanneries, coal depots, and domestic waste sources.
Within Khulna district				
S5	89.51664	22.91769	Urban	Wastewater discharge points in proximity to brick fields, cement factories, and cable manufacturing industries.
S6	89.5566	22.85071	Urban	Area influenced by wastewater discharge, power plants, oil depots, and textile industries.
S7	89.56664	22.81968	Urban	Located near the city center, affected by solid waste dumping and wastewater discharge.
S8	89.58246	22.80136	Urban	Industrial zone with shipyard operations, port activities, and urban wastewater discharge.

Table S2. Sub-index formula utilized in this study to measure RMS-WQI score (Uddin et al., 2022a)

WQ Indicator	Conditions	Sub-Index equation
TEMP	(i) $TEMP \leq 25$	100
	(ii) $TEMP > 25$	0.0
EC, Cl ⁻ , TS, BOD	-	$SI = (SI_u - SI_l) - \frac{(SI_u \times WQ_m)}{(STD_u - STD_l)}$
DO	-	$SI = (SI_u - SI_l) - \frac{(SI_u \times WQ_m)}{(STD_u - STD_l)} \times SI_u$
pH	(i) If, $pH < 6.5$	$SI = \frac{(WQ_m - STD_l)}{(STD_u - STD_l)} \times SI_u$
	(ii) If, $pH > 8.5$ and $pH \leq 9.0$	Where SI_u and SI_l are the lower and upper bounds of SI values (0 and 100, respectively), STD_l and STD_u are the lower and upper reference values, and WQ_m is the measured WQ indicator value. $SI = (SI_u - SI_l) - \frac{(SI_u \times WQ_m)}{(STD_u - STD_l)} \times SI_u$
	(iii) If $pH \geq 7.5$ and $pH \leq 8.5$	100

Table S3. Eclipsing criteria utilized in this study (Uddin et al., 2022b)

Water quality status	Expected number of water quality indicators that breach the guideline value
Good	0 indicator
Fair	1-2 indicators
Marginal	3 indicators
Poor	More than 3 indicators

2.5.2 ML/AI algorithms

(i) *Adaptive Boosting*: Adaptive Boosting is a machine learning technique that employs a sample weighting mechanism to combine several weak learners into a stronger and accurate predictor (Yousefi et al., 2024). It does not require prior knowledge about the weak learner's performance which makes it adaptable to various base models. Nonetheless, AdaBoost is sensitive to noisy data and outliers because it assigns higher weights to misclassified instances, including those that might be errors or anomalies. As a result, it leads to overfitting on noise (Schapire et al., 2013).

(ii) *Artificial Neural Networks*: Artificial Neural Networks are a distinctive class of non-linear models, inspired by the functioning of the human brain. Its interconnected neurons mirror the structure of biological neurons (Zhu & Heddiam, 2019). On the positive side, ANNs excel at handling complex, non-linear relationships in data, and can learn from large datasets. While, it can be computationally intensive, require large amounts of labeled data, as well as decision-making mechanism of hidden layers make it difficult to understand (Tu, 1996).

(iii) *Categorical Boosting*: Categorical Boosting model is a gradient boosting algorithm designed to address target leakage and prediction shift. Its unique statistical method improves model robustness and makes it effective for small and challenging datasets (Chen et al., 2024). It also employs techniques like ordered boosting and symmetric trees, which act as natural regularizers to prevent overfitting and improve model generalization. A limitation of this model is that unlike XGBoost and LightGBM which build asymmetric trees, CatBoost builds symmetric trees which limits its ability to capture highly complex, irregular patterns in some datasets (Chen et al., 2020; Hancock et al., 2020).

(iv) *Gradient Boosting*: Gradient Boosting is a machine learning method that combines weak classifiers, typically decision trees, to build a robust model for classification and regression. It adjusts weights for misclassified instances and optimizes a cost function (Shams et al., 2023). The model provides feature importance scores, which is useful to understand the models' decision-making process and gain insights from data. An issue with GBR is that it requires careful tuning of various parameters (e.g., learning rate, tree depth, regularization) to achieve optimal performance. In addition, the model is prone to overfitting, especially if the learning rate is high or the number of trees is excessive (Zhang et al., 2015).

(v) *Multiple Linear Regression*: Multiple Linear Regression is a prediction model that establishes a linear relationship between known and unknown data values, using the ordinary least squares (OLS) method to estimate parameters (Su et al., 2012). By including more variables, MLR can reduce the bias that might occur when important predictors are left out of a model, as in simple regression. As the number of variables increases, however, its results become more difficult to interpret, especially with smaller datasets (Shams et al., 2021).

(vi) *Random Forest*: The Random Forest algorithm combines multiple decision trees to improve prediction accuracy. It builds several independent decision trees by training each one on a random sample of the dataset and then compares the outputs to select the best prediction (Hidayat and Astsauri, 2022; Khan et al., 2022). RF can effectively manage datasets with a large number of features without requiring explicit dimensionality reduction. It can also identify important features. In cases of highly imbalanced datasets, the model often exhibits bias towards the majority class. Moreover, optimal performance necessitates careful tuning of hyperparameters such as the number of trees and the number of features considered at each split (Salman et al., 2024).

(vii) *Support Vector Machine*: Support Vector Machine is a popular and powerful algorithm in supervised statistical machine learning. It works by identifying a hyperplane that maximizes the margin of error while minimizing the prediction error for continuous data (Nafsin & Li, 2022). The ‘kernel trick’ allows SVMs to model non-linear decision boundaries and separate data that is not linearly separable. Few problems of SVMs include sensitivity to the choice of kernel function and regularization parameter. On top of that, selecting the appropriate parameters requires careful tuning and can significantly impact model performance (Abdullah et al., 2021).

(viii) *Extreme Gradient Boosting*: Extreme Gradient Boosting is an enhanced version of the Gradient Boosting algorithm, first introduced by Chen et al. in 2014. It combines multiple decision trees (weak learners) to predict residuals and correct the errors made by previous decision trees to improve overall model performance (Nguyen, 2025). XGB incorporates built-in regularization techniques (e.g. L1 and L2) to prevent overfitting and improve the models’ generalization ability. While it includes regularization, improper tuning or excessive tree depth can still lead to overfitting, particularly on smaller datasets (Zhang et al., 2022).

Table S4. Shapiro–Wilk Statistic showing the distribution of data utilized in this study ($p < 0.05$)

Indicators	Shapiro–Wilk Statistic		p-value	Distribution
2021				
TEMP		0.9344	0.5574	Normal
pH		0.8759	0.1719	Normal
EC		0.881	0.1926	Normal
Cl		0.8799	0.1878	Normal
TS		0.9142	0.3848	Normal
DO		0.9258	0.4783	Normal
BOD ₅		0.8485	0.0919	Normal
RMS-WQI		0.9294	0.5104	Normal
2022				
TEMP		0.9187	0.4195	Normal
pH		0.9356	0.5683	Normal
EC		0.9141	0.3835	Normal
Cl		0.9208	0.4362	Normal
TS		0.9319	0.5337	Normal
DO		0.8855	0.2124	Normal
BOD ₅		0.5345	0	Not Normal
RMS-WQI		0.9086	0.3441	Normal

2023			
TEMP	0.8419	0.0788	Normal
pH	0.9433	0.6441	Normal
EC	0.9282	0.4996	Normal
Cl	0.9226	0.4513	Normal
TS	0.8772	0.1772	Normal
DO	0.9654	0.8594	Normal
BOD	0.8999	0.2885	Normal
RMS	0.9368	0.5794	Normal
2024			
TEMP	0.9334	0.5474	Normal
pH	0.9689	0.8889	Normal
EC	0.9685	0.8857	Normal
Cl	0.6962	0.002	Not Normal
TS	0.9777	0.9508	Normal
DO	0.8511	0.0978	Normal
BOD ₅	0.9221	0.4471	Normal
RMS-WQI	0.8848	0.2093	Normal

Table S5. RMS-WQI calculation at each monitoring site during 2021-2021

Station ID	Sub-index score							RMS-WQI	Rating
	TEMP	pH	EC	Cl	TS	DO	BOD		
2021									
S1	100	100	12.64	72.85	0.00	0	65.00	65	FAIR
S2	0	100	45.14	51.63	26.58	87.89	4.38	58	FAIR
S3	0	100	66.14	77.33	56.87	86.59	6.92	67	FAIR
S4	0	100	42.82	55.61	32.93	77.30	12.75	56	FAIR
S5	0	100	39.56	80.06	24.63	76.43	75.08	66	FAIR
S6	0	100	61.03	82.02	48.63	62.50	70.83	67	FAIR
S7	0	100	67.16	72.99	36.18	73.33	49.44	64	FAIR
S8	0	100	59.27	69.36	25.53	77.42	55.56	63	FAIR
2022									
S1	0	100	78.93	0.00	64.94	0	51.25	57	FAIR
S2	0	100	50.88	21.11	33.06	0	48.00	48	MARGINAL
S3	0	100	62.68	62.25	46.36	0	63.33	59	FAIR
S4	0	100	66.07	69.26	54.69	84.59	68.89	70	FAIR
S5	0	100	68.43	45.65	59.07	93.40	57.50	68	FAIR
S6	0	100	68.43	45.65	59.07	93.40	57.50	68	FAIR
S7	0	100	64.06	27.37	48.57	0	59.03	54	FAIR
S8	0	100	68.93	72.38	54.24	0	0	57	FAIR
2023									
S1	0	30.50	61.70	78.36	50.07	88.19	0	55	FAIR
S2	0	36.71	42.34	68.20	30.41	23.56	0	36	MARGINAL
S3	0	41.50	51.79	73.07	40.64	17.25	0	41	MARGINAL
S4	0	37.21	61.93	78.60	52.77	42.81	0	48	MARGINAL

S5	0	34.15	24.74	57.57	39.03	73.20	0	41	MARGINAL
S6	0	41.75	25.07	57.02	9.48	54.61	0	35	MARGINAL
S7	0	32.50	0.00	43.23	0.00	69.97	0	33	MARGINAL
S8	100	49.63	10.19	48.88	0.00	46.11	0	49	FAIR
2024									
S1	0	37.2	0	0	0	66.5	23.8	30	MARGINAL
S2	0	32.9	0	0	0	57.3	0.0	25	POOR
S3	0	40.9	0	5.9	0	57.9	0.0	27	POOR
S4	0	36.5	0	0	0	54.6	0.0	25	POOR
S5	0	47.8	0	0	0	0	0.0	18	POOR
S6	0	39.9	0	0	0	0	13.2	16	POOR
S7	0	46.6	0	0	0	6.9	0.0	18	POOR
S8	0	43.4	0	0	0	0	0.0	16	POOR

Table S6. ML model performance and ranking

ML Models	Training set										Testing set										Scoring	
	R2	Rank	RME	Rank	MS E	Rank	MA E	Rank	PAB E	Rank	R2	Rank	RME	Rank	MS E	Rank	MA E	Rank	PAB E	Rank	Total score	Rank
2021																						
AdaB	-0.56	8	5.04	8	25.44	8	4.04	8	0.0707	8	0.58	7	2.52	7	6.36	7	1.01	7	0.0177	7	75	7
CatB	0.49	3	2.9	3	8.4	3	2.11	3	0.0374	3	0.86	3	1.45	3	2.1	3	0.53	1	0.0093	1	26	3
XGB	0.81	2	1.77	2	3.12	2	1.28	2	0.0227	2	0.94	2	0.97	2	0.95	2	0.62	2	0.0103	2	20	2
GBR	0.28	6	3.42	6	11.7	6	2.62	6	0.0462	6	0.8	6	1.72	6	2.97	6	0.79	5	0.0138	5	58	6
MLR	0.34	5	3.28	5	10.74	5	2.54	5	0.0447	5	0.82	5	1.66	5	2.77	5	0.86	6	0.0147	6	52	5
SVM	0.37	4	3.22	4	10.36	4	2.53	4	0.0443	4	0.83	4	1.62	4	2.61	4	0.73	4	0.0127	4	40	4
RF	-0.32	7	4.64	7	21.55	7	3.59	7	0.0631	7	0.56	8	2.58	8	6.65	8	1.76	8	0.0295	8	75	7
ANN	0.97	1	0.73	1	0.54	1	0.6	1	0.0105	1	0.96	1	0.82	1	0.67	1	0.72	3	0.0115	3	14	1
2022																						
AdaB	0.83	3	3.2	3	10.24	3	2.99	3	0.0512	4	0.95	3	1.6	3	2.56	3	0.75	3	0.0128	4	32	3
CatB	0.74	4	3.91	4	15.31	4	3.34	4	0.0506	3	0.92	4	1.96	4	3.83	4	0.84	4	0.0126	3	38	4
XGB	0.71	5	4.12	5	17	5	4.1	6	0.0661	6	0.91	5	2.07	5	4.29	5	1.17	6	0.0189	6	54	5
GBR	0.51	7	5.36	7	28.69	7	4.83	7	0.0744	7	0.86	7	2.69	7	7.23	7	1.36	7	0.0214	7	70	7
MLR	0.7	6	4.22	6	17.83	6	4	5	0.0628	5	0.91	5	2.11	6	4.46	6	1	5	0.0157	5	55	6
SVM	0.96	1	1.54	1	2.36	1	1.48	1	0.0235	1	0.99	1	0.77	1	0.59	1	0.38	1	0.006	1	10	1
RF	0.24	8	6.72	8	45.17	8	6.24	8	0.097	8	0.72	8	3.78	8	14.25	8	2.61	8	0.0433	8	80	8
ANN	0.89	2	2.5	2	6.23	2	2.39	2	0.0377	2	0.97	2	1.26	2	1.58	2	0.69	2	0.0112	2	20	2
2023																						

AdaB	0.51	6	5.03	6	25.3 4	6	4.72	6	0.112	6	0.88	6	2.52	6	6.34	6	1.18	6	0.028	6	60	6
CatB	0.82	5	3.05	5	9.33	5	2.85	5	0.077 3	5	0.95	5	1.53	5	2.33	5	0.71	5	0.019 3	5	50	5
XGB	0.98	3	0.89	3	0.79	3	0.81	3	0.022 3	3	0.99	1	0.7	2	0.49	2	0.61	4	0.015 6	4	28	3
GBR	- 0.01	8	7.25	8	52.6 3	8	7.2	8	0.186 9	8	- 0.02	8	7.2	8	51.9	8	5.99	8	0.139 4	8	80	8
MLR	1	1	0.31	2	0.09	1	0.27	1	0.006 2	1	0.99	1	0.67	1	0.46	1	0.58	2	0.014 1	2	13	1
SVM	1	1	0.3	1	0.09	1	0.3	2	0.007 5	2	0.99	1	0.78	3	0.61	3	0.47	1	0.012 9	1	16	2
RF	0.16	7	6.62	7	43.7 8	7	6.19	7	0.167 8	7	0.64	7	4.3	7	18.5 2	7	3.47	7	0.083 6	7	70	7
ANN	0.88	4	2.45	4	5.99	4	2.31	4	0.055	4	0.97	4	1.22	4	1.5	4	0.59	3	0.014 1	2	37	4
2024																						
AdaB	1	1	0.22	3	0.05	3	0.22	3	0.010 9	3	1	1	0.11	1	0.01	1	0.06	1	0.002 7	1	18	1
CatB	1	1	0.22	3	0.05	3	0.22	3	0.010 9	3	1	1	0.11	1	0.01	1	0.06	1	0.002 7	1	18	1
XGB	1	1	0.16	2	0.03	2	0.15	2	0.006 5	2	1	1	0.19	3	0.04	3	0.14	3	0.005 9	3	22	3
GBR	0	8	3.5	8	12.2 2	8	3.5	8	0.168 6	8	- 0.01	8	5.14	8	26.4 2	8	4.83	8	0.225 6	8	80	8
MLR	0.81	7	1.52	7	2.3	7	1.51	7	0.074	7	0.79	7	2.32	7	5.39	7	2.08	7	0.096 8	7	70	7
SVM	1	1	0.06	1	0	1	0.05	1	0.002 6	1	0.88	5	1.77	5	3.12	5	1.02	4	0.039 3	4	28	4
RF	0.93	6	0.91	6	0.82	6	0.71	5	0.038 7	5	0.8	6	2.26	6	5.11	6	1.74	6	0.080 5	6	58	6
ANN	0.94	5	0.85	5	0.73	5	0.85	6	0.041 3	6	0.9	4	1.63	4	2.66	4	1.1	5	0.044 9	5	49	5

References

- Abdullah, D. M., & Abdulazeez, A. M. (2021). Machine learning applications based on SVM classification a review. *Qubahan Academic Journal*, 1(2), 81-90.
- Chen, B., Chen, Y., & Chen, H. (2024). An interpretable CatBoost model guided by spectral morphological features for the inversion of coastal water quality parameters. *Water*, 16(24), 3615. <https://doi.org/10.3390/w16243615>
- Chen, T., T. He, M. Benesty, V. Khotilovich, Y. Tang, H. Cho, K. Chen, R. Mitchell, I. Cano and T. Zhou. (2022). *xgboost: Extreme gradient boosting*. R package version 1.6. 0.1.
- Chen, Y., Song, L., Liu, Y., Yang, L., & Li, D. (2020). A review of the artificial neural network models for water quality prediction. *Applied Sciences*, 10(17), 5776.
- Hancock, J. T., & Khoshgoftaar, T. M. (2020). CatBoost for big data: an interdisciplinary review. *Journal of big data*, 7(1), 94.
- Hidayat, F. and T. M. S. Astsauri. (2022). Applied random forest for parameter sensitivity of low salinity water Injection (LSWI) implementation on carbonate reservoir. *Alexandria Engineering Journal* 61(3): 2408–2417.
- Khan, M. A., M. I. Shah, M. F. Javed, M. I. Khan, S. Rasheed, M. El-Shorbagy, E. R. El-Zahar and M. Malik. (2022). Application of random forest for modelling of surface water salinity. *Ain Shams Engineering Journal* 13(4): 101635.
- Nafsin, N., & Li, J. (2022). Prediction of 5-day biochemical oxygen demand in the Buriganga River of Bangladesh using novel hybrid machine learning algorithms. *Water Environment Research*, 94(5). <https://doi.org/10.1002/wer.10718>
- Nguyen, H. D. (2025). Assessing water quality in the context of climate change in the Red River Delta using the hybrid machine learning. *www.jeeng.net*. <https://doi.org/10.12911/22998993/208093>
- Salman, H. A., Kalakech, A., & Steiti, A. (2024). Random forest algorithm overview. *Babylonian Journal of Machine Learning*, 2024, 69-79.
- Schapire, R. E. (2013). Explaining adaboost. In *Empirical inference: festschrift in honor of vladimir N. Vapnik* (pp. 37-52). Berlin, Heidelberg: Springer Berlin Heidelberg.
- Shams, M. Y., Elshewey, A. M., El-Kenawy, E. M., Ibrahim, A., Talaat, F. M., & Tarek, Z. (2023). Water quality prediction using machine learning models based on grid search method. *Multimedia Tools and Applications*, 83(12), 35307–35334. <https://doi.org/10.1007/s11042-023-16737-4>
- Shams, S. R., Jahani, A., Kalantary, S., Moeinaddini, M., & Khorasani, N. (2021). The evaluation on artificial neural networks (ANN) and multiple linear regressions (MLR) models for predicting SO₂ concentration. *Urban Climate*, 37, 100837.
- Su, X., X. Yan and C. L. Tsai. (2012). Linear regression. *Wiley Interdisciplinary Reviews: Computational Statistics* 4(3): 275–294.
- Tu, J. V. (1996). Advantages and disadvantages of using artificial neural networks versus logistic regression for predicting medical outcomes. *Journal of Clinical Epidemiology*, 49(11), 1225–1231. [https://doi.org/10.1016/s0895-4356\(96\)00002-9](https://doi.org/10.1016/s0895-4356(96)00002-9)
- Uddin, M. G., Nash, S., Rahman, A., & Olbert, A. I. (2022a). A comprehensive method for improvement of water quality index (WQI) models for coastal water quality assessment. *Water Research*, 219, 118532. <https://doi.org/10.1016/j.watres.2022.118532>
- Uddin, M. G., Nash, S., Rahman, A., & Olbert, A. I. (2022b). Performance analysis of the water quality index model for predicting water state using machine learning techniques. *Process Safety and Environmental Protection*, 169, 808–828. <https://doi.org/10.1016/j.psep.2022.11.073>

- Yousefi, M., Oskoei, V., Esmaeli, H. R., & Baziar, M. (2024). An Innovative Combination of Extra Trees within AdaBoost for Accurate Prediction of Agricultural Water Quality Indices. *Results in Engineering*, 24, 103534. <https://doi.org/10.1016/j.rineng.2024.103534>
- Zhang, P., Jia, Y., & Shang, Y. (2022). Research and application of XGBoost in imbalanced data. *International Journal of Distributed Sensor Networks*, 18(6), 15501329221106935.
- Zhang, Y., & Haghani, A. (2015). A gradient boosting method to improve travel time prediction. *Transportation Research Part C: Emerging Technologies*, 58, 308-324.
- Zhu, S., & Heddam, S. (2019). Prediction of dissolved oxygen in urban rivers at the Three Gorges Reservoir, China: extreme learning machines (ELM) versus artificial neural network (ANN). *Water Quality Research Journal*, 55(1), 106–118. <https://doi.org/10.2166/wqrj.2019.053>